Evidence for the biological functions of Histone acetyltransferase Gcn5 and Adaptor protein Ada2 in *Zea mays* L.

Riyaz Ahmad Bhat

Evidence for the biological functions of Histone acetyltransferase Gcn5 and Adaptor protein Ada2 in *Zea mays* L.

Inaugural-Dissertation

zur

Erlangung des Doktorgrades

der Mathematisch-Naturwissenschaftlichen Fakultät

der Universität zu Köln

vorgelegt von

Riyaz Ahmad Bhat

aus Kashmir, Indien

Köln, July 2002

Die vorliegende Arbeit wurde am *Max-Planck-Institut für Züchtungsforschung* in Köln in der Abteilung für Pflanzenzüchtung und Ertragsphysiologie unter der Leitung von Prof. Dr. Francesco Salamini angefertigt.

Berichterstatter: **Priv. -Doz. Dr. Richard D. Thompson**
Prof Dr. Martin Hülskamp

Tag der mündlichen Prüfung: 2nd July 2002

Read: In the name of thy Lord who createth,
Createth man from a clot.
Read: and thy Lord is the most bounteous,
Who teacheth by the pen,
Teacheth man that which he knew not.

(Holy Qur'an)

Dedicated to my parents, to whom I owe the gift of life.

Standard Abbreviations

Abbreviation	Significance
Amp	Ampicillin
APS	Ammonium persulphate
A. tumefaciens	*Agrobacterium tumefaciens*
ATP	Adenosine 5-triphosphate
bp	Base pair
BSA	Bovine serum albumin
˚C	Degree centigrade
cDNA	Complementary deoxyribonucleic acid
Cellulase	1, 4-[1,3;1,4]-β-D-Glucan 4-glucano-hydrolase
Ci	Curie
DAP	Days after pollination
dATP	Deoxyadenosinetriphosphate
dCTP	Deoxycytidinetriphosphate
DEPC	Diethylpolycarbonate
dGTP	Deoxyguanosinetriphosphate
DMSO	Dimythysulfoxide
DNA	Deoxyribonuleic acid
DNase	Deoxyribonuclease
dNTP	Deoxynucleosidetriphosphate
DTT	Dithiothrietol
dTTP	Dioxythimydinetriphophate
E. coli	*Escherichia coli*
EDTA	Ethylenediaminetetraacetic acid
EtBr	Ethidium bromide
EtOH	Ethanol
g	Gram
X g	Gravitation constant (980 cm/s)
GFP	Green fluorescent protein
h	Hour
HAT	Histone acetyltransferase
HDAC	Histone deacetylase
HEPES	4-(2-hydroxyethyl)-1-piperazinethanesulfonic acid
H_2O	Water
HRP	Horseradish peroxidase
kb	Kilobase (s)
kDa	Kilodalton (s)
kV	Kilovolt
l	Litre
LiOAc	Lithium acetate
mA	Milliampere
MES	4-morpholin-ethanesulphonic acid
min	Minute(s)
mmol	Millimolar
MOPS	3-(N-morpholino)-propanesulphonic acid
mRNA	Messenger ribonucleic acid
NaOAc	Sodium acetate
ng	Nanogram
NAA	α-naphthalene acetic acid
OD_x	Optical density at specific wavelength
PAA	Polyacrylamide
PAGE	Polyacrylamide gel electrophoresis
PCR	Polymerase chain reaction

PEG	Polyethylene glycol
pg	Picogram
pmol	Picomol
PMSF	Phenylmethanesulphonfluoride
PVPP	Polyvinylpyrrolidone
RNA	Ribonucleic acid
rRNA	Ribosomal ribonucleic acid
RT	Room temperature
RT-PCR	Reverse transcription-polymerase chain reaction
SDS	Sodium dodecyl sulphate
SDS-PAGE	SDS polyacrylamide gel electrophoresis
sec	Second(s)
TCA	Trichloroacetic acid
TEMED	N,N,N',N'-Tetramethylethylenediamine
TRIS	Tris-(hydroxymethyl)-aminomethane
U	Unit
O/N	Over night
V	Volt
%(v/v)	Volume-percent
%(w/v)	Weight-percent

Contents

CHAPTER 1: GENERAL INTRODUCTION		1-22
1.1	Eukaryotic transcription	1
1.2	Chromatin modifying mechanisms	3
1.2.1	Chromatin disruption by DNA polymerase, RNA polymerase and SWI/SNF complexes	4
1.2.2	Structural and functional consequences of acetylation of core histones	5
1.2.3	Phosphorylation, ubiquitination, ADP-ribosylation and methylation as rivals to core histone acetylation	8
1.2.4	HAT's and their biological functions	9
1.2.4.1	Histone acetyltransferase Gcn5	9
1.2.4.2	Adaptor protein Ada2	12
1.2.5	The histone acetyltransferase superfamily	14
1.2.6	HDAC's and their biological functions	15
1.2.7	Histone deacetylase inhibitors	16
1.3	Histone acetylation in plants	17
1.4	Role of transcriptional activators with acidic activation domains	20
	Aim of the project	23
CHAPTER 2: MATERIALS & METHODS		24-49
2.1	**Materials**	24
2.1.1	Antibiotics	24
2.1.2	Plant materials	24
2.1.3	Bacterial strains, cloning vectors and oligonucleotides	24
2.1.3.1	*E coli* strains	24
2.1.3.2	*Agrobacterium tumefaciens* strains	24
2.1.3.3	Cloning vectors	25
2.1.3.4	Oligonucleotides used for cloning and PCR analysis	25
2.1.4	Chemicals	26
2.1.5	Photographic material	26
2.1.6	Enzymes	26
2.1.6.1	Restriction enzymes	26
2.1.6.2	Nucleic acid modifying enzymes	26
2.1.7	Proteases and protease inhibitors	27

2.1.8	Media	27
2.1.9	Buffers and solutions	28
2.1.9.1	General buffers and solutions	28
2.1.9.2	DNA buffers	29
2.1.9.3	Hybridisation buffers	29
2.1.9.4	Protein buffers	29
2.1.9.5	RNA buffers	30
2.2	**Methods**	31
2.2.1	Nucleic acid manipulations	31
2.2.1.1	Polymerase chain reaction (PCR) amplification	31
2.2.1.2	Cloning PCR products	31
2.2.1.3	Primer extension	32
2.2.2	Transformation of *E. coli*	33
2.2.2.1	Preparation of electro-competent *E. coli* cells	33
2.2.2.2	Transformation of electro-competent *E. coli* cells	33
2.2.3	DNA analysis	34
2.2.3.1	Plasmid DNA isolation	34
2.2.3.2	Isolation of maize DNA for PCR screening	34
2.2.3.3	Southern blotting	34
2.2.4	RNA analysis	35
2.2.4.1	Isolation of total and poly $(A)^+$ RNA from plant tissues	35
2.2.4.2	*In vitro* transcription for the production of spiking RNA control for microarrays	35
2.2.4.3	RNA electrophoresis	36
2.2.4.4	Northern blot analysis	36
2.2.5	Preparation of radioactively labelled probes	36
2.2.5.1	Random prime [α-^{32}P] dCTP labelled probes	36
2.2.5.2	First strand cDNA synthesis with [α-^{33}P] dCTP	37
2.2.6	Expression profiling using cDNA microarrays	38
2.2.6.1	Amplification of cDNA inserts from maize cDNA and expressed sequence tag (EST) collection	39
2.2.6.2	Spotting of cDNA onto nylon filters	40
2.2.6.3	Hybridisation of nylon-array filters	40
2.2.6.4	Microarray quantifications	41
2.2.7	Protein analysis	41
2.2.7.1	Crude nuclear pellet isolation from maize cell lines	41
2.2.7.2	Crude histone purification from maize cell lines	41

2.2.7.3	Western blot analysis	42
2.2.8	Isolation of genomic clones	42
2.2.8.1	Screening of lambda (λ) phage libraries	42
2.2.8.2	Production of high titre phage lysate	44
2.2.8.3	Production of phage DNA	44
2.2.9	DNA sequencing	44
2.2.10	Transient gene expression in plant protoplasts *via* PEG mediated transfection	44
2.2.10.1	Preparation of protoplasts from tobacco BY2 cell line	44
2.2.10.2	Preparation of mesophyll protoplasts from tobacco (SR1) and Cowpea leaves	45
2.2.10.3	Transfection of protoplasts	45
2.2.11	Microscopy	46
2.2.11.1	Light fluorescence microscopy	46
2.2.11.2	Confocal laser scanning microscopy (CLSM)	46
2.2.11.3	Fluorescence spectral imaging microscopy (FSPIM)	46
2.2.12	Plant transformation	47
2.2.12.1	Maize transformation, regeneration and maintenance of transgenic callus and suspension cell lines	47
2.2.12.2	SR1 tobacco cultivar transformation	47
2.12.12.3	BY2 tobacco cell line transformation	48
2.2.13	Chemical treatment of HE-89 cell maize line	48
2.2.14	Computer software	48
2.2.14.1	Visualisation and quantification of DNA and RNA blots by PhosphorImager technology	48
2.2.14.2	DNA sequence analysis	49

CHAPTERS 3-6: RESULTS 50-102

CHAPTER 3: Characterisation of a *ZmGCN5* genomic clone 50-58

3.1	Introduction	50
3.2	Isolation and characterisation of a *ZmGCN5* genomic clone	51
3.3	Identification of transcription start site and putative promoter elements of *ZmGCN5* gene	55
3.4	The *ZmGCN5* promoter drives the expression of green fluorescent protein (GFP) in transiently and stably transformed BY2 and SR1 tobacco protoplasts	57

CHAPTER 4: Localisation and targeting of ZmGcn5		59-62
4.1	ZmGcn5 is a nuclear type A histone acetyltransferase	59
4.2	The extended N-terminal region of ZmGcn5 contains a functional nuclear localisation sequence (NLS)	60
CHAPTER 5: *In vivo* interaction studies between the putative co-activators ZmGcn5, ZmAda2 & a plant transcriptional activator Opaque 2		63-76
5.1	Introduction	63
5.2	The Split-ubiquitin system	64
5.2.1	Establishment of split-ubiquitin system to study *in vivo* protein interactions in plant cells	64
5.2.2	The split-ubiquitin system detects a strong *in vivo* interaction between ZmGcn5 HAT and the adaptor ZmAda2	67
5.3	The Fluorescence resonance energy transfer (FRET) system	69
5.3.1	*In vivo* FRET to study interaction between ZmGcn5, ZmAda2 and plant transcriptional activator ZmO2	70
5.3.2	Colocalisation of ZmGcn5 HAT, adaptor ZmAda2 and plant transcriptional activator ZmO2 in living plant cells	71
5.3.3	FRET studies between ZmGcn5, ZmAda2 and ZmO2	72
5.3.2.1	FRET between ZmGcn5 HAT and the adaptor ZmAda2	72
5.3.2.2	FRET between adaptor ZmAda2 and plant transcriptional activator ZmO2	74
CHAPTER 6: Biological impact of Core Histone Acetylation		77-102
6.1	Introduction	77
6.2	Histone hyper-acetylation studies using Trichostatin A (TSA)	78
6.2.1	TSA treatment results in a dosage dependent acetylation response in maize cell lines	78
6.2.2	Increase in acetylation on TSA treatment is accompanied by decrease in ZmGcn5 levels	79
6.2.3	Microarray analysis on TSA treated and untreated cell lines	80
6.2.3.1	Correction and normalisation of array filters	81
6.2.3.2	Development of non-varying Nebulin poly A^+ RNA reference	82
6.2.3.3	Sensitivity of the microarray system	83
6.2.3.4	Quantification of the TSA treatment transcript profiles	85
6.2.3.5	Differential gene expression between filters hybridised with cDNA prepared from control and TSA treated cell lines	86

6.2.3.6	Inhibiting deacetylases by TSA treatment affects many classes of genes related to stress, development, pathogenesis etc	91
6.2.4	Increase in histone transcripts upon TSA treatment does not change the overall histone abundance in the cell	92
6.3	Transgenic approach to study the impact of histone acetylation	93
6.3.1	Generation of antisense transgenic cell lines of *ZmGCN5*	93
6.3.2	Characterisation of the antisense transgenic callus lines of *ZmGCN5*	94
6.3.3	Reducing *ZmGCN5* results in decreased protein levels of histone deacetylase HD1B-I (ZmRpd3)	96
6.3.4	Microarray analysis on transgenic maize lines containing the *ZmGCN5* antisense construct	98
6.3.4.1	Differential expression between filters hybridised with cDNA prepared from antisense *ZmGCN5* and vector transformed control maize cell lines	98
6.3.4.2	Reducing *ZmGCN5* levels affects similar classes of genes to those affected by TSA treatment	99
6.3.4.3	Overall trend of genes differentially expressed on TSA treatment or in the *ZmGCN5* knockout line	102
CHAPTER 7: DISCUSSION & CONCLUSIONS		103-116
7.1	Role of histone acetylation in transcriptional activation	103
7.1.1	Plant Gcn5 HAT's do not contain a PCAF domain	103
7.1.2	The N-terminal region of ZmGcn5 is essential for the nuclear localisation of the protein	104
7.2	ZmGcn5 HAT interacts with the adaptor ZmAda2 *in vivo*	105
7.2.1	FRET analysis identifies a transient interaction between the adaptor ZmAda2 and plant transcriptional activator ZmO2	107
7.2.2	Split-ubiquitin as a sensor for *in vivo* protein-protein interaction studies in living plant cells	108
7.3	Contribution of histone acetylation to overall chromatin status in maize	109
7.3.1	The cell responds to the changes in histone acetylation by regulating the levels of acetylases and deacetylases	110
7.3.2	Histone acetylation affects many classes of genes related to stress, development and pathogenesis etc	111

7.3.3	ZmGcn5 contributes significantly to the overall nuclear histone acetylation in maize	112
7.4	Future directions	115
SUMMARY:		117-118
ZUSAMMENFASSUNG:		119-120
APPENDICES:		121-125
Appendix I:	Schematic of different constructs used for FRET analysis between putative transcriptional co-activators ZmGcn5, ZmAda2 and transcriptional activator ZmO2.	121
Appendix II:	Sensitivity of microarray system	122
Appendix III:	Clones up-regulated in *ZmGCN5* antisense microarrays	123
Appendix IV:	Clones down-regulated in *ZmGCN5* antisense microarrays	124
LITERATURE CITED:		126-135
ERKLÄRUNG:		136
PUBLICATIONS:		137
ACKNOWLEDGEMENTS:		138
LEBENSLAUF:		139

General Introduction

1.1 Eukaryotic transcription

The eukaryotic genome is packaged into the compact state of chromatin that forms the scaffold from which the fundamental nuclear processes of transcription, replication and DNA repair occur. Chromatin is composed of nucleosomes that are comprised of DNA wrapped around an octameric core containing two molecules each of histones, H2A, H2B, H3 and H4 (Wolffe and Hayes, 1999). The assembly of a stable nucleosome core depends on the initial hetero-dimerization of H3 with H4 and the subsequent dimerization of two H3/H4 dimers to form the $(H3/H4)_2$ tetramer (Eickbusch and Moudrianakis, 1993). Histones H2A and H2B form a stable heterodimer in a manner structurally homologous to H3/H4, but do not self-assemble into stable tetramer complexes. Rather, dimers of (H2A/H2B) bind to either side of the $(H3/H4)_2$ tetramer to form the core which can wrap >160 bp of DNA (Wolffe and Hayes, 1999). The linker histone H1 stabilises the assembly of the octameric core into higher order structures characteristic of chromatin (Marmorstein, 2001). Whereas core histones are essential for chromatin and chromosome assembly, linker histones are not required (Dasso, *et al.,* 1994; Shen *et al.,* 1995).

Each core histone contains a highly helical globular carboxy-terminal domain that comprises about 75% of the amino acid content and forms the interior core of the nucleosome particle (Marmorstein, 2001). External to these folded globular domains, ~25% of the mass of the core histones is contained within flexible and highly basic tail domains that are highly conserved across various species (Wolffe and Hayes, 1999). These domains are located at the N-termini of all four-core histone proteins and at the C-termini of histone H2A (Bohm and Robinson, 1984). These N-termini, if fully extended, can project well beyond the superhelical turns of DNA in the nucleosome (Luger *et al.,* 1997). A schematic of chromatin scaffold along with histone tail domains is shown in figure 1.1.

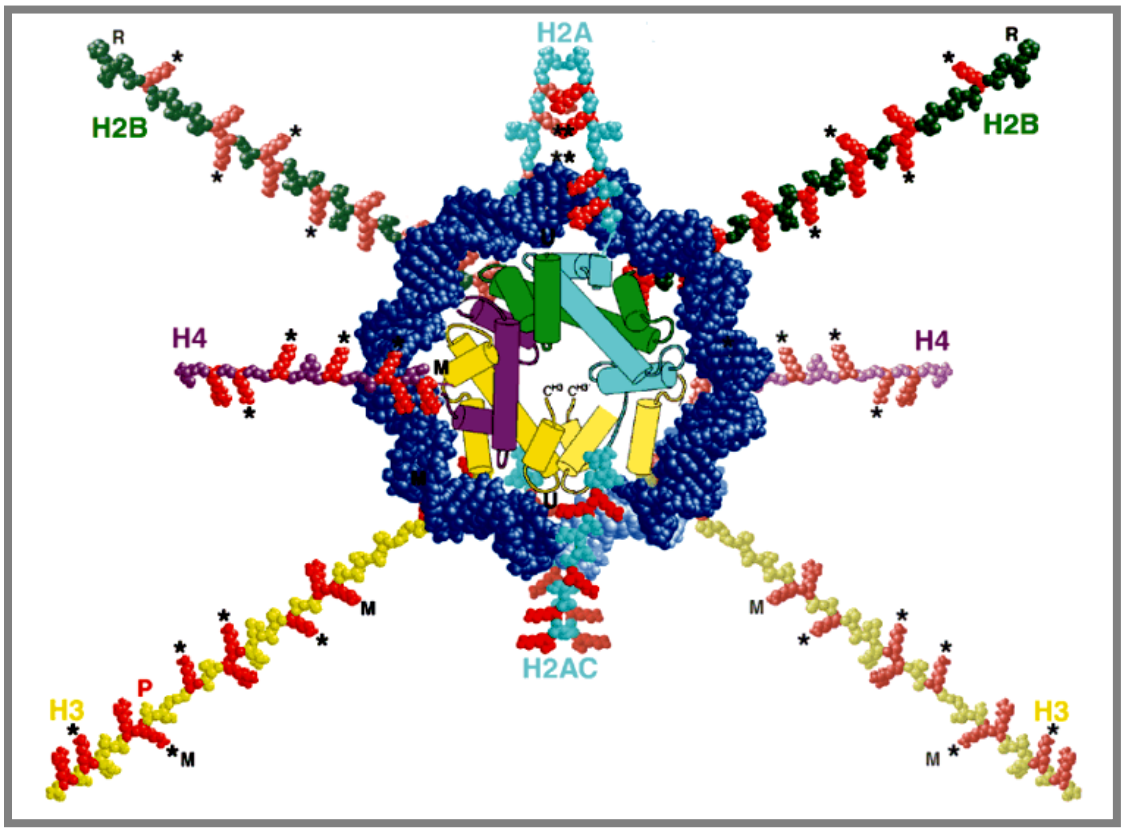

Figure 1.1) Chromatin scaffold along with sites for post-translational modifications within the histone tail domains. The histone tail domains and the nucleosome core proper are viewed along the superhelical DNA axis. The tail domains are modelled as fully extended polypeptide chains to show the approximate length of these domains with respect to the histone fold domains (columns). The top and bottom superhelical turns of core DNA are coloured blue and light blue, respectively. H2A, H2B, H3 and H4 are coloured cyan, green, yellow and magenta, respectively, while arginine and lysine residues in the tails are coloured red. The H2A C-terminal tail is indicated as H2AC. Only the top four polypeptides are shown in their entirety. Tails from histones in the bottom half of the nucleosome are shaded lighter than those from the top half. Well-characterized sites of acetylation on lysines are indicated by an asterisk. Sites of methylation (M), the site of phosphorylation (P) in the H3 tail (Ser10), and sites of ribosylation (R) and ubiquitination (U) in H2A and H2B are also indicated. See text for details about various modifications of histone tails (Wolffe and Hayes, 1999).

Histone tails mediate internucleosomal contacts as extended chains of nucleosomes are compacted to form chromatin fibre (Garcia-Ramirez *et al.,* 1992). Furthermore, the tails are critical for the self-assembly of condensed fibres into higher order structures (Tse and Hansen; 1997; Tse, *et al.,* 1998). Histone tail interactions change as the chromatin fibre undergoes folding or compaction suggesting that specific tail interactions are correlated with specific conformations of the fibre (Fletcher and Hansen, 1996).

Regulatory expression of genes is pivotal to almost all the biological phenomena including development, differentiation, cell growth and response

to environmental cues. Transcriptional regulation of gene expression is a commonly utilised regulatory mechanism and is largely mediated through sequence-specific DNA binding proteins that recognise *cis*-acting elements located on the promoter and the enhancer regions of the target genes. Binding of such transcription factors to the relevant *cis*-acting elements facilitates other components of the transcription machinery to initiate the mRNA synthesis. However chromatin (as described above) appears to be an inhospitable environment for the molecular machines that use it as a substrate for various nuclear processes (Wolffe and Hayes, 1999). DNA in the nucleosomes is in a highly condensed and repressive state. Nucleosomes are remarkably stable to physical perturbation and under physiological conditions nucleosomal arrays fold into stable higher order structures that self-associate within the nucleus to achieve concentrations in excess of 50 mg/ml (Wolffe and Hayes, 1999). Under such repressive conditions the access of the transcription machinery to the target promoters is not possible. Packaging promoters in nucleosomes prevents the initiation of transcription by bacterial and eukaryotic RNA polymerases *in vitro* (Kornberg and Lorch, 1999). Nucleosomes exert a similar inhibitory effect upon transcription *in vivo*. Turning off histone synthesis by genetic means in yeast, leading to nucleosome loss, turns on transcription of all previously inactive genes (Han and Grunstein, 1988). Despite this repression complex metabolic processes involving DNA occur very efficiently in the cell. This contrasting requirement between the storage and the functional utility is met through the use of specialized molecular machines that reversibly disrupt and modify chromatin. Eukaryotic transcription machinery includes certain classes of non-DNA binding transcriptional co-activators (or adaptors) that modify or alter the chromatin structure in such a way as to facilitate access by the transcription machinery to the DNA (Roth and Allis, 1996).

1.2 Chromatin modifying mechanisms

Research done over the last decade has shown that at least two different, yet highly conserved, mechanisms are used by eukaryotic cells to relieve nucleosomal repression and facilitate transcription (Kuo and Allis,

1998). The two mechanisms, described below, differ in whether or not they use covalent modification to alter chromatin structure (Kingston and Narlikar, 1999).

a) **Chromatin remodelling complexes,** which use the energy of ATP hydrolysis to locally disrupt or alter the association of histones with DNA (Vignali *et al.,* 2000). These structural changes are accomplished without covalent modification and can be involved in either activation or repression (Kingston and Narlikar, 1999).

b) **Histone acetyltransferase (HAT) and histone deacetylase (HDAC) complexes**, which regulate the transcriptional activity of genes by determining the level of acetylation of the amino-terminal domains of nucleosomal histones associated with them (Kuo and Allis, 1998).

1.2.1 Chromatin disruption by DNA polymerase, RNA polymerase and SWI/SNF Complexes

Molecular machines driven by ATP hydrolysis, including DNA and RNA polymerases and SWI/SNF-type complexes, can disrupt chromatin structure. Nucleosomes are disrupted by DNA polymerase with the pre-existing histone $(H3/H4)_2$ tetramers being distributed between both daughter DNA duplexes and reassociating with pre-existing and newly synthesized histone (H2A/H2B) dimers (Wolffe and Hayes, 1999). Half of the newly assembled nucleosomes on nascent DNA contain newly synthesized diacetylated histone H4 and consequently will be more accessible to the transcriptional machinery (Ura *et al.,* 1997). RNA polymerase needs to disrupt histone-DNA contacts in half of the nucleosome in order to effect cooperative displacement of the remaining histone-DNA interactions (Studitsky *et al.,* 1994). Prokaryotic DNA and RNA polymerases have remarkable success in traversing chromatin templates (Bonne-Andrea *et al.,* 1990). On the other hand eukaryotic RNA polymerases II and III have difficulty progressing along nucleosomal arrays (Wolffe and Hayes, 1999).

Eukaryotic polymerases make use of additional factors to promote elongation through chromatin. These include proteins of the SWI/SNF (SWI, mating type SWItching; SNF, Sucrose Non Fermenting) class of genes

(Brown *et al.,* 1996). These genes were first identified in yeast and their products were shown to oppose the inhibition of transcription by histones *in vivo* (Kornberg and Lorch, 1999). Mono-nucleosomal substrates lose the rotational constraint of DNA on the histone surface in the presence of yeast or mammalian SWI/SNF complexes (Kwon *et al.,* 1994; Imbalzano *et al.,* 1994). This loss requires ATP hydrolysis and facilitates the access of DNA-binding proteins to DNA in the nucleosome. Examples of plant proteins involved in ATP dependent chromatin remodelling are the products of *Arabidopsis thaliana* L. DDM1 and MOM loci (Kakutani *et al.,* 1995, Amedeo *et al.,* 2000).

The mechanism of action of ATP dependent chromatin remodelling factors is not clearly understood. One of the models is that histones H2A and H2B are displaced or destabilized within the nucleosome (Peterson and Tamkun, 1995). Removal of H2A and H2B facilitates access of transcription factors to nucleosomal DNA (Hayes and Wolffe, 1992) and facilitates transcription (Hansen and Wolffe, 1994).

1.2.2 Structural and functional consequences of acetylation of core histones

The histone tail domains provide sites for several different types of post-translational modifications including methylation, ADP ribosylation, phosphorylation, ubiquitination and acetylation (Allfrey *et al.,* 1964; Bradbury, 1992; Marmorstein, 2001). Such post-translational modifications have long been correlated with various nuclear activities, including replication, chromatin assembly and transcription (Grunstein, 1997; Durrin *et al.,* 1991).

Of such modifications, acetylation and deacetylation have generated most interest since gene activity was first correlated with histone acetylation. Nearly 40 years ago it was proposed that the acetylation state of the core histones within chromatin is associated with gene regulation (Allfrey *et al.,* 1964; Pogo *et al.,* 1966) whereby genes containing hypoacetylated histones were transcriptionally repressed, while genes containing hyperacetylated histones were transcriptionally active. However, a direct link between chromatin function and acetylation was established by the discovery that coactivator complexes required for transcriptional activation function as

histone acetyltransferases (HAT's; Brownell *et al.,* 1996; Ogryzko *et al.,* 1996; Kou *et al.,* 1998), while co-repressors containing histone deacetylases (HDAC's) confer transcriptional repression (Taunton *et al.,* 1996; Alland *et al.,* 1997; Hassig *et al.,* 1998).

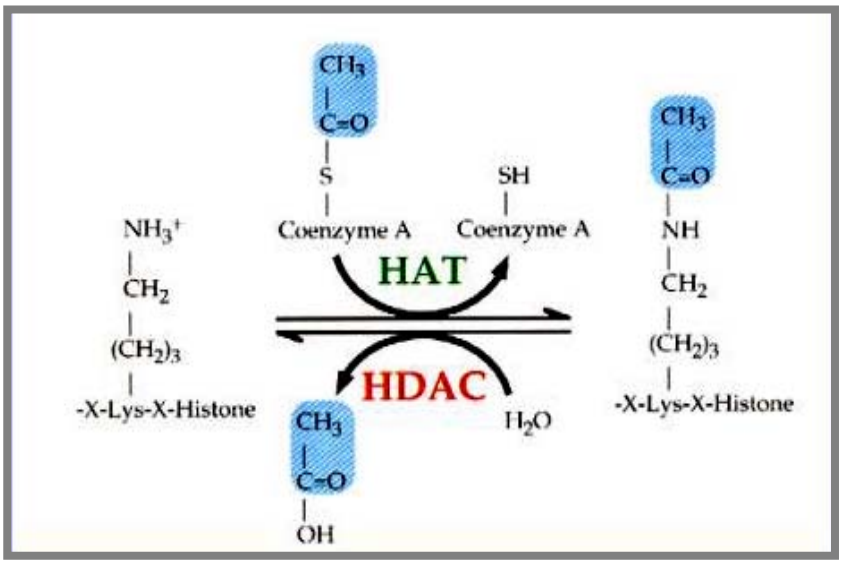

Figure 1.2) Equilibrium of steady-state histone acetylation is maintained by opposing activities of HAT's and HDAC's. Acetyl coenzyme A is the high-energy acetyl moiety donor for histone acetylation. HAT's transfer the acetyl moiety to the ε-NH_3^+ groups of internal lysine residues of histone N-terminal domains. Reversible reaction is catalysed by HDAC (Kuo and Allis, 1998).

Histone acetylation is a reversible process (figure 1.2). HAT's transfer the acetyl moiety from acetyl coenzyme A onto the ε-NH_3^+ group of specific lysine residues present in the amino-terminal tails of each of the core histones resulting in the neutralisation of a single positive charge on each residue (Allfrey *et al.,* 1964). Deacetylation catalysed by histone deacetylases, on the other hand, involves the removal of the acetyl moiety and, accordingly, the restoration of a positive charge on the histone tail (Brownell and Allis, 1996).

Histones are locally modified on target promoters and specific lysines in particular histones are functional targets for acetyltransferases and deacetylases (Kuo *et al.,* 1998; Kruger *et al.,* 1995; Rundlett et al 1998). A hypothetical model of the mechanism of action of HAT's is shown in figure 1.3.

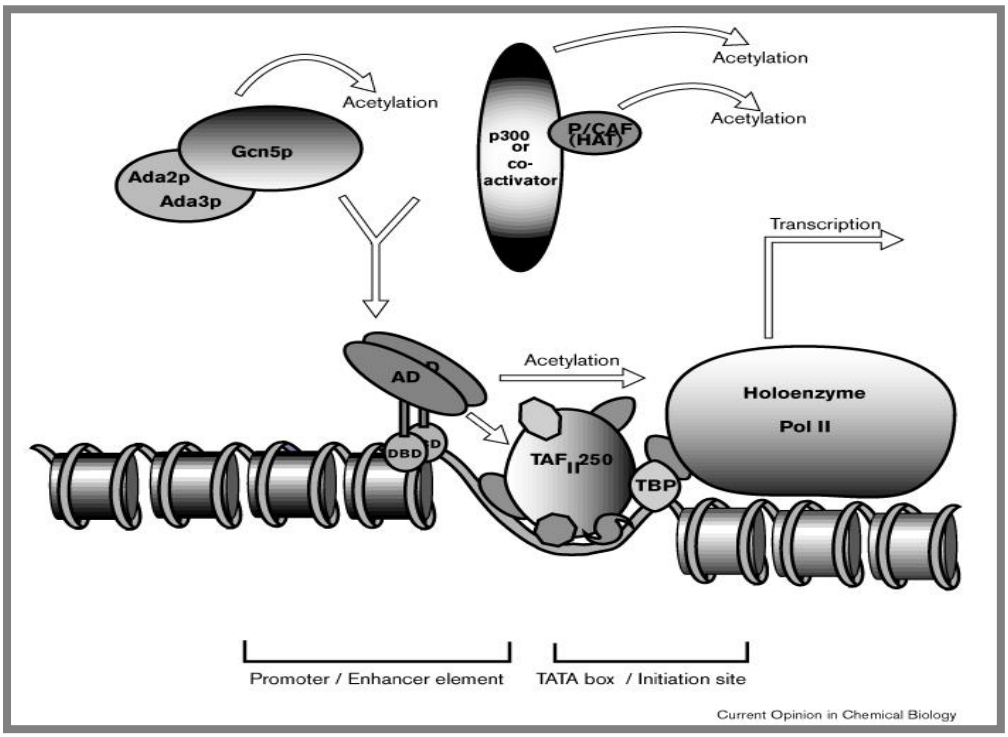

Figure 1.3) A model for the mechanism of action of histone acetylation. Transcription factors bind DNA at enhancer sites or promoter sites near to the TATA box and initiation site via the DNA-binding domains (DBD) and recruit co-activators (like Gcn5 and P/CAF) to specific DNA sites using their activation domains (AD). The yeast nuclear histone acetyltransferase Gcn5p, in association with Ada2/3p, forms a co-activator complex that is thought to function in a targeted manner. In mammalian cells, the co-activator p300/CBP (which also functions as a HAT) and its associated HAT, PCAF, are recruited in the same fashion. These activities of the HAT's are thought to enhance transcription by RNA polymerase II (pol II) holoenzymes on a nucleosomal template by acetylating nucleosomes. (Hassig and Schreiber, 1997)

Several possibilities for the biological effects of lysine acetylation on chromatin structure have been suggested. These can be summarised below:

a) Each acetylation reaction neutralises a positive charge and thus potentially weakens the interaction of the core histones with the negatively charged DNA. This may destabilise the nucleosomes and facilitate the binding of transcription factors to their recognition elements within isolated nucleosomes (Graessle *et al.,* 2001).
b) Acetylated histones wrap DNA less tightly in mono-nucleosomes, which may result in a decrease in the amount of DNA superhelical writhe constrained by the nucleosome (Wolffe and Hayes, 1999).
c) Acetylation may disrupt the secondary structures that are known to exist within the H3- and H4 N-termini when they are bound to

nucleosomal DNA (Baneres *et al.,* 1997). This might further destabilize interactions with DNA and the nucleosome itself.

d) Acetylation may also facilitate factor access and transcription from nucleosomal arrays by decreasing the stability of the completely compacted 30 nm chromatin fibre (Tse *et al.,* 1998; Ura *et al.,* 1997; Nightingale *et al.,* 1998). It is also likely that acetylation leads to the destabilisation of long range structures through which the chromatin fibre is folded into chromosome itself (Annunziato *et al.,* 1988).

e) Acetylation may act as a highly specific signal that alters histone-protein interactions. This possibility is supported by the finding that non-histone proteins can also be acetylated and deacetylated by HAT's and HDAC's (Graessle *et al.,* 2001). Among these proteins are structural proteins (HMG proteins), transcriptional activators (e.g. p53, c-myb, GATA-1, MyoD, E2F etc.), nuclear receptor co-activators (ACTR, TIF2), general transcription factors (TFIIE, TEIIF).

1.2.3 Phosphorylation, ubiquitination, ADP-ribosylation and methylation as rivals to core histone acetylation

In contrast to the studies on the structural and functional consequences of histone acetylation, the impact of other post-translational modifications of the core histones is relatively unexplored. Histone H3 is rapidly phosphorylated on serine/threonine residues within its basic N-terminal domain, when extracellular signals such as growth factors stimulate quiescent cells to proliferate (Mahadevan *et al.,* 1991). Based on charge effects phosphorylation of histone H3 might be expected to have structural consequences comparable with acetylation.

Ubiquitin is a 76 amino acid peptide that is attached to the C-terminal tail of histone H2A and perhaps H2B. Ubiquitinated H2A is incorporated into nucleosomes, without major changes in the organization of nucleosome cores (Wolffe and Guschin, 2000). Only one nucleosome in 25 contains ubiquitinated histone H2A within non-transcribed chromatin. This increases to one nucleosome in two for the transcriptionally active *HSP70* genes (Levinger and Varshavsky, 1982).

ADP-ribosylation of core histones may lead to localized unfolding of the chromatin fibre. The synthesis of long negatively charged chains of ADP-ribose may well facilitate a partial disruption of nucleosomes, presumably by exchange of histones to this competitor polyanion (Wolffe and Hayes, 1999).

Core histones are methylated on their lysine residues. Most methylation in vertebrates occurs on histone H3 at Lys9 and Lys27 and histone H4 at Lys20. The lysine positions on H3 are not known sites of acetylation while lysine 20 on H4 is subject to acetylation in plants (Wolffe and Hayes, 1999; Waterborg, 1990). Methylation of H3 seems to be correlated with acetylated regions of chromatin while methylation of H4 seems to have the opposite correlation (Annunziato *et al.,* 1995). The exact role(s) of this modification has not been elucidated.

1.2.4 HAT's and their biological functions

HAT's can be classified with respect to their intracellular location and substrate specificity as either nuclear A-type (HAT A) or cytoplasmic B-type (HAT B). A-type HAT's are involved in the post-synthetic acetylation of all four nucleosomal core histones and have long been thought to promote transcription related acetylation although their involvement in other processes such as DNA repair and replication is also likely (Kuo and Allis, 1999). Conversely B-type HAT's are believed to have a housekeeping role in the cell, acetylating newly synthesised free histones (primarily histone H4 at lysines 5 and 12) in the cytoplasm for transport into the nucleus, where they may be deacetylated and incorporated into chromatin (Kölle *et al.,* 1998; Ruiz-Carrillo *et al.,* 1975; Allis *et al.,* 1985).

1.2.4.1 Histone acetyltransferase Gcn5

The first type-A HAT of known function, *viz. GCN5* (General Control Nonderepressible-5) was identified in a genetic screen in yeast designed to isolate mutants unable to grow under conditions of amino acid limitation (Georgakopoulos and Thireos, 1992). The yeast cells' response to changes in amino acid regime is coordinated by the activity of a bZip transcription factor, *GCN4*. Gcn4 activates the transcription of a large number of amino acid

biosynthesis genes when yeast cells are starved for amino acids (Hinnebusch, 1990). However the ability of Gcn4 to activate a target promoter depends on the products of a number of *gcn* loci identified in this screen, including *GCN5.* Later it was suggested that the encoded protein (Gcn5) could function as an adaptor that mediates and enhances the interaction of the transcriptional activation domain of the DNA bound activators like Gcn4 with the basal transcriptional machinery (Georgakopoulos and Thireos, 1992). The *GCN5* locus was recognized to be a HAT on the basis of sequence homology with the first functionally identified histone acetyltransferase gene from Tetrahymena (Brownell *et al.,* 1996) and was subsequently shown to encode an active enzyme. Functional characterisation of yeast Gcn5 revealed a direct correlation between the ability of the protein to acetylate histones and its ability to activate transcription (Wang *et al.,* 1998; Kuo *et al.,* 1998). Various studies have mapped and characterised the functional domains of yeast Gcn5 (figure 1.4).

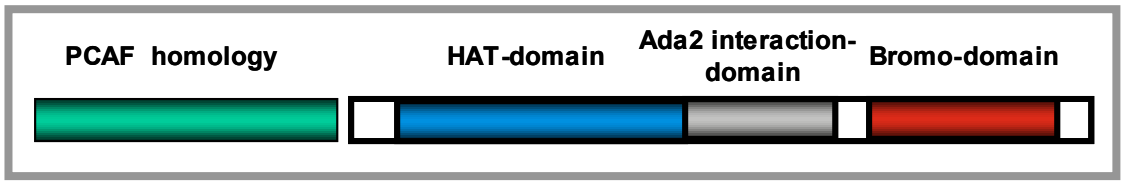

Figure 1.4) Typical domain structure of Gcn5 proteins. An N-terminal HAT domain, a central Ada2 interaction-domain and a C-terminal bromo-domain. Also shown is the PCAF homology domain found in mammalian Gcn5 proteins (see text for details).

The domains identified include a C-terminal bromo-domain (Tamkun *et al.,* 1992), which interacts with the histone N-termini (Ornaghi *et al.,* 1999), a central domain responsible for interaction with adaptor protein Ada2 (Alteration/Deficiency in activation), and an N-terminal HAT-domain.

Functional analysis of mutagenised Gcn5 HAT-domain identified conserved residues critical to HAT activity and demonstrated the direct correlation of Gcn5 HAT function with cell growth, *in vivo* transcription and histone acetylation at Gcn5 dependent promoters' *in vivo* (Kuo *et al.,* 1998). Further studies on these mutants showed that Gcn5 HAT activity also has an effect on chromatin remodelling (Gregory *et al.,* 1998).

Gcn5-homologous proteins have been cloned from humans, plants, fungi and protozoa (Smith *et al.,* 1998). Mammalian Gcn5 HAT's contain an

additional domain at the N-terminal end. This domain shows homology to PCAF (p300/CREB binding associated factor; CREB, cAMP response element-binding protein) protein and is known as PCAF homology-domain (Forsberg *et al.,* 1997). The PCAF-domain of mammalian Gcn5 has been implicated in the acetylation of histones in nucleosomes (Xu *et al.,* 1998). It has also been shown to bind to CBP (CREB binding protein) and p300 (Yang, *et al.,* 1996), both of which are transcriptional co-activators and interact with a large number of developmentally important transcription factors (Kamei, *et al.* 1996).

Nuclear histone acetyltransferases are often subunits of large protein complexes. Among known nuclear HAT's, TAF_{250} (TATA binding protein associated factor) is a subunit of large TFIID complex and CBP/p300, SRC-1 (steroid receptor cofactor 1) and ACTR (activator of thyroid and RA receptor) may all be components of a single, large co-activator complex that facilitates the functioning of nuclear hormone receptors (Pollard and Peterson, 1998).

The yeast Gcn5 is a catalytic subunit of three distinct complexes: Ada complex (0.8 Mda), SAGA (Spt, Ada, Gcn5, Acetyltransferase) complex (1.8 Mda) and a 200 kDa complex (Grant *et al.,* 1997; Pollard and Peterson, 1997; Saleh *et al.,* 1997). Models of Ada and SAGA complexes are shown in figure 1.5. In addition to several unknown subunits, each complex contains the adaptor Ada2 and Ada3 gene products, and SAGA also contains Spt (suppressor of transcription) proteins *viz.* Spt3, Spt7, Spt8 and Spt20 (Grant *et al.,* 1997). Unlike the isolated catalytic HAT subunits, which can only acetylate isolated core histones, these complexes are able to acetylate histones within nucleosomes (Grant *et al.,* 1997).

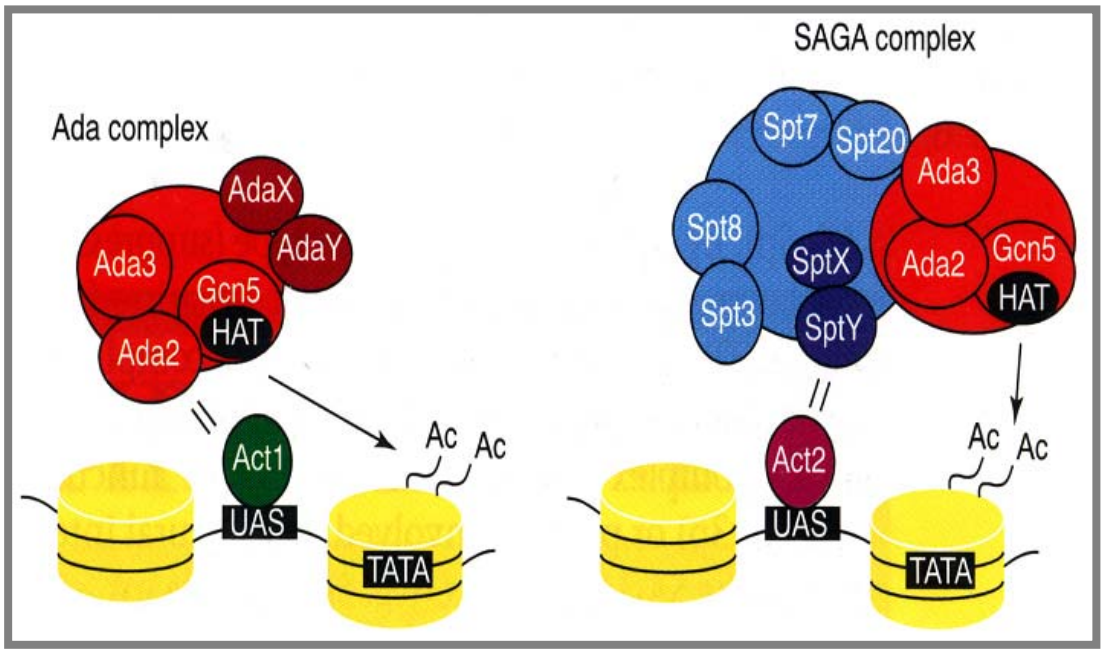

Figure 1.5) Models of Ada and SAGA structure and function. The scenario shows that the Ada and SAGA complexes are distinct in terms of function and composition. Both complexes would contain the nucleosome acetylating function of GCN5 but might possess some unique uncharacterised subunits (e.g. AdaX and AdaY, SptX and SptY) and interact with different types of activators (Act1 and Act2, Grant *et al.,* 1998).

1.2.4.2 Adaptor protein Ada2

A genetic screen in yeast identified proteins that could functionally interact with the activation domain of the herpes simplex virus activator, VP16 (Berger *et al.,* 1992). Several genes, Ada2 (Alteration/Deficiency in activation; Berger *et al.,* 1992), Ada3 (Pina *et al.,* 1993), Ada4 (Marcus *et al.,* 1994) and Ada5 (Marcus *et al.,* 1996; Roberts and Winston, 1996) were identified and cloned. Mutations in any one of them slowed yeast growth and reduced the activation by acidic activators such as VP16 and yeast Gcn4. Ada4 was shown to be identical to Gcn5 while Ada5 was shown to be Spt20 (Barlev *et al.,* 1995; Grant *et al.,* 1998). Ada2, Ada3 and Gcn5 (Ada4) interact with each other *in vitro* (Horiuchi *et al.,* 1995) and *in vivo* (Candau and Berger, 1996), which strongly argues for the existence of a physiologically relevant Ada complex. This is further supported by the fact that mutant strains in either *ada3* (Pina *et al.,* 1993) or *gcn5* (Marcus *et al.,* 1994) have properties similar to *ada2* mutants. The role of such an Ada complex could be to constitute a physical link to allow productive interaction between the activation domains of transcription factors and the basal transcription machinery. Ada2 may play a

central role in such a complex since it physically interacts with activation domains from VP16 (Silverman *et al.,* 1994; Barlev *et al.,* 1995), Gcn4 and also with TBP (TATA binding protein; Barlev *et al.,* 1995). Further studies proved that indeed Gcn5 and Ada2 are present in multi-protein complexes (Grant *et al.,* 1997; Pollard and Peterson, 1997; Saleh *et al.,* 1997; figure 1.4). Gcn5 mediated HAT activity of these complexes is lost in strains bearing disruptions of Ada2 or Ada3 (Grant *et al.,* 1998) indicating the crucial role of Ada2 and Ada3.

Genes encoding putative adaptor proteins have been isolated and cloned from a range of eukaryotes including plants as for Gcn5. The sequence similarity between Ada2 proteins from different organisms is less highly conserved than Gcn5. Nevertheless various studies have characterised a number of functional domains in Ada2 proteins (figure 1.6).

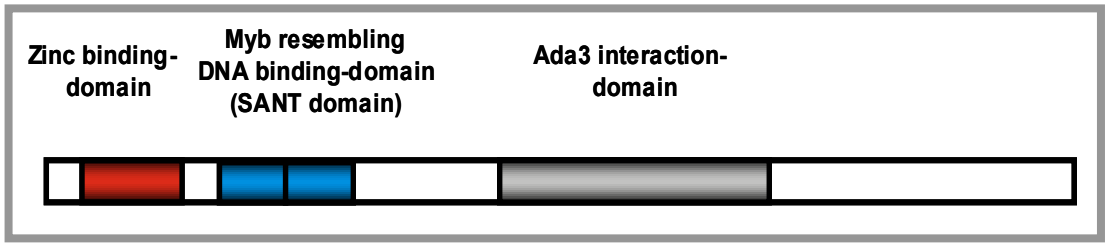

Figure 1.6) Typical domain structure of Ada2 proteins. All proteins contain a zinc binding- and a myb-resembling DNA binding-domain at the N-terminal end and a central Ada3 interaction-domain.

The similarity between various Ada2 proteins is found primarily in three regions. The most N-terminal region includes a cysteine-rich zinc binding domain (comprising of 2 zinc fingers with 6 conserved cysteine and 2 flanking histidine residues). This region is capable of binding to both Gcn5 and the transcriptional activation domain of VP16 (Candau *et al.,* 1996; Barlev *et al.,* 1995). Deletion of the cysteine rich region from yeast Ada2 reduces co-immunoprecipitation of Gcn5 but has little discernible phenotype *in vivo* (Candau and Berger, 1996). The N-terminal segment of Ada2 also contains one copy of a motif present three times in the DNA binding domain of the Myb protein family (Lane *et al.,* 1990; Berger *et al.,* 1992). Deletion of the myb motif does not affect co-immunoprecipitation of Gcn5 but cripples the ability of Ada2 to support transcriptional activation *in vivo* (Candau and Berger, 1996).

Recently it was shown that this domain is required for the normal acetylation of histones by the SAGA complex (Sterner *et al.,* 2002). The central region is responsible for interaction with Ada3 (Candau *et al.,* 1996) and its deletion causes debilitating phenotypes *in vivo* (Stockinger *et al.,* 2001).

1.2.5 The histone acetyltransferase superfamily

A large number of transcriptional regulators have been found to possess intrinsic HAT activity (Table 1.1; Sterner and Berger, 2000).

HAT	HAT complex	Function	Organism
Gcn5-related N-acetyltransferases (GNAT)			
Gcn5	Ada, SAGA	Coactivator of transcription	Ubiquitous
Hat1	Complex with Rbap48	Cytoplasmic acetylation of H4 (deposition-related)	Ubiquitous
PCAF	PCAF complex	Coactivator of transcription	Mammals
Hpa2	–	Unknown	Yeast
Elp3	RNA polymerase II complex	Transcription (elongation)	Yeast
CBP/p300	Associates with different regulatory proteins	Coactivator of transcription	Ubiquitous
Nuclear receptor coactivators			
ACTR	–	Coactivator of transcription	Mammals
SRC-1	–	Coactivator of transcription	Mammals
TIF2	–	Coactivator of transcription	Mammals
$TAF_{II}250$	TFIID	Factor associated with TBP	Ubiquitous
TFIIIC (90, 110, 220)	TFIIIC complex	RNA polymerase III transcription	Human
MYST-family			
Sas3	Nun	Silencing	Yeast
Esa1	Nun	Cell cycle regulation	Yeast
MOF	MSL complex	Gene dosage compensation	Insects
MOZ	–	Malignant diseases	Human
Tip60	Tip60 complex	HIV-Tat interaction	Human
HBO1	HBO complex	Interacts with replication origin recognition complex	Human

Table 1.1) HAT families and their transcription-related functions. **ACTR**–activator of thyroid and RA receptor; **HAT**–histone acetyltransferase; **MOF**–male absent on first; **MYST** – MOZ, Ybf2/Sas3, Sas2, Tip60; **PCAF**–p300/CBP associated factor; **rOX**–RNA on X; **SRC-1** – steroid receptor cofactor 1; **-**, not known (Lusser *et al.,* 2001).

Sequence analysis of these proteins reveals that they fall into distinct families that show high similarity within families but poor to no sequence similarity between families (Kuo *et al.,* 1998). Gcn5/PCAF family of HAT proteins (GNAT family) function as coactivators for a subset of transcriptional activators. This family contains a catalytic HAT domain that preferentially acetylates lysine 14 of histone 3 and to a lesser extent lysine 8 and lysine 16 of histone H4 (Wang *et al.,* 1998; Kuo *et al.,* 1998; Kuo *et al.,* 1996).

1.2.6 HDAC's and their biological functions

The connection between acetylation and transcription is further augmented by the fact that deacetylation can cause transcriptional repression (Grunstein, 1997; Struhl, 1998). Histone deacetylases from various organisms are shown in table 1.2.

HDAC-family (examples)	Enzymes	Organisms	Proteins associated directly or indirectly with HDAC-complexes
RPD3-like			
	RPD3, HOS1-3	Yeast	
	RPDA, HOSA	*Aspergillus*	Sin3, Rbap, SAP, MAD, MAX, *Nco*R,
	DHDAC1-3	*Drosophila melanogastor*	SMRT, Mi2, MTA2, MBD3, MeCP1,
	HDA1-3	*Caenorhabditis elegans*	MeCP2, Ikaros, UME6, Ski, p53, HPV
	HDm	*Xenopus laevis*	E7, PcG, YY1, LIM, Hunchback,
	HDAC1-3	Chicken, mammals	Groucho, LAZ3, PLZF, BRCA1, HDAC4,
	HDAC7, 8	Chicken, mammals	HDAC5
	RPD3/HD1-B	*Zea mays*	
HDA1-like			
	HDA1	Yeast	
	DHDA2	*D. melanogastor*	HDAC3, MEF2A, *Nco*R, SMRT
	MHDA1, 2	Mouse	
	HDAC4-6	Human	
HD2-like			
	HD2	Plants	Homopolymer of HD2-p39 and phosphorylated forms
SIR2-like			
NAD-dependent			
	SIR2	Yeast	Sir3, Sir4, Net 1
	SIR2-homolog	Mouse	

Table 1.2) HDAC families of various organisms. **HDAC-**histone deacetylase (Lusser *et al.,* 2001).

Rpd3, a yeast co-repressor, was first identified in genetic screenings as a positive and negative regulator for a subset of yeast genes (Vidal and Gaber, 1991). Later on it was discovered that *RPD3* locus encodes the catalytic subunit of histone deacetylase complexes (Kuo and Allis, 1998). The deacetylation-repression connection was most clearly demonstrated by the isolation of a human histone deacetylase, *HDAC1 (HD1),* whose sequence was highly similar to that of yeast *RPD3* (Kornberg and Lorch, 1999). Another histone deacetylase RbAp48, a protein previously found to interact with retinoblastoma (Rb) is also a subunit of chromatin assembly factor *CAF1* (Verreault *et al.,* 1996) and is implicated with chromatin assembly as well. Biochemical fractionation of yeast extracts led to the discovery of two distinct

yeast deacetylation activities, HDA (350 kDa complex) and HDB (600 kDa complex). Protein microsequencing and subsequent sub-cloning demonstrated that the catalytic subunits for these deacetylase complexes were encoded by *HDA1* (HDA complex) and *RPD3* (HDB complex) genes. In yeast deletion of HDA1 or Rpd3 leads to hyperacetylation of histones H3 and H4 (Rundlett *et al.,* 1996).

All of the known deacetylases occur in multiprotein complexes. The complexes are able to deacetylate histones only in nucleosomes, where as the isolated deacetylase subunits cannot. These deacetylase complexes interact with DNA-binding proteins, to be recruited to specific promoters (Kornberg and Lorch, 1999).

1.2.7 Histone deacetylase inhibitors

The discovery of compounds capable of inhibiting the enzymatic hydrolysis of acetamido groups (deacetylation) has proved instrumental in the study of histone acetylation. No such inhibitors are known for HAT's (Lusser *et al.,* 2001). Inhibitors used are butyrate and microbially derived compounds of diverse chemical composition, such as Trichostatin A (TSA) and Trapoxin (TPX).

Millimolar concentrations of butyric acid inhibit HDAC's. However butyric acid also causes additional effects on cellular activities *in vivo* that are not directly linked to histone hyperacetylation (Yoshida *et al.,* 1995). On the other hand, highly potent and specific small molecule HDAC inhibitors like TPX and TSA, provide useful tools for studying effects of acetylation while avoiding unwanted side effects.

TPX is an irreversible inhibitor belonging to a family of histone deacetylase inhibitors whose conserved structural motif consists of a 12-atom cyclic tetrapeptide backbone that mimics the acetyl lysine and may bind in the vicinity of the enzyme's active site (figure 1.7). The *Streptomyces* metabolite TSA is a nonpeptidic HDAC inhibitor that lacks structural similarity to the TPX family, but has a lysine side chain mimic with a terminal hydroxamic acid, which is a likely ligand for the presumptive metal in the HDAC enzyme active site (Hassig and Schreiber, 1997).

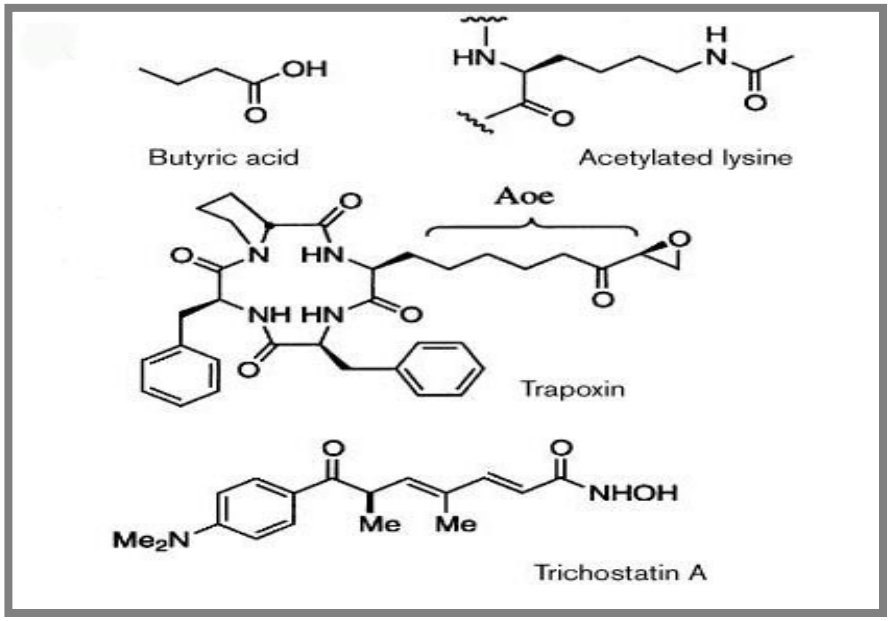

Figure 1.7) Chemical structures of some HDAC inhibitors. (a) Butyric acid, TPX and TSA inhibit HDAC's at low concentrations *in vivo* and *in vitro*. The structure of the epoxydecanoic acid (Aoe) side chain of Trapoxin approximates acetyl lysine and may bind in the vicinity of the enzyme's active site. Biochemical experiments suggest that TSA and TPX bind the same inhibitory site of HDAC1 (Taunton *et al.,* 1996). Hydrolysis or reduction of the epoxide results in complete loss of biological activity, suggesting that Trapoxin may form a covalent adduct with an HDAC active site residue (Hassig and Schreiber, 1997).

1.3 Histone acetylation in plants

Both histone acetylation and deacetylation occur in plants, and it is likely that these processes regulate similar functions to those identified in other eukaryotes. The most extensively acetylated histone in plants is H3, in contrast to the situation in non-plant eukaryotes where H4 is most highly acetylated (Waterborg, 1990). A further difference is that in plants, H4 is acetylated (mono- to penta-acetylated forms) at five lysine residues (Lys 5, 8, 12, 16 and 20). Lysine 20 in animals and yeast is not acetylated but is methylated instead, and is therefore unavailable for acetylation (Lusser *et al.,* 2001). Monocotyledonous maize (*Z. mays* L.) has been employed as a plant model for detailed biochemical, enzymatic and molecular characterisation of different HAT and HDAC types, their substrate specificities and developmental regulation (Graessle *et al.,* 2001). In germinating seedlings of maize three HAT and four distinct HDAC activities have been detected by chromatographic fractionation of cellular extracts (Loidl, 1994; Lechner *et al.,* 1996).

Fractionation of cellular extracts from germinated embryos yielded 3 distinct HAT activities (Lechner *et al.,* 1996), HAT-A1, HAT-A2, and HAT-B. Maize HAT-B was shown to acetylate newly synthesised H4 at lysine 5 and 12, before chromatin assembly (Kölle *et al.,* 1998). HAT-B (similar to Hat1p from yeast), found at least partly in the cytoplasm is thought to be important for the transport of newly synthesised H4 into the nucleus and also for its correct assembly into the nucleosomes (Lusser *et al.,* 1999). However deletion of the Hat1 gene from yeast does not reveal any mutant phenotype. Recently it has been shown that the histones need not be acetylated to interact with chromatin assembly factor CAF-1 or to be deposited onto chromatin (Verreault, 2000). Since H4 and H3 N-termini in yeast are functionally redundant, it was suggested that the acetylation of H3 N-termini by another, unidentified enzyme could complement the lack in H4 acetylation (Graessle *et al.,* 2001).

In plants, genes involved in the process of histone deacetylation have been cloned and analysed for their activity (Rossi *et al.,* 1998; Wu *et al.,* 2000 a and b; Tian and Chen, 2001). HDAC's have been categorized into three classes (table 1.2; Davie and Chadee, 1998). Classes 1 and 2 contain enzymes that are homologous to the yeast proteins Rpd3 and Hda1, respectively. Proteins related to maize HD2 belong to class 3. Recently, the yeast-silencing information protein Sir2 (silent information regulator 2) has been shown to be an NAD-dependent (Nicotineamide adenine dinucleotide) HDAC (Guarente, 2000), thus defining a fourth class. Three biochemically distinct HDAC activities have been identified in pea and four in maize (HD1A, HD1BI, HD1BII and HD2; Loidl, 1996; Lechner *et al.,* 2000). Maize HD1BI (ZmRpd3) and HD1BII are class 1 HDAC (Lusser *et al.,* 2001). Several EST clones from *Z. mays*, *A. thaliana* and other plant species are also available that are homologous to the HDA-1 family, although none of them has been studied in detail (Lusser *et al.,* 2001).

HD2-like HDAC's (Wu *et al.,* 2000) form multigene families of highly similar members within the plant kingdom (Lusser *et al.,* 2001) but no closely related proteins have been identified so far in animals or fungi. The nucleolar location of HD2 in maize cells suggests a possible role in the regulation of

rRNA genes (Lusser *et al.,* 1997). Targeting a deacetylase, AtHD2A, to a reporter gene *in vivo*, caused its repression (Wu *et al.,* 2000a).

The phenomenon of histone acetylation in plants has been mainly addressed via biochemical studies of purified complexes and the analysis of histone acetylation patterns on isolated chromatin components, although transcriptional adapter proteins have been characterized recently in *A. thaliana* (Stockinger *et al.,* 2001), and several HAT sequence types (GCN5, MYST, ESA, HAT-B) are present in plant genome databases (Lusser *et al.,* 2001).

The isolation of the putative transcriptional co-activators (*GCN5* and *ADA2*) from maize has been previously reported (Becker *et al.,* 1999). The *GCN5* homologous sequence from maize (*ZmGCN5;* GenBank Acc.: AJ428540) was isolated by two hybrid screening using an RT-PCR *At*Ada2 as a bait. The isolated cDNA contained an open reading frame of 1545 bases, predicting a polypeptide of 515 amino acids. Further analysis showed that *ZmGCN5* is a single copy gene and is constitutively expressed in dividing cells. *In vitro* acetylation assays showed that the isolated protein could acetylate the core histones (H2A, H2B, H3 and H4) but not nucleosomes *in vitro* (Marcus Riehl, Diplomarbeit, Universität Giessen, 1999).

Database searches identified a barley EST (clone BCD450, GenBank Acc.: AA231679) homologous to *At*Ada2. Primers were designed based on this sequence, and a 226bp fragment amplified by genomic PCR was used to screen a barley cDNA library. A cDNA clone ca. 1kb in length was used in turn to screen an amplified maize silk cDNA library. The screen yielded 2 positive clones, of which one possessed an open reading frame of 1695 bp predicting a polypeptide of 565 amino acids. The ZmAda2 cDNA (GenBank Acc.: AJ430205) clone was sequenced, and showed homology to the published Ada2 genes from *A. thaliana* (Heinz-Albert Becker, personal communication). Ada2 is a small multigene family in maize and is expressed in all tissues and at all stages of development examined. GST spin-down experiments showed that ZmGcn5 could interact with ZmAda2 *in vitro* (Marcus Riehl, Doktorarbeit, Universität Köln, 2002). Both ZmGcn5 and ZmAda2 proteins were over-expressed in *E. coli* and antibodies were raised against them.

1.4 Role of transcriptional activators with acidic activation domains

The eukaryotic transcription initiation machinery, consisting of RNA polymerase II and at least 50 other additional components is recruited to the promoters of target genes by activators (Holstege *et al.,* 1998). Specific activator proteins bind at one or more locations upstream (known as enhancer or upstream activation sequences or UASs) of the TATA sequence, the site where TATA box binding protein (TBP) nucleates the assembly of basic transcription factors and RNA polymerase II (Drysdale *et al.,* 1995; Banerji *et al.,* 1981; Guarente *et al.,* 1982). These transcriptional activator proteins contain two functional domains, one that dictates the DNA binding and a second that activates transcription (Brent and Ptashne, 1985). The activation domains interact with other factors including TFIID or TFIIB (TF–transcription factor) and facilitate the binding of RNA polymerase II at the start site of mRNA synthesis (Schmitz *et al.,* 1997). The activation domains of several yeast activators are characterised by a high content of acidic amino acids (Hope and Struhl, 1986; Ma and Ptashne, 1987 a, b) while activation domains from metazoans consist of many classes, including acidic, glutamine-rich and proline-rich types. Acidic activators such as yeast GAL4 (Ma and Ptashne, 1987 a, b) and Gcn4 (Hope and Struhl, 1986) activate transcription in many eukaryotic organisms. Metazoan acidic activators work in yeast, while non-acidic activators such as the glutamine-rich activator Sp1 (Courey and Tijan, 1988) appear not to function. Thus the mechanism by which acidic activation domains function seems to be conserved (Berger *et al.,* 1992).

Activators can directly interact with one of the basic transcription factors (Geisberg *et al.,* 1994; Ingles *et al.,* 1991; Lin *et al.,* 1991) however there are indications that activators interact with basic factors through mediators or co-activators (Drysdale *et al.,* 1995). Transcriptional activator Gcn4 is one of the activators that have been shown to interact with Ada2 of the Ada2-Gcn5 coactivator complex. Gcn4 is a transcriptional activator of genes encoding amino acid biosynthesis enzymes in *Saccharomyces cerevisiae* L.. Gcn4 is a member of the bZIP (basic/leucine zipper) family of transcriptional activators that binds to DNA as a homodimer (Landshulz *et al.,*

1988; Hope and Struhl, 1987). The activator domain of Gcn4 resides in the stretch of acidic amino acids located roughly in the centre of the protein while the N-terminal region serves as a sequence-specific DNA binding domain (Hope and Struhl, 1986; Hope *et al.,* 1988). Furthermore the activation domain of Gcn4 can also interact with TBP (Melcher and Johnston, 1995). There are also indications that activation by Gcn4 is mediated by the RNA Pol II holoenzyme (Kim *et al.,* 1994) and by TFIID (Klebanow *et al.,* 1996). These findings suggest that Gcn4 may interact with multiple GTFs (General transcription factors) and co-activator proteins in order to stimulate transcription. A model summarising the role of Gcn4 is shown in figure 1.8.

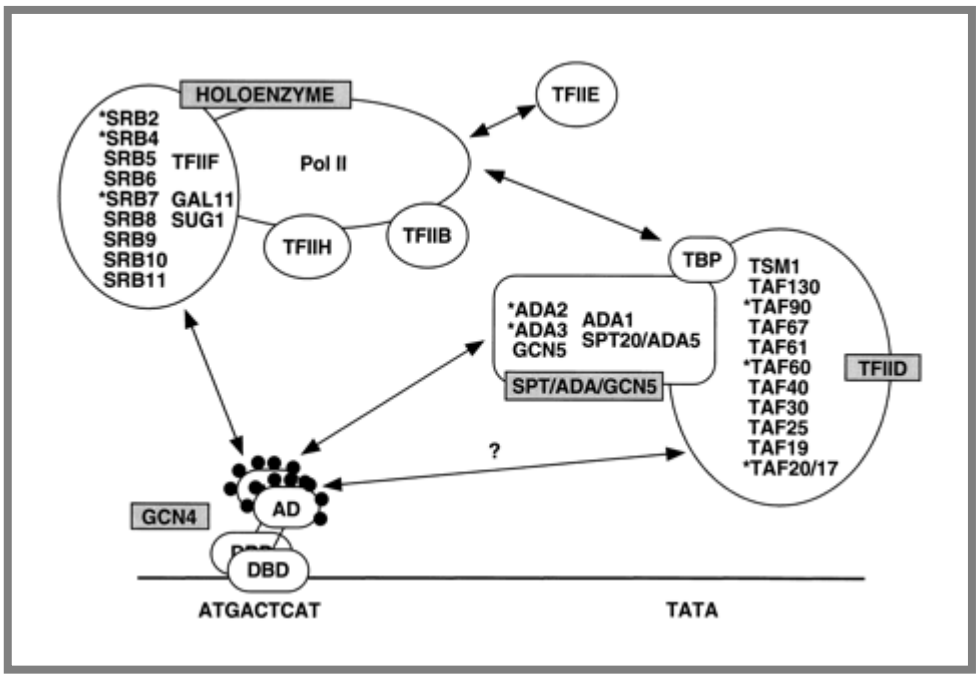

Figure 1.8) Model summarizing the *in vitro* interactions between the Gcn4 activation domain and RNA polymerase II holoenzyme, TFIID and Gcn5-Ada2 coactivator complex. A dimer of Gcn4 is depicted to bind to a Gcn4 binding site located upstream from the TATA element in a Gcn4-regulated promoter. The activation domain (AD) of Gcn4 is shown interacting independently with the mediator complex of RNA Pol II holoenzyme (containing *SRB*-encoded proteins, TFIIF, Gal11p, and Sug1p) and the Spt-Ada-Gcn5 complex (Drysdale 1998). DBD - DNA-binding domain.

A number of transcriptional activators have been identified from plants. Among these maize Opaque-2 (*ZmO2*), a member of the bZIP transcription factor family, is expressed during late endosperm development (Gallusci *et al.,* 1994). *ZmO2*, located on the chromosome 7 was cloned by transposon tagging (Schmidt *et al.,* 1987; Motto *et al.,* 1989) and is involved in

the regulation of seed storage protein synthesis, modulating the transcription of 22 kDa zein genes and of the b-32 albumin (Kodrzycki *et al.,* 1989; Schmidt *et al.,* 1990; Lohmer *et al.,* 1991). The 22-kDa zeins are most abundant endosperm storage proteins in maize. The function of b-32 albumin in endosperm development is not clear but the protein shares homology with type I ribosome inactivating proteins (Maddaloni *et al.,* 1991). A number of distinct functional domains have been identified on the O2 protein. These include a basic region followed by a leucine zipper, responsible for DNA-binding and dimerization (Hartings *et al.,* 1989; Aukerman *et al.,* 1991) and an N-terminally located acidic activation domain responsible for transcriptional activation (Schmitz *et al.,* 1997).

ZmO2 shows many similarities to yeast Gcn4. Both possess bZip DNA-binding-domains, have acidic activation-domains and also share similar DNA target sequences (Vinson *et al.,* 1989; Ziff 1990; Katagiri and Chua, 1992; Lohmer *et al.,* 1991). Homology between the basic regions of ZmO2 shows 50% similarity and 40% identity to Gcn4 at the amino acid level (Hartings *et al.,* 1989). Furthermore, *ZmO2* partially complements the *GCN4* mutation in yeast (Mauri *et al.,* 1993). Such a high degree of conservation between ZmO2 and Gcn4 suggests that these bZip proteins might be functionally equivalent and raises the possibility that ZmO2 might also recruit the Gcn5-mediated co-activator complexes via an interaction with ZmAda2.

Aim of the project

At the commencement of this project, two maize genes encoding putative transcriptional co-activator proteins *viz.* ZmGcn5 histone acetyltransferase and the adaptor ZmAda2 had been isolated in the Thomson laboratory at Max Planck Institute, Köln (Becker *et al.,* 1999). Evidence from other eukaryotes shows that Gcn5 is a histone acetyltransferase, which modifies the N-terminal tails of the lysine residues of the histones in nucleosomes (Brownell *et al.,* 1996). This reduces the strength of histone-DNA interaction and the DNA becomes accessible to transcription machinery resulting in increased levels of transcription of specific gene products (Wang *et al.,* 1998; Kuo *et al.,* 1998). Ada2 is an adaptor protein (Berger *et al.,* 1992), which interacts with Gcn5 (Candau and Berger *et al.,* 1996). Ada2 can also directly interact with transcriptional activators to evoke transcription of specific genes (Silverman *et al.,* 1994; Barlev *et al.,* 1995). Both these proteins are present inside the cell in multi-protein complexes. Two such complexes have been characterised in yeast *viz.* the Ada and SAGA complexes (Grant *et al.,* 1997; Pollard and Peterson, 1997). These complexes show intrinsic HAT activity due to Gcn5. Gcn5 interacts with the rest of these complexes through Ada2 (Candau and Berger *et al.,* 1996). Most of this information has been accumulated by research on *S. cerevisiae* or mammalian systems (discussed in the introduction). Little is known about organisation and mechanism of action of these proteins in plants. Experiments performed in the Thompson lab at MPIZ showed that ZmGcn5 can acetylate free histones (at lysine positions 5, 8, 12 and 16) and can also interact with ZmAda2 *in vitro* (Marcus Riehl, Diplomarbeit, 1999, Doktorarbeit, 2002). The purpose of this research was to functionally characterise these genes and to add to the basic knowledge and understanding of transcriptional activation in plants. Specifically the objectives of the study were to:

1. Understand and characterise the Gcn5-Ada2 complexes in plants and
2. Establish the role of histone acetylation and deacetylation in regulating plant gene expression.

Materials and Methods

2.1 Materials

2.1.1 Antibiotics

Name	Stock	Final concentration	Organism
Ampicillin	Water	100 µg/ml	*Escherichia coli* L.
Carbenicillin	Water	100 µg/ml	*Agrobacterium tumefaciens* L.
Claforan	Water	250 µg/ml	*A. tumefaciens* L.
Kanamycin	Water	25 µg or 100 µg/ml	*E. coli* L. */A. tumefaciens* L.
Phosphinothricin	Water	200 µg/ml	*Z. mays* L.
Rifampicin	Methanol	100 µg/ml	*A. tumefaciens* L.
Tetracycline	Ethanol	100 µg/ml	*A. tumefaciens* L.

2.1.2 Plant materials

Zea mays L. cv. A69Y

Zea mays L. cv. B37

Zea mays L. cv. HE-89 Cell line

Nicotiana tabacum L. cv. BY2 (suspension cell line)

Nicotiana tabacum L. cv. SR1 (greenhouse cultivar)

Vigna unguiculata L. (Cowpea)

2.1.3 Bacterial Strains, cloning vectors and oligonucleotides

2.1.3.1 *E. coli* strains

- **DH10B:** F^-, mcrAΔ(mrr-hsdRMS-mcrBC)Φ80dlacX74, deoR, recA1, endA1, araD139, Δ(ara,leu)7607, galU, galK, λ $^-$rspl, nupG (GIBCO BRL)
- **XL1 Blue MRF´:** Δ*(mcrA)*183, Δ(*mcr*CB-*hsd*SMR-*mrr)173* endA1 *supE44 thi1 recA1 gyrA69 relA1 lac[*F*' proAB* $lac^qZ\Delta M15$Tn*10*(Tet^r)]

2.1.3.2 *Agrobacterium tumefaciens* strain

- **LBA-4404:** Sm^r, (Rif^r) (Hoekma, *et al.,* 1983)

2.1.3.3 Cloning vectors

Vector	Origin
pBluescript® SK(+/-)	Stratagene (Alting-Mees *et al.,* 1992)
pBin19	Clontech (Bevan, M., 1984)
pRTO2	Schmitz *et al.,* 1997
pRT 100- pRT 107	Töpfer *et al.,* 1988
pGFP-JS	Sheen *et al.,* 1995
pMON999 CFP/YFP	Shah *et al.,* 2001
pGEMTEasy	Promega, (Robles, 1994)
pAHC25	Christiansen and Quail, 1996

2.1.3.4 Oligonucleotides used for cloning and PCR analysis

The oligonucleotides used in the current study are listed below and were purchased from Life Technologies, Gibco BRL or MWG Biotech.

Primer name	Primer sequence 5'→3'
Gcn5PromterFwd:	GCCACCATGGAAATATTTTTGGGT
Gcn5PromterRev:	GCCGTCCATGGGGGGAAAGAGGGGA
***Nco*1Gcn5Fwd:**	TCCCCTCTTTCCCCCCATGGACGGCCT
***Nco*1Gcn5Rev:**	GCGCCCATGGTTGAGAGTTGTGCAAG
Gcn5NtermRev:	CATACCATGGGTTCATCAACGCCGTCA
Gcn5HatFwd:	GAACCCATGGTATGGTTGGTA
Gcn5Ada2IntFwd:	GCGCCCATGGAGTGTAAAATTGACCCA
Gcn5Ada2IntRev:	GCCCATGGGTTGCCTGTAAGTATTATAGT
***Apa*IN$_{ub}$Fwd:**	GCGGGCCCATGCAGATTTTCGTCAAGACT
***Sac*IN$_{ub}$Rev:**	GCGAGCTCTAGCGTCGACCCCGGGCTCGA
***Bgl*IIAda2Fwd:**	GCAGATCTCATGGGGCGGTCGCGAGGGGT
***Sal*IAda2Rev:**	GCGTCGACCGTAGGCAACTCCACATGGTT
***Eco*RIGcn5Fwd:**	GCGAATTCATGGACGGCCTCGTGGCGCCGT
AgeIGcn5Rev:	GCACCGGTGCTCTTGGTTGAGAGTTGTGCA
***Nco*IAda2Fwd:**	GCCATGGGGCGGTCGCGAGGGGTGCAGAA
***Nco*IAda2Rev:**	GCCCATGGCCGTAGGCAACTCCACAT
***Cla*IO2Fwd:**	GCATCGATATGGAGCACGTCATCTCAATG
***Xba*IO2Rev:**	GCTCTAGAATACATGTCCATGTGTATGGC
35SFwd	GATACAGTCTCAGAAGACCAGAGGGCTA
Gcn5As	TGGCAAGGGTACATTAAAGATTATGAC
PextGcn5:	CCGTCCATGCGGGGAAAGAGGGGAAG
Universal	GTA AAA CGA CGG CCA GT
Reverse	CAG GAA ACA GCT ATG AC

2.1.4 Chemicals

Laboratory grade chemicals and reagents were purchased from Roth (Karlsruhe), Serva (Heidelberg), Boehringer (Mannheim), Merck (Darmstadt), Beckman (München), GIBCO BRL (Neu Isenburg) and Sigma (Deisenhofen) unless otherwise stated. Filter paper was obtained from Whatman. Radioactive nucleotides were obtained from Amersham Buchler (Braunschweig). Tissue culture chemicals were obtained from Sigma, Merck, Duchefa and Roche unless otherwise stated.

2.1.5 Photographic material

Kodak X-omat film was used for autoradiography in conjunction with exposure cassettes fitted with high speed Trimax intensifying screens. For the detection of rare messages PhosphorImager system from Molecular Dynamics was used. Mitsubishi film (Mitsubishi Electric Corporation, Japan) was used to photograph ethidium bromide stained gels using Bio-Rad Gel-doc electrophoresis photosystem.

2.1.6 Enzymes

2.1.6.1 Restriction enzymes

Restriction enzymes were purchased from Boehringer (Mannheim), GIBCO BRL, Pharmacia Biotech (Braunschweig), New England Biolabs (Schwalbach) and Stratagene (Heidelberg) unless otherwise stated. 10 x buffers for restriction enzymes were those supplied by manufacturers.

2.1.6.2 Nucleic acid modifying enzymes

Standard PCR reactions were performed using homemade *Taq* DNA polymerase while for the cloning of the PCR products, cloned *pfu* or platinum *pfx* polymerases (Gibco BRL) were used. Following modifying enzymes were purchased from Gibco BRL and Roche Ltd, except otherwise stated:

- T4 DNA ligase
- T4 Polynucleotide kinase
- DNase I, from bovine pancrease
- RNase I, from bovine pancrease

- Shrimp alkaline phosphatase
- Taq DNA polymerase
- Platinum pfx polymerase
- Cloned pfu polymerase
- Lysozyme
- Superscript II RT

2.1.7 Proteases and Protease inhibitors

Proteinase K	Merck
Protease inhibitor cocktail	Sigma

2.1.8 Media

Unless otherwise stated all the media were sterilised by autoclaving at 121°C for 20 minutes. Heat labile solutions were sterilised using Steritop filter sterilisation units from Millipore prior to addition of autoclaved components. For the addition of antibiotics the solutions were cooled down to 50°C.

- **BY2 culture medium:** MS plant salt mixture (as per supplier's instruction), 3% sucrose, 200 mg/l KH_2PO_4, 1 mg/l Thiamine HCl, 0.2 mg/l 2,4-dichlorophenoxyacetic acid (2,4-D), 100 mg/l *myo*-inositol.
- **Lauria Bertani (LB) broth:** 1% tryptone peptone, 0.5% yeast extract, 1% NaCl. For the preparation of solid media 1.5-2% agar was added to the above broth.
- **N6 maize culture medium:** N6M medium is a version of N6 (Chu *et al.,* 1975) medium where the microelements are substituted for MS microelements. The aqueous N6M medium was used for suspension culture while the solidified N6M medium for the maintenance of callus.
- **Protoplast culture medium (K3/0.4 M sucrose):** Macro-salt stock solution 10 ml, micro-salt stock solution 1 ml, MS vitamins 1 ml, Fe/EDTA 5 ml, *myo*-inositol 100 mg, Xylose 250 mg, Sucrose (0.4 M) 136.92 g, NAA 1 mg, Kinetin 0.2 mg. (For stock solutions see section 2.1.9.1).
- **YEB broth:** 0.5% (w/v) beef extract, 0.1% (w/v) yeast extract, 0.5% (w/v) peptone, 0.5% (w/v) sucrose, 2 mM $MgSO_4$ pH 7.4.

2.1.9 Buffers and Solutions

2.1.9.1 General buffers and solutions:

- **30% Acrylamide:** 29.2% (w/v) acrylamide, 0.8% (w/v) N-N'–methylene bisacrylamide in deionised water.
- **Denhardt's solution (100x):** 2% (w/v) BSA, 2% (w/v) Ficoll, 2% (w/v) PVPP360.
- **DEPC water 0,1% (w/v):** DEPC in deionised water shaking over night at 25°C followed by autoclaving.
- **Ethidium bromide stock:** 5 mg/ml ethidium bromide in sterile deionised water. Stored at 4°C.
- **K3 Fe/EDTA (1 L) (x200):** 5.57 g $FeSO_4$.$7H_2O$, 7.45 g Na_2EDTA. The two components are dissolved separately by heating, then they are mixed and boiled for 10 minutes.
- **K3 Macro-salt stock solution (200 ml) (x100):** 3g $FeSO_4$, 18 g $CaCl_2.2H_2O$, 50 g KNO_3, 2.7 g $(NH_4)_2SO_4$, 5 g $MgSO_4.7H_2O$.
- **K3 Micro-salt stock solution (1 L) (x1000):** 6.2 g H_3BO_3, 22.3 g $MnSO_4.4H_2O$, 10.6 g $ZnSO_4.7H_2O$, 0.83 g KI, 0.25 g $Na_2MoO_4.2H_2O$, and 0.025 g $CuSO_4.5H_2O$.
- **K3 Vitamin-solution (200 ml) (x1000):** 400 mg Glycine, 400 mg Nicotinic acid, 900 mg Pyridoxine HCl, and 20 mg Thiamine HCl.
- **Magnesium mannitol solution (MaMg):** 0.2% MES, 0.5 M Mannitol, 0.015 M $MgCl_2.6H_2O$. Solution is brought to pH 5.7 with KOH and filter sterilized or autoclaved.
- **PEG solution:** 25% PEG 1500 or 40% PEG 4000, 0.1 M $MgCl_2.6H_2O$, 0.45 M mannitol, 0.02 M HEPES pH 6.0 with KOH.
- **20 x SSC:** 3M NaCl, 300 mM sodium citrate.
- **20 x SSPE:** 200 mM disodium hydrogen phosphate, 20 mM sodium di-hydrogen phosphate, 3.6 M NaCl, 20 mM EDTA pH8.
- **TAE buffer:** 400 mM Tris-HCl, 200 mM NaOAc, 18 mM EDTA pH 7,8 with glacial acetic acid.
- **W-5 solution:** 0.154 M NaCl, 0.125 M $CaCl_2.2H_2O$, 0.005 M KCl and 0.005 M Glucose. Solution is brought to pH 5.7 with KOH and filter sterilized.

- **SM phage dilution buffer:** 50 mM Tris-HCl pH 8.0, 10 mM NaCl, 8 mM $MgSO_4.7H_2O$, 0.01% (w/v) gelatine.

2.1.9.2 DNA buffers

- **DNA extraction buffer:** 100 mM Tris-HCl pH 8,5, 100 mM NaCl, 50 mM EDTA pH 8, 2% SDS and 0.1 mg/ml proteinase K (added at the time of use).
- **DNA loading buffer (10x):** 30% (v/v) glycerol, 1 x TAE, 0.025% (w/v) bromophenol blue, 0.025% (w/v) xylene-glycol. Stored at 4°C.

2.1.9.3 Hybridisation buffers:

- **Microarray (cDNA) hybridisation buffer:** 0.5 M Na-Phosphate pH 7.2, 7% SDS, 1 mM EDTA pH 8.0, and 100 µg/ml salmon sperm DNA at 65°C.
- **Northern hybridisation buffer:** 5 x SSPE, 50% deionised formamide, 5 x denhardt solution, 0.5% SDS, 200 µg/ml denatured salmon sperm DNA at 42°C.
- **Southern hybridisation buffer:** 5 x SSC, 0.5% SDS, 5 x denhardt´s and 50 µg/ml denatured salmon sperm DNA at 65°C.
- **Stripping buffer for cDNA arrays:** Boiling solution of 5 mM Na-phosphate pH 7.2, 0.1% SDS followed by rising in 2 x SSC.
- **Stripping buffer for Northern/Southern blots:** Boiling solution of 0.1% (w/v) SDS or 0.2 M NaOH at 42°C followed by rising in 2 x SSC.

2.1.9.4 Protein buffers:

- **Histone (crude) extraction buffer:** 0.4 M sucrose, 10 mM Tris-HCl pH 8.0, 0.10 mM $MgCl_2$, 5 mM β-mercaptoethanol and protease inhibitor cocktail.
- **Laemmli buffer (4x):** 0.25 M Tris-HCl pH 8.2, 0.4% (w/v) SDS, 767 mM Glycine, and protease inhibitor cocktail.
- **Nuclei extraction buffer:** 0.5 M sucrose, 5 mM EDTA, 5 mM DTT, 30 mM Tris brought to pH 7.7 with 0.5 M MES and protease inhibitor cocktail.

- **Pellet buffer:** 1.7 M sucrose, 10 mM Tris-HCl pH 8.0, 0.15% Triton X-100, 2 mM $MgCl_2$, 5 mM β-mercaptoethanol and protease inhibitor cocktail.
- **Protein blocking solution:** 500 mM NaCl, 20 mM Tris-HCl pH 7.5, 0.05% Tween 20, and 5% non-fat milk powder.
- **Protein blotting buffer:** 25 mM Tris-HCl pH 8,3, 192 mM Glycine, and 20% methanol.
- **Roti load protein sample buffer (4x):** Roti-load buffer concentrate, (Roth) was used for loading protein samples onto SDS-PAGE gels.
- **Stripping buffer for protein blots:** 100 mM β-mercaptoethanol, 2% SDS, and 62.5 mM Tris-HCl pH 6.7.
- **T-TBS (1x)**: 500 mM NaCl, 20 mM Tris-HCl pH 7,5, 0,05% Tween-20.

2.1.9.5 RNA buffers:

- **Extraction buffers**
  - **Buffer I:** 0.1 M NaCl, 0.05 M Tris-HCl pH 9, 0.01 M EDTA, 2% SDS and 0.2 mg/ml proteinase K (added at the time of use).
  - **Buffer II:** 0.4 M NaCl, 0.01 Tris-HCl pH 7.5, 0.2% SDS.
  - **Buffer III:** 0.1 M NaCl, 0.02 M Tris-HCl pH 7.5, 0.01% SDS.
  - **Buffer IV:** 0.01 M Tris-HCl pH 7.5.

For extraction of total RNA: 0.2 M Tris-HCl pH 7.5, 0.1 M LiCl, 5 mM EDTA, 1% SDS. All buffers are prepared in 0.1% DEPC water.

- **Formaldehyde gel-running buffer (5xMOPS):** 0.1 M MOPS pH 7.0, 40 mM NaOAc, 5 mM EDTA pH 8.0, DEPC to a final volume of 0.1%. Left overnight shaking at 25°C and then sterilised by filtration through a 0.2 µ Millipore filter. Stored at room temperature protected from light.
- **Formaldehyde gel-loading buffer:** 50% glycerol, 1 mM EDTA (pH 8.0), and 0.025% bromophenol blue.
- **RNA incubation buffer:** 1 x MOPS, 1.75% formaldehyde, 0.5% deionised formamide. Made up in DEPC water at the time of use.

2.2 Methods

2.2.1 Nucleic acid manipulations

All nucleic acid manipulations *viz.* restriction digestion of DNA, dephosphorylation of plasmid vectors and ligation of DNA molecules etc were performed as per standard laboratory methods (Maniatis *et al.,* 1989).

2.2.1.1 Polymerase chain reaction (PCR) amplification

For plasmid or genomic PCR, 10-50 ng of DNA was used while for RT-PCR the amount of DNA template depended on the transcript abundance and varied between 20 and 100 ng. The reaction was done in 50 µl final volume with following components (Innis *et al.,* 1990)

20-50 ng of Template DNA (genomic or plasmid)
1x PCR amplification buffer without Mg
0.2 mM each dNTP mix (dATP, dGTP, dCTP, dTTP)
1.5 mM $MgCl_2$
0.5 µM of each primer
2.5 U homemade *Taq* DNA polymerase.

The amplification was carried out in a Biometra® Thermal Reactor using the below given parameters:

1	Initial denaturation	3 minutes at 95°C
2	Denaturation	1 minute at 94°C
3	Annealing	1 minutes at 58-60°C
4	Extension	1 minutes at 72°C

The steps 2 to 4 were cycled 30-35 times, followed by a final extension of 10 minutes to ensure the completion of the reactions. For direct PCR on bacterial colonies the initial denaturation was increased to 5 minutes.

2.2.1.2 Cloning PCR products

The PCR products were cloned into Promega pGEM®-T Easy Vector system. The system utilises the tendency of *Taq* DNA polymerase to generate fragments with a 5' A nucleotide overhangs. PCR products ran on the gel

were purified using High PCR purification kit (Boehringer Mannheim) and ligated into the pGEM®-T Easy vector as per standard laboratory protocols.

2.2.1.3 Primer extension (Current protocols in molecular biology)

50 µg of total maize RNA was used as a template for primer extension. 100 ng of primer (PextGcn5, see section 2.1.3.4) was labelled with γP^{32}-ATP by incubation for 1 hour at 37°C with 10 U T4 polynucleotide kinase. The reaction was carried out in 10 µl volume with following components:

1 µl 100 ng/µl Oligonucleotide primer
1 µl 10x T4 Polynucleotide kinase buffer
1 µl 1 mM Spermidine
1 µl 100 mM DDT
3 µl 10 µCi/µl γ^{-32}P-ATP
10 U T4 Polynucleotide kinase
H_2O to 10 µl final volume

After labelling the reaction was stopped by adding 2 µl of 0.5 M EDTA and 50 µl TE buffer and incubating at 65°C for 5 minutes. The labelled primer was purified using an oligonucleotide purification kit from Gibco BRL and resuspended in 100 µl H_2O. The purified radiolabeled oligonucleotide was then hybridised to the maize total RNA at 65°C for 90 minutes. The reaction was carried out in 15 µl volume with following components:

10 µl total maize RNA (50 µg)
1.5 µl 10x Hybridisation buffer (1.5 M KCl, 0.1 M Tris-Cl, pH 8.3, 10 mM EDTA)
3.5 µl radiolabeled oligonucleotide (from the step described above)

The primer extension reaction was carried on the hybridised RNA-primer mixture at 45°C for 1 hour using 200 U of Superscript II reverse transcriptase (Gibco BRL). The reaction was carried out in a final volume of 45 µl total volume with following components:

15 µl RNA/primer in hybridisation buffer
0.9 µl 1 M Tris-HCl, pH 8.3
0.9 µl 0.5 M $MgCl_2$
0.25 µl 1 M DTT
6.75 µl 1 mg/ml actinomycin D
1.33 µl 5 mM dNTP mix
200 U Superscript II RT
H_2O to 45 µl final volume

The reaction was stopped by adding 105 µl RNase reaction mix (100 µg/ml salmon sperm DNA; 20 µg/ml RNase A) and incubating at 37°C for 15 minutes. Following phenol/chloroform extraction the product was analysed on a 9% acrylamide/7 M urea gel. The same primer (PextGcn5) was used for a sequencing reaction on the genomic template of *ZmGCN5* using T7 sequencing kit (Amersham Pharmacia) according to manufacturer's protocol. The sequencing reaction was used as a size marker for the primer extension product. After the run, the gel was dried and subjected to PhosphorImager analysis.

2.2.2 Transformation of *E. coli*

2.2.2.1 Preparation of electro-competent *E. coli* cells

10 ml of an overnight culture of *E. coli* strain (XL1 Blue or DH10B, see section 2.1.3.1) was added to 1 litre of LB broth and shaken at 37°C until the bacterial growth reached an OD_{600} = 0.5-0.6. The bacteria were pelleted at 3000 x g for 10 minutes at 4°C and the pellet gently resuspended in ice-cold sterile water. The cells were pelleted as before and again resuspended in ice-cold water. The process was repeated twice. Finally the cells were gently resuspended in a 1/100 volume of the initial culture in 10% sterile glycerol, pelleted once more and then resuspended in 5 ml 10% glycerol. 50 µl aliquots of cells were frozen in liquid nitrogen and stored at –70 till use.

2.2.2.2 Transformation of electro-competent *E. coli* cells

20 to 50 ng of salt-free ligated plasmid DNA was mixed with 50 µl of electro-competent cells, and transferred to the 0.2 cm cold BioRad electroporation cuvette. The BioRad gene pulse apparatus was set to 25 µF

capacitance, 1.6 kV voltage and the pulse controller to 200 ohms. The cells were pulsed once at the above settings for 5 seconds and 500 µl of LB broth was immediately added to the cuvette and the cells were quickly resuspended and incubated at 37°C for I hour. A fraction of the transformation mixture was plated out onto selection media plates.

2.2.3 DNA analysis

2.2.3.1 Plasmid DNA isolation

Plasmid DNA was isolated by alkaline lysis method of Birnboim and Doly (1979). High quality DNA for sequencing or plant transformation was isolated using Qiagen Mini-, Midi- or Maxi-prep kit (Qiagen Plasmid Purification Handbook, September 2000)

2.2.3.2 Isolation of maize DNA for PCR screening

Maize DNA for PCR screening was isolated by following the protocol of Edwards *et al.* (1991).

2.2.3.3 Southern blotting (Maniatis *et al.,* 1989)

10 µg of genomic DNA or 1 µg of Plasmid DNA, digested to completion with appropriate restriction enzymes, was electrophoretically separated on 1% agarose gels in TAE buffer. The gels were treated with 0.125 N HCl solution to depurinate the DNA, followed by denaturation for 30 minutes in 0.5 M NaOH and 1.5 M NaCl. The DNA was neutralised by washing the gels in 0.5 M Tris-HCl pH 7.5, 1.5 M NaCl for 30 minutes. The denatured/neutralised DNA was then transferred and bound to a Hybond N membrane (Amersham) following the standard capillary transfer procedure (Maniatis *et al.,* 1989). Filters were UV cross-linked (120000 µJoules cm^{-2} for 30 s, using Stratagene UV cross linker), prehybridised (2 hours) and hybridised (overnight) in southern hybridisation buffer (section 2.1.9.3) at 65°C. Following hybridisation with appropriate probes, the filters were washed twice in 2x SSC, 0.1% SDS for 10 minutes and twice in 1x SSC, 0.1% SDS for 10 minutes. After washing the filters were sealed in plastic bags and exposed to autoradiography at -

80°C using Kodak XOMAT film and intensifying screens or subjected to PhosphorImager analysis.

2.2.4 RNA analysis

2.2.4.1 Isolation of total and poly $(A)^+$ RNA from plant tissues

Plant material finely ground in liquid nitrogen was resuspended in the total RNA extraction buffer and incubated at 37°C for 1 hour. Following three phenol/chloroform extractions RNA was precipitated with 1 volume 8 M LiCl prepared in DEPC (Diethylpolycarbonate) water, washed with 70% ethanol and resuspended in DEPC treated water.

Poly $(A)^+$ enriched RNA was isolated according to Bartels and Thompson (1983). Finely ground plant material resuspended in RNA buffer I and incubated at 37°C for 1 hour was extracted with phenol/chloroform three times. Oligo dT cellulose was added to the aqueous phase (0.1 g oligo dT cellulose/10 g of starting plant tissue). Following slow agitation at room temperature for 15 minutes the cellulose was spun down and washed thrice with buffer II and subsequently three times with buffer III till the optical density of the eluate was $A_{260} \leq 0.05$. Poly $(A)^+$ RNA bound to the oligo dT cellulose was eluted at 55°C with 5 ml of pre-warmed buffer IV (for the description of the buffers see section see section 2.1.9.5). RNA was precipitated with 4 M NaCl and 2.5 volumes of absolute ethanol, pelleted at 13000 x g for 30 minutes at 0°C and then washed thrice with 70% ethanol. Pellet was dried and resuspended in DEPC treated water and stored at –70°C.

2.2.4.2 *In vitro* transcription for the production of spiking RNA control for microarrays

2.5 µg of DNA (Nebulin cDNA cloned into pBluescript) was used for *in vitro* transcription. The reaction mix included following components:

1 M DTT
100 mM of A, G, C and U ribonucleotides
10x T7 polymerase buffer
50 U RNase inhibitor
25 U T7 RNA polymerase

The components were mixed in a total reaction volume of 50 µl. The reaction was carried out at 37°C for 1 hour and was stopped by adding 0.5 µl of DNase I. The RNA was aliquoted and stored at -70°C.

2.2.4.3 RNA electrophoresis

In order to avoid RNase contamination an electrophoresis tank was specifically designated for separating RNA samples on denaturing agarose gels. 15 µl of RNA incubation buffer was added to 50 µg of total RNA in a total volume of 20 µl and incubated at 65°C for 15 minutes. Following the incubation, the denatured RNA samples were mixed with 5 µl of formaldehyde gel loading buffer and separated in a I% (w/v) denaturing agarose gel containing 1 x MOPS, 2.2 M formaldehyde and using 0.2% 5 x MOPS, 0.08% formaldehyde as the running buffer.

2.2.4.4 Northern blot analysis (Maniatis *et al.,* 1989)

After electrophoresis, the samples were blotted onto Hybond N nylon membranes (Amersham) following the standard capillary transfer procedure (Maniatis *et al.,* 1989). RNA was fixed to the membrane by UV cross-linking as described in Southern blotting (see section 2.2.3.3). Prehybridisation (2 hours) and hybridisation (overnight) of the filters was done in Northern hybridisation (section 2.1.9.3) buffer at 42°C. Following hybridisation, filters were washed in 2 x SSC, 0.1% SDS, once at 45°C and twice at 65°C and exposed to autoradiography or subjected to PhosphorImager analysis.

2.2.5 Preparation of radioactively labelled probes

2.2.5.1 Random prime [α-^{32}P] dCTP labelled probes

For Northern and Southern blot analysis radioactive probes were prepared from agarose gel electrophoresis-separated DNA fragments using the T7 QuickPrime®Kit (Pharmacia Biotech) as follows:

34 µl denatured DNA (50 to 100 ng)
10 µl reaction mix (containing buffer, nucleotides and random primers)
5 µl (3000 Ci/mmol) [α-^{32}P] dCTP
1 µl T7 DNA polymerase

The reaction was incubated at 37°C during 30 minutes. Following the removal of unincorporated nucleotides using High Pure PCR purification kit (Boehringer Mannheim) the eluate was denatured at 95°C for 5 minutes and immediately chilled on ice prior to use.

2.2.5.2 First strand cDNA synthesis with [α-^{33}P] dCTP

Radioactive cDNA probes for microarray filter hybridisations were prepared following the protocol of Hoheisel *et al.,* 1993. The different steps are summarized below.

❖ **Oligo hybridisation**

Total RNA (30 µg)	X µl
Poly A$^+$ RNA Nebuin (0.5%)	X µl
DEPC water	X µl
Oligo dT primer (500 ng)	X µl
Total reaction volume	11 µl

Following an incubation at 70°C for 10 minutes, the reaction was equilibrated at 43°C for 5 minutes and then the first strand cDNA synthesis reaction was carried out at 42°C for 1 hour with following components:

❖ **First strand cDNA synthesis**

Oligo hybridised RNA	11 µl
Reverse transcription buffer 5X	6 µl
0.1 M DTT (freshly prepared)	3 µl
10 mM [dATP, dGTP, dTTP]	3 µl
50 µM dCTP	3 µl
[α-^{33}P] dCTP 30 µCi	3 µl
Superscript II RT (200 U)	1 µl
Total reaction volume	30 µl

After the cDNA synthesis the RNA was hydrolysed at 65°C for 30 minutes in presence of 1% SDS, 0.5 M EDTA and 3 M NaOH followed by incubation at room temperature for 15 minutes. The reaction was neutralised with 2N HCl and the cDNA was pelleted down using 3 M Na acetate pH 5.3 and 10 mg/ml yeast t-RNA carrier and 2.5 volumes of absolute ethanol. The pellet was dried and resuspended in water.

2.2.6 Expression profiling using cDNA microarrays

Whole genome expression profiling facilitated by the development of cDNA microarrays (Schena *et al.,* 1995; Lockhart *et al.,* 1996) represents a major advance in genome wide functional analysis (Hughes *et al.,* 2000). Microarrays have become an indispensable too for the investigation of gene expression profiles and gene polymorphisms. In a single assay, the transcriptional response of each gene to a change in cellular state can be measured, whether it is disease, a process such as cell division, or a response to a chemical or genetic perturbation (DeRisi *et al.,* 1997; Heller *et al.,* 1997; Holstege *et al.,* 1998). The method makes it possible to survey thousands of genes in parallel and has several areas of application. One is expression monitoring (Chee *et al.,* 1996) in which the transcript levels of genes are measured in different physiological conditions both in cultured cells and tissues, to search for regulatory expression patterns. Understanding patterns of expressed genes is expected to improve our knowledge of highly complex networks that cross communicate in hitherto unknown ways. The microarray technology can be divided into four main steps (figure 2.1):

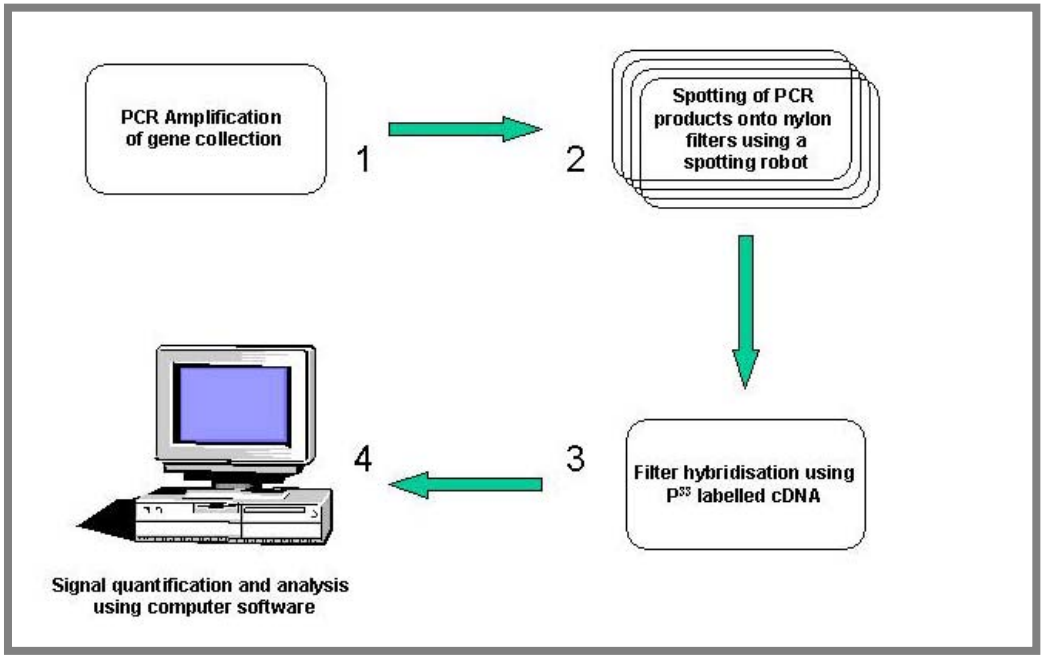

Figure 2.1) Key steps in cDNA microarray procedure

a) PCR amplification of the gene collection organised in a 384 well microtiter plate.
b) Transfer of PCR products, in duplicates, onto nylon membranes (or glass chips) using a "gridding" robot. In this step replica filters are generated.
c) Hybridisation of independent filters to complex probes prepared from cDNA reverse transcribed from total or poly A^+ RNA extracted from control and treatments.
d) Filter analysis. This involves reading the filters using a scanning device (e.g. PhosphorImager from Molecular Dynamics), quantification and analysis of signals using specialised computer software (e.g. Array Vision/Array Stat from Imaging Research Inc.)

2.2.6.1 Amplification of cDNA inserts from maize cDNA and expressed sequence tag (EST) collection

The maize cDNA collection comprising of 800 EST clones from Missouri (Monsanto, USA) and around 1800 EST clones collected in Thompson lab (Ricardo Velasco, Max Planck Institute, Köln, unpublished results) were amplified by PCR with universal and reverse primers in 96-mirowell plates (Advanced biotechnologies) in a Peltier Thermal Cycler (PTC-225 DNA Engine Tetrad, MJ Research, Inc.). The clone identities can be found at http://www.mpiz-koeln.mpg.de/~riehl/ArrayDB/MzArrayDB.htm. Since most of the cDNAs were cloned into pBluescript® or pBluescript® derived vectors (see section 2.1.3.3), universal and reverse primers were used for amplification of desired inserts. In cases where the cDNAs were cloned into other vectors, PCR amplification was done with vector specific primers or the primers specific for amplifying inserts in those vectors. 1 µl of each clone (taken from plasmid stock or directly from bacterial stock) was loaded into 96 micro-well plates. A PCR master mix was prepared (as described in section 2.2.1.1) and 99 µl was dispensed into each well. For difficult to amplify templates dimethyl sulfophoxide (DMSO) was added to a final concentration of 5%. PCR amplification was carried out as described earlier (section 2.2.1.1).

2.2.6.2 Spotting of cDNA onto nylon filters

30 µl of each PCR reaction was loaded onto a 384 well microtiter plate (NUNC), sized 12.5 x 8 cm^2. Seven such plates contained all the cDNA clones while an empty 8^{th} plate served as a blank control for subtraction of any background during micro-array analysis. The microtiter plates were placed onto a bio-gridder robot (BioGrid/MicroGrid with cooling, BioRobotics). 22 cm^2 Hybond N^+ nylon filter placed on top of 3 sheets of Whatman paper soaked in denaturing solution (1.5 M NaCl, 0.5 M NaOH) was also placed at the appropriate place on the robot.

The bio-gridder was programmed to produce DNA spots in a pattern of 4 x 4 so that a repetition of each PCR product was present in each nylon filter. The final spotting pattern in a 4 x 4 field was as shown in the table 2.1. The numericals from 1 to 8 represent the eight 384 well microtiter plates used for spotting. As can be seen each PCR product was spotted twice in a 4 x 4 field. The spotting plan and the final organisation of the clones on the nylon filters can be found at http://www.mpiz-koeln.mpg.de/~riehl/ArrayDB/AllPlates.htm.

2	6	2	3
1	4	7	5
7	8	3	6
1	5	4	3

Table 2.1) Spotting pattern on nylon filters. Spotting was done from eight 384well microtiter plates containing 2600 maize EST's. The numbers in the boxes represent the plate number from which the clone was taken for spotting. Each clone was represented on the filter twice.

After spotting, nylon filters were placed two times for 4 minutes on top of 3 MM Whatman paper pre-wetted in neutralising solution (1 M Tris pH 7.6, 1.5 M NaCl). The DNA was fixed to the membrane by UV irradiation at 20000 µjoules cm^{-2} for 30 seconds using Stratalinker (Stratagene).

2.2.6.3 Hybridisation of nylon-array filters

Array filters were hybridised according to Hoheisel, 1993 with some minor modifications. Prehybridisation was done in 20 ml of microarray

hybridisation buffer (see section 2.1.9.3) at 65°C for 2 hours. After prehybridisation, 10 ml of microarray hybridisation buffer along with 50 ng of labelled probe (section 2.2.5.2) was added to the prehybridisation solution and the hybridisation was carried over night at 65°C. The filters were washed twice in 40 mM Na-Phosphate pH 7.2, 0.1% SDS at 65°C. Finally filters were blotted dry and subjected to PhosphorImager (Molecular Dynamics) analysis by exposing to a phosphor screen overnight.

2.2.6.4 Microarray quantifications

The imaging of the array filters was done with the software supplied with the Storm 860 Scanner. The ArrayVision (ARV), Imaging Research Inc., 6.0 software version was used for the quantification, analysis and interpretation of the DNA array data. The software gave a final output of spot volume quantifications (in MDC, molecular dynamics count), which were already normalised to a control and also included background corrections.

2.2.7 Protein analysis

2.2.7.1 Crude nuclear pellet isolation from maize cell lines

The protocol was based on Nagahshi and Hiraike, 1982. Essentially 5 g of callus from pelleted HE-89 cell lines; finely ground in liquid nitrogen was mixed with 10 ml of ice-cold nuclei extraction buffer (see section 2.1.9.4) and filtered through a 2 layers of Miracloth into a 15 ml falcon tube. The solution was centrifuged at 1000 x g for 5 minutes at 4°C. The pellet was resuspended in 0.5 ml of the extraction buffer and the protein concentration checked by performing a Bradford reaction (using BioRad Protein assay system). The resuspended nuclear pellet was aliquoted and stored at -80°C for further use.

2.2.7.2 Crude histone purification from maize cell lines

The protocol was based on Moehs *et al.,* 1988. 5 g of pelleted HE-89 cell line (callus), finely ground in liquid nitrogen was mixed with 20 ml of ice-cold histone extraction buffer (see section 2.1.9.4) and filtered through two layers of Miracloth and pelleted at 12000 x g for 10 minutes. The pellet was completely homogenised in 10 ml of pellet buffer (section 2.1.9.4) and

centrifuged again at 27000 x g for 30 minutes. The pellet was thoroughly resuspended in 1 ml 0.4 M HCl and put into an eppendorf tube and centrifuged at 13000 rpm for 1 minute. Supernatant was collected and neutralised with ammonia and precipitated with 5 volumes of ice-cold acetone. The acetone was washed off and the pellet dried and resuspended in nuclei resuspension buffer (0.35 M NaCl, 1 mM Tris pH 8, 0.1 mM PMSF). Protein concentration was determined using the BioRad Protein assay (Bio-Rad) and the samples frozen in small aliquots and stored at -80°C for further use.

2.2.7.3 Western blot analysis (Maniatis *et al.,* 1989)

Protein samples were run overnight on a discontinuous SDS-PAGE gel, electro-blotted in protein blotting buffer onto supported nitrocellulose membrane (Schleicher and Schuell) and blocked overnight at 4°C or for 1 hour at room temperature in TTBS (see section 2.1.9.4) containing 5% (w/v) non-fat powdered milk. The primary antibody was diluted to the working concentration in blocking solution (TTBS containing 5% milk) and then incubated with the membrane at room temperature for 3 hours. The membrane was washed 3 x 10 minutes in TTBS and then incubated with biotinylated-goat-anti-rabbit-antibody (Sigma) diluted 5000 fold in blocking solution. The membrane was again washed 5 x 5 minutes in TTBS followed by antibody detection by ECL reagent as per the manufacturer's instructions (ECL system, Amersham Pharmacia). The image was captured using Lumi-imager system from Boehringer Mannheim (Roche).

2.2.8 Isolation of genomic clones

2.2.8.1 Screening of lambda (λ) phage libraries

A maize genomic library (EMBL-3) from Clontech was screened for a *ZmGCN5* genomic clone using the following method. 5-10 ml of LB broth (containing 0.2% maltose + 10 mM $MgSO_4$) was inoculated with a single colony of *E. coli* (K803 strain) and incubated at 37°C, shaking at 300 rpm overnight. In the morning a fresh culture was initiated (from the overnight culture) for 3-4 hours under same conditions till the OD_{600} reached 1.0. The culture was spun down at 3000 x g and the pellet resuspended and diluted to

OD_{600}=0.5 with 10mM $MgSO_4$. The titer of the library was calculated by diluting 2 µl of the phage stock library in 1ml SM buffer (see section 2.1.9.1; 1: 500 dilution). 2µl from the first dilution were mixed with fresh 1 ml SM buffer (1:250000 dilution). 2, 5, 10 and 20µl from the second dilution were used to inoculate 200 µl of *E. coli* (in 10 mM $MgSO_4$). The culture was pre-incubated for 15 minutes at 37°C and the inoculated *E. coli* mixed with 4 ml of LB top agarose (pre-warmed to ~ 48°C) before plating out evenly on LB plates. The plates were incubated at 37°C overnight. The following formula was used to calculate the titer (plaque forming units (pfu) per ml) of the library.

$$\text{Pfu / ml} = \frac{\text{Number of plaques}}{\text{µl of dilution used}} \text{ x dilution factor x } 10^3 \text{µl /ml}$$

Typically 12 almost confluent 22cm x 22cm plates were used for first screen, which represented a total of approximately 2.6 x 10^6 plaques. The plates were blotted for 5 minutes with individually numbered Amersham Hybond-N nylon membranes. The blots were placed DNA side up, on to 3 MM Whatman paper soaked in denaturation solution for 5 minutes, neutralised by placing on to a paper soaked with neutralisation solution for 5 minutes and then rinsed in 2 x SSC. After drying on a Whatman paper, the DNA was linked to the membranes using Stratagene UV cross-linker (Stratalinker®). The membranes were prehybridised (2 hours) and then hybridised with a [α-^{32}P] - dCTP labelled fragment of ZmGCN5 cDNA. The hybridisation buffer consisted of 0.5 M Na-Phosphate pH 7.2, 7% SDS, 1 mM EDTA pH 8.0, and 100 µg/ml salmon sperm DNA at 65°C. The blots were washed and exposed to autoradiography. The putative positive plaques were picked out of the plate using the wide bore end of a Pasteur pipette and the phage particles eluted into 1 ml SM buffer by shaking at 400 rpm at room temperature for 2-3 hours, or eluting at 4°C overnight. The phage particles were re-screened as above and the process was repeated until plaque purity was achieved i.e. all the plaques present on the plates were positive. The positive plaques were picked and used for the production of high titer phage lysate for the purification of phage DNA.

2.2.8.2 Production of high titer phage lysate

100 µl of an overnight culture of *E. coli* K 803 was mixed with 10^5 pfu of bacteriophage and incubated at 37°C for 15 minutes. 3 ml of molten (48°C) top agarose (0.7%) was added to the inoculated bacteria and evenly poured onto a 90mm plate containing 30-35 ml of hardened bottom agar. Plates were incubated for 6-8 hours at 37°C. When the plates were almost confluently lysed they were removed from the incubator and 5 ml of SM buffer was added to the plates. Plates were stored at 4°C overnight with intermittent, gentle shaking. A Pasteur pipette was used to harvest the SM buffer from the plates. Another 1 ml of SM buffer was added to the plates to recover all the bacteriophage. 100 µl of chloroform was added to the pooled SM, vortexed briefly and centrifuged at 4000 x g for 10 minutes at 4°C. Supernatant was recovered and stored at 4°C with a drop of chloroform. This lysate was serially diluted, as in phage library screening and the phage titer calculated.

2.2.8.3 Purification of phage DNA

Qiagen λ-DNA purification method was used for the purification of the phage DNA (Qiagen® Lambda Handbook, August 1998).

2.2.9 DNA sequencing

DNA sequences were determined by the MPIZ DNA core facility on Applied Biosystems (Weiterstadt, Germany) Abi Prism 377 and 3700 sequencers using Big Dye-terminator chemistry. Premixed reagents were from Applied Biosystems. Oligonucleotides were purchased from Life technologies.

2.2.10 Transient gene expression in plant protoplasts *via* PEG mediated transfection

2.2.10.1 Preparation of protoplasts from tobacco BY2 cell line

Tobacco cell line BY2, derived from *Nicotiana tabacum* L. cv. Bright Yellow 2 (Kato *et al.* 1972) was propagated and used for protoplast isolation according to Nagata *et al.* (1981). 5 ml of the 7-day-old stationary culture was transferred to 95 ml of fresh culture medium (see section 2.1.8). After three

days of culture, cells in the exponential phase were harvested by passing through a 100 µm sieve and used for protoplast preparation.

2.2.10.2 Preparation of mesophyll protoplasts from tobacco (SR1) and cowpea leaves

Tobacco SR1 plants (Maliga *et al.,* 1973) were grown under sterile conditions until 7 cm tall (leaves were approximately 4 cm at this stage). Leaves were cut and transferred to 155 mm petridishes containing 40ml K3/0.4M (see section 2.1.8), macerozyme (0.1%) and cellulase (0.4%) for 20-22 hours in dark at 26°C. After overnight incubation the petridishes were shaken slowly for 30 minutes at room temperature. For the preparation of protoplasts from cowpea (*Vigna unguiculata*) the under-epidermis of the leaves was removed and the leaves were incubated (with the removed under-epidermis down) in the K3/0.4 M/cellulase/macerozyme solution for 3-4 hours at 26°C while gently shaking. After the appropriate incubation the protoplast/debris solution was filtered through double sieves (upper 250 µm, lower 100 µm) and the flow through transferred to 50 ml Falcon tubes and the volume adjusted to 50 ml using K3/0.4M sucrose (see section 2.1.8). The falcon tubes were centrifuged at 500 rpm for 15 minutes. The protoplasts band at the top of the solution was removed and resuspended very carefully in Ca-man solution (0.6 M mannitol, 10mM $CaCl_2$ solution) and washed three times. Finally the protoplasts were resuspended in 10 ml of W5 solution. The protoplast titer was determined using the Fuchs-Rosenthal counting chamber and the protoplasts pelleted at 500 rpm for 5 minutes and resuspended to 2 x 10^6 protoplasts/300 µl in MaMg solution (section 2.1.9.1).

2.2.10.3 Transfection of protoplasts

Transfection of protoplasts was performed according to Negrutiu *et al.* (1987) with some minor modifications. 10-20 µg of DNA was mixed with 0.3 ml aliquots of freshly isolated protoplasts (about 2 x 10^6), followed by mixing with 0.6 ml of PEG solution (section 2.1.9.1). The PEG-protoplast mixture was incubated for 20 minutes at room temperature and diluted by adding 10 ml of W5 solution (see section 2.1.9.1). Protoplasts were centrifuged at 100 x g for 5 minutes and the pellet was resuspended in 5 ml of protoplast culture

medium (K3, 0.4 M sucrose solution; see section 2.1.8). Transfected protoplasts were incubated at 28°C in the dark. Sample aliquots for transient GFP fluorescence were taken 18-24 hours after the treatment of the protoplasts.

2.2.11 Microscopy

2.2.11.1 Light fluorescence microscopy

Protoplasts transfected with fluorescent proteins were examined under Leica DMRB or Zeiss Axiophot light microscopes equipped with epifluorescence optics (GFP specific fluorescence observed using HQ GFP, HQ GFP LP filters; blue light exciter BP 450-490 nm; beam splitter RKP 510 nm; emitter LP 520 nm). DsRed (Ds or ds- *Discosoma sp*.: excitation 558nm, emission 583nm) fluorescence was observed using specific filters.

2.2.11.2 Confocal laser scanning microscopy (CLSM)

Detailed analysis of intracellular fluorescence was done by confocal laser scanning microscopy (CLSM) using a Zeiss LSM 510 microscopy system (Carl-Zeiss) based on an Axiovert inverted microscope equipped with an Argon ion laser as an excitation source. CFP and YFP tagged proteins expressed in protoplasts were excited by the 458 nm and the 514 nm laser lines sequentially. CFP fluorescence was selectively detected by HFT 458 dichroic mirror and BP 470-500 band pass emission filter while YFP fluorescence was selectively detected by using HFt 514 dichroic mirror and BP 535-590 band pass emission filter. In both cases the chlorophyll autofluorescence was filtered out and detected in another channel using a LP650 long pass filter. A 25 x Plan-Neofluar water immersable objective lens (numerical aperture 0.8) was used for scanning protoplasts. The pinhole size was 66 µm for CFP, 76 µm for YFP and 90 µm for chlorophyll autofluorescence. Images and data captures were analysed with Zeiss LSM510 software.

2.2.11.3 Fluorescence spectral imaging microscopy (FSPIM)

Fluorescence resonance energy transfer (FRET) between the fluorescently labelled probes was measured by FSPIM. Spectral imaging was

done using a Leica DMR epifluorescence microscope equipped with a Chromex 250 IS imaging spectrograph (Albuquerque, NM, USA) coupled to a Photometrics CH250 CCD (Charged coupled device) camera (Tucson, AZ, USA). The excitation light source was a 100 watt mercury lamp coupled to an excitation filter wheel. Fluorescent spectral images were acquired using a 20 x Plan Neofluar objective (numerical aperture 0.5), an omega 435 df10m band pass excitation filter, an omega 430 DCLP dichroic mirror and a 455 long pass emission filter (Schott, Mainz, Germany). Spectral images were acquired using a 150 groove/mm grating, set at a central wavelength of 500 nm and a slit width of 175-250 µm. Typical exposure and CCD integration time was 2-5 seconds. Data processing and background autofluorescence was performed as described (Gadella *et al.,* 1997).

2.2.12 Plant transformation

2.2.12.1 Maize transformation, regeneration and maintenance of transgenic callus and suspension cell lines

Transformation of maize suspension cell line HE-89 (Morocz *et al*, 1990) was kindly carried out by Anja Siedel/Dr. Steinbiss (Monocot Transformation Group, MPIZ) or by Dr. Günter Donn (Maize transformation group, Aventis Crop Sciences, Frankfurt). Transformation procedure was based on the protoplast PEG uptake method (Morocz *et al*, 1990). The protoplasts were co-transformed with the plasmid containing the gene of interest and with a plasmid containing Phosphinothricin (BASTA) resistance gene for the selection of transformants. Once the transgenic callus lines were established and characterised by PCR and Northern blots, they were put into suspension culture and maintained on the suitable selection (BASTA) and sub-cultured as recommended (Morocz *et al*, 1990).

2.2.12.2 SR1 tobacco cultivar transformation

A single colony of *Agrobacterium* containing the transformation vector was inoculated in 5 ml of YEB containing the selection antibiotics and grown under dark at 28°C for 48 hours. Sterile plant material (SRI tobacco) was grown for 6-8 weeks on MS medium. Leaf discs of approximately 1-3 cm were cut and placed in 20 ml of liquid MS medium (BY2 subculture medium; section

2.1.8). 2 ml of the fresh bacterial culture was added and incubated with the tobacco leaf discs for 30 minutes at room temperature. Leaf discs were then removed from the solution and laid upside down on solidified MS medium and incubated for 2 days at 26°C. After washing thrice in liquid MS medium, the leaf discs were transferred to fresh MS plates containing claforan (500 mg/l), kinetin (0.2 mg/l), auxin (1.0 mg/l) and the proper antibiotic to select for the growth of transgenic calli. After one week the calli were again transferred to fresh plates containing claforan, kinetin, auxin and selective antibiotic. Between 3-4 weeks, calli formed at the periphery of the leaf discs and subsequently shoots developed from these calli. Once the shoots were 0.5-1.0 cm in size they were removed and placed on MS medium with claforan but lacking auxin and kinetin for the development of roots. When each plantlet developed roots, they were transferred to small pots and transferred to greenhouse for further growth and genetic analysis.

2.2.12.3 BY2 tobacco cell line transformation

Tobacco cell line BY2, maintained as described earlier (2.2.10.1) was stably transformed as per the method described by An G (1987).

2.2.13 Chemical treatment of HE-89 cell line

Maize suspension cell line HE-89 was cultured weekly as recommended (Morocz *et al.* 1990). For Trichostatin A treatment, rapidly dividing cells, 3 days after the subculture, were treated with different concentrations of TSA (0.5 – 5.0 µM) and cultured further for 10 -12 hours under the same conditions. After the treatment the cells were pelleted and frozen at -70^{o}C until further use.

2.2.14 Computer Software

2.2.14.1 Visualisation and quantification of DNA and RNA blots by PhosphorImager technology

The PhosphorImager from Molecular Dynamics (Johnston *et al.,* 1990) was used to quantify the activity of radioactive bands on the nylon membranes. Image Quant software version 1.0 for Macintosh (1995),

Molecular Dynamics was used for basic analysis and data reporting/graphing functions.

2.2.14.2 DNA sequence analysis

DNA sequences were characterised by using GCG software package version 9.0 from Genetic computer group (Madison, WI) and the BLAST network service (Altschul *et al.,* 1990).

Characterisation of a *ZmGCN5* genomic clone

3.1 Introduction

A database search for plant orthologues of histone acetyltransferase *gcn5* and adaptor *ada2* (in 1998) yielded two *A. thaliana* sequences, a cDNA for *AtGCN5* (AF037442), and an *AtADA2* genomic sequence (GenBank Acc.: Z97341). Primers designed on *AtADA2* genomic sequence were used to isolate the corresponding *AtADA2* cDNA by RT-PCR (Heinz Albert-Becker, MPIZ, personal communication). This cDNA was used as bait in yeast two hybrid system to screen maize 7 DAP, endosperm hybri-ZAP cDNA library. The screening yielded 16 clones out of which one clone showed sequence homology to *GCN5* histone acetyltransferase (Becker *et al.,* 1999). Full-length *ZmGCN5* cDNA was afterwards isolated by screening a maize pistil (silk) cDNA library (Marcus Riehl, Diplomarbeit, Universität Giessen, 1999). The cDNA (GenBank Acc: AJ428540) contained an open reading frame of 1545 bases, predicting a polypeptide of 515 amino acids.

Protein sequence comparison of ZmGcn5 (figure 3.1), with other members of GNAT (GCN5 related N-acetyltransferase; Sterner and Berger, 2000) superfamily showed that three functional domains present in other Gcn5 sequences are shared by ZmGcn5: the catalytic domain at the N-terminus responsible for the acetyltransferase activity, a centrally located domain responsible for the interaction with adaptor protein Ada2, and the C-terminal bromo-domain, which interacts with the histone N-termini (Ornaghi *et al.,* 1999).

Sequence comparison with other Gcn5 proteins also pinpointed an N-terminal extension in ZmGcn5. However this extension showed no homology to the PCAF domain in mammalian GCN5 HAT's (discussed in section 1.2.4.1). Recently, full length AtGcn5 (Stockinger *et al.,* 2001) and TgGcn5, a Gcn5 HAT protein from a protozoan parasite (Hettmann and Soldati, 1999) were reported to have N-terminal extensions, but these are unrelated in sequences to that present in ZmGcn5.

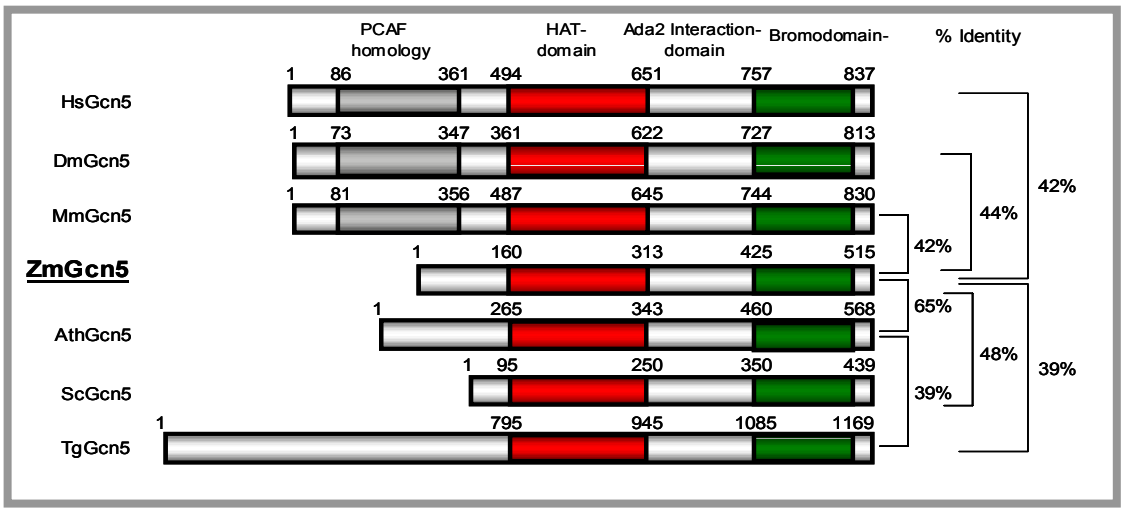

Figure 3.1) Comparison of ZmGcn5 with other members of GNAT protein family. All family members (Human, Drosophila, Rat, Maize, Arabidopsis, Yeast and Taxoplasma) share a catalytic HAT domain, the Ada2 interaction domain and the bromo-domain. A PCAF homology is present only in the metazoan family members. Amino acid positions of the putative domains are indicated above the diagram. The percentage of identical amino acid residues is shown on the right. Acc. Nr: HsGcn5, AF029777; DmGcn5, AF029776; MmGcn5, AF254441; ZmGcn5, AJ428540; AtGcn5, AF338768; ScGcn5, X68628; TgGcn5, AF197953.

At the time of the isolation of *ZmGCN5*, the full-length clones of *AtGCN5* and *TgGCN5* were not known. The N-terminal extension in *ZmGCN5* raised many questions:

1. Is the N-terminal extension in *ZmGCN5* part of the encoded protein or is it part of an unspliced intron sequence?
2. Do plant *GCN5* genes contain the PCAF homology domain?

A database search for any plant protein sharing homology with the PCAF region of mammalian Gcn5 gave no hits, so a genomic clone of *ZmGCN5* was isolated to characterise the 5´ end of the gene.

3.2 Isolation and characterisation of a ZmGCN5 genomic clone

Full-length cDNA sequence of *ZmGCN5* (1.54Kb) was used as a probe to screen the maize genomic library EMBL3 from Clontech (section 2.2.8). The Clontech EMBL 3 library was generated from the DNA extracted from 2-leaf stage maize seedlings (B73 cultivar). The DNA was partially digested with restriction endonuclease *Mbo*I and the fragments between the size range 8 to 22 Kb were cloned into the *Bam*HI site of vector EMBL-3. *Sal*I is one of the

flanking multiple cloning sites and the insert DNA can be excised from the clones by digestion with endonuclease *Sal*I.

2 x 10^6 pfu were screened and 12 hybridising clones were obtained after three successive rounds of screening. To confirm the clone authenticity and generate subclones, phage DNA was prepared using Qiagen Lambda DNA purification kit (Qiagen). The inserts were excised from the λ-vector and the products, run on an agarose gel were Southern blotted onto a nylon membrane and hybridised using the *ZmGCN5* cDNA as a probe. The size of the insert within the lambda vector was approximately 17 kb (figure 3.2, *Sal*I digest).

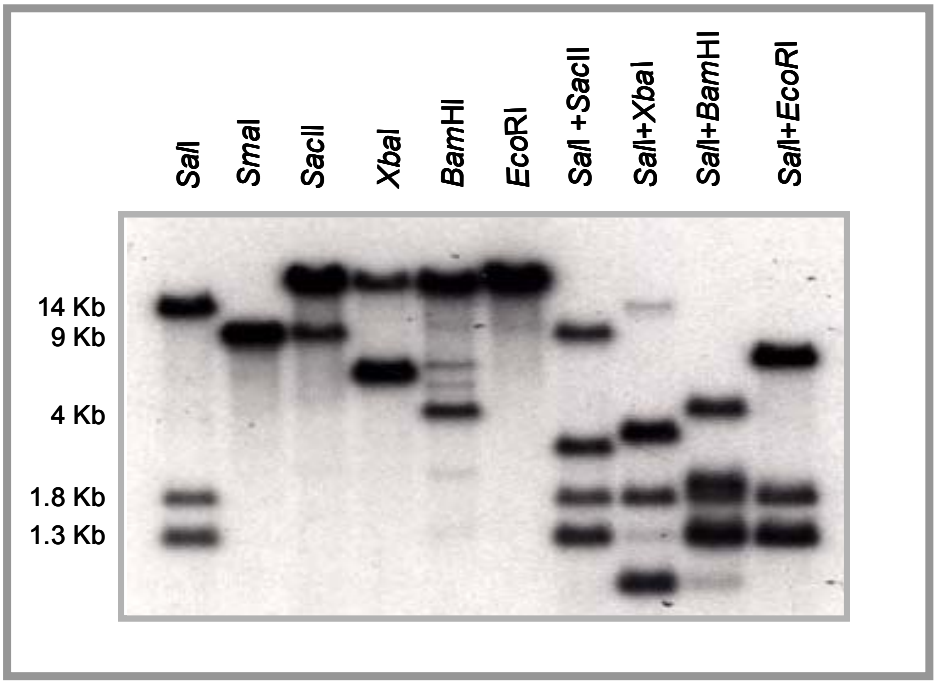

Figure 3.2) Southern blot on *λ-ZmGCN5.1* genomic clone. The λ-DNA was digested with different restriction endonucleases as indicated and probed with full length *ZmGCN5* cDNA.

All the 12 clones showed the same digestion and hybridisation pattern indicating that the isolated clone was over-represented in the lambda library. Further analysis was carried out on a representative clone (*viz. λ-ZmGCN5.1*). In order to ascertain that the isolated clone contained both N- and C-terminal regions of the gene, specific 5´and 3´ probes were generated and used to hybridise restricted λ clones. Both types of probes gave strong hybridisation signals indicating that whole *GCN5* gene was present in a single lambda

clone. DNA, single and double digested with different restriction enzymes, was Southern blotted and the sizes of the bands were used to construct the detailed restriction map of *ZmGCN5* genomic clone. The detailed restriction map is shown in figure 3.3.

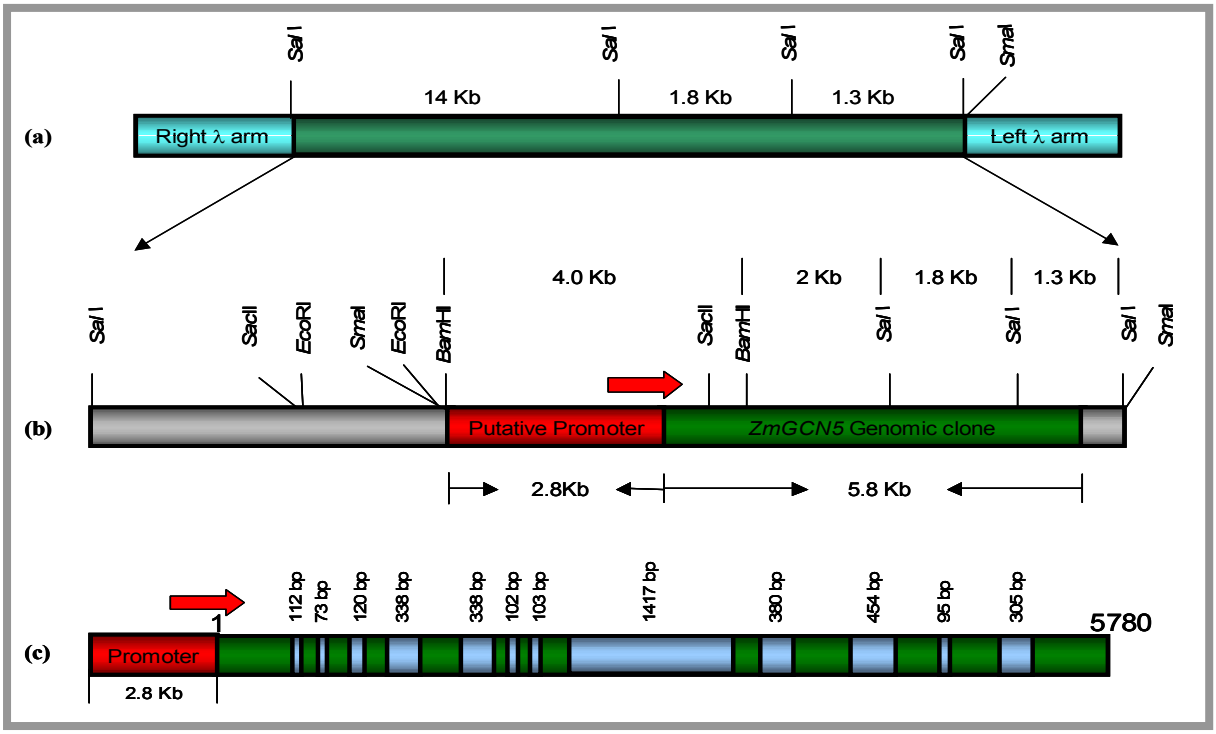

Figure 3.3) Restriction map of *maize λGCN5* genomic clone. (a) 17Kb *Z. mays* genomic insert within left and right λ arms. (b) Orientation of *ZmGCN5* within the λ vector along with relative restriction sites. (c) Intron-exon structure of *ZmGCN5* genomic clone. (Not scaled)

Based on the deduced restriction map a series of digests were made to generate fragments, which would cover entire *GCN5* coding sequence and the putative promoter region. DNA was double digested with *Bam*HI and *Sma*I and the 4Kb *Bam*HI fragment and 5.1Kb *Bam*HI/*Sma*I fragments were cloned into pBluescript vector digested with *Bam*HI and *Bam*HI / *Eco*RV respectively. Putative sub-clones generated were digested with appropriate enzymes, Southern blotted onto a nylon membrane and hybridised with specific 5´ and 3´ *ZmGCN5* cDNA probes to confirm the clone authenticity and their orientation and position within the genomic fragment. The sub-clones were sequenced, initially using the universal and reverse primers from

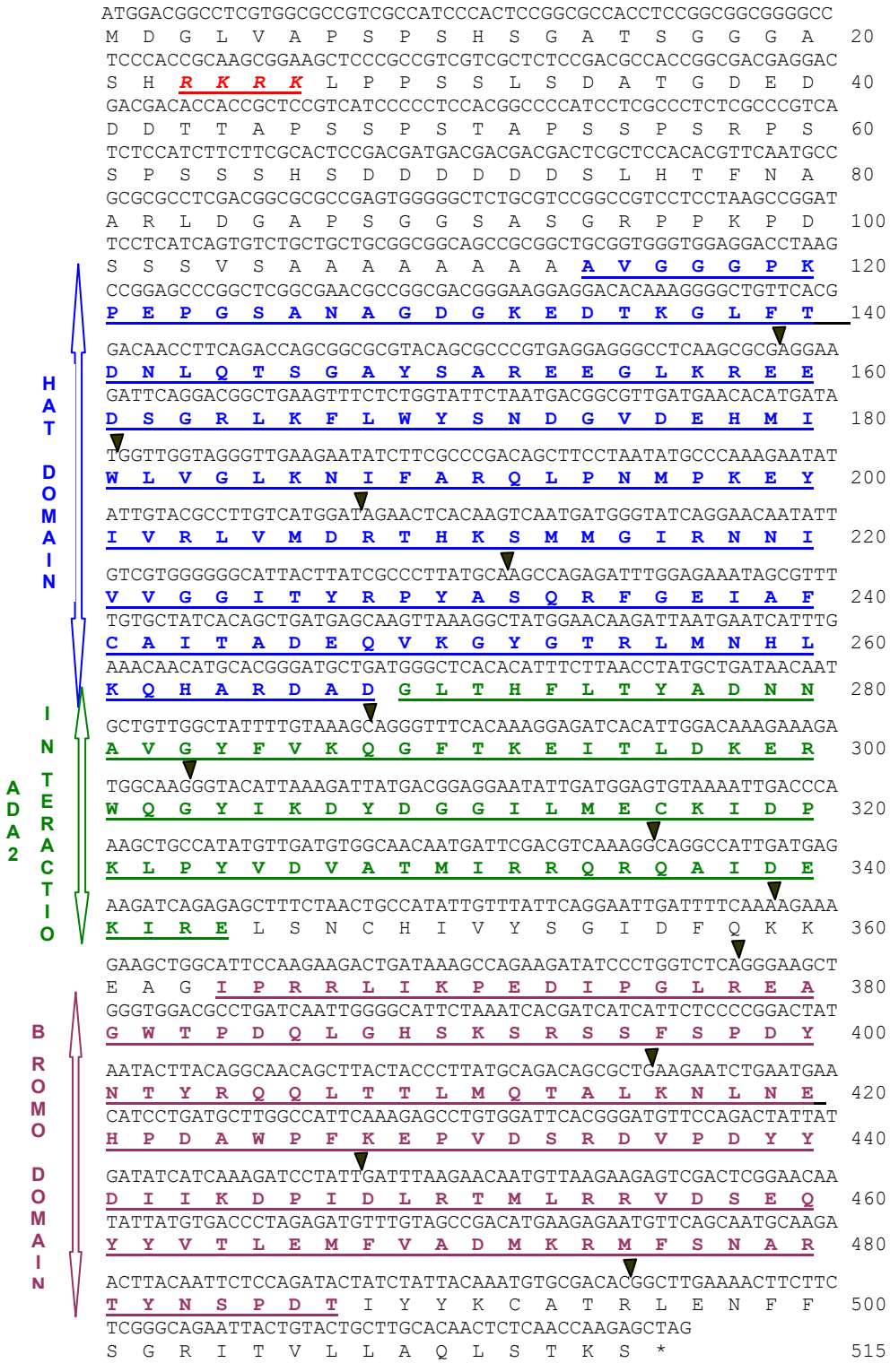

Figure 3.4) *ZmGCN5* open reading frame. Sequence of the coded cDNA for ZmGCN5 and its deduced amino acid sequence. Predicted protein domains are colour coded, underlined and identified in the left hand column. Intron positions within the cDNA are marked with black arrowheads. Position of mapped nuclear localisation sequence (NLS) in the N-terminal is shown in bold, underlined italic letters (red).

pBluescript and afterwards by designing gene specific primers till the full-length genomic clone of *ZmGCN5* was assembled. The sequencing also gave 2.8 kb upstream region of *ZmGCN5* gene.

Sequence comparison of genomic clone with the cDNA sequence identified 12 introns, ranging in size from 73 bp to 1.4 kb. The latter was situated in the middle of the gene (figure 3.3 c). The *ZmGCN5* cDNA open reading frame and the positions of the identified introns are shown in the figure 3.4.

3.3 Identification of the transcription start site and the putative promoter elements of *ZmGCN5* gene

Identification of the N-terminal methionine residue within the genomic clone was an important step towards characterisation of the *ZmGCN5* gene. The sequenced 2.8 kb upstream region of the *ZmGCN5* genomic clone did not show any homology with the PCAF domain of metazoan *GCN5* HAT's or any other protein. This led to the conclusion that most likely there is no other domain missing in *ZmGCN5*.

Primer extension was performed to map the transcription start site. Initial efforts to generate a primer extension product were not successful because of the very high GC content in the N-terminal of *ZmGCN5* leading to very stable RNA secondary structures. In order to circumvent this problem a primer was designed at the putative translation start site. The primer sequence (PextGcn5) is shown section 2.1.3.4 and also in figure 3.6. Primer extension reaction (section 2.2.1.3) was performed on the total RNA extracted from maize leaves with PextGcn5 primer labelled with γ-^{32}P-ATP. Products were separated on a 9% acrylamide/7 M urea gel. The sizes of the products were estimated from α^{33}P-dCTP labelled sequencing reaction on the genomic sequence using the same primer. The results are shown in figure 3.5. Three bands at 80, 96 and 111 bp were identified. These products may have originated from three different transcription start sites or the lower bands may represent premature termination of the reverse transcription reaction. The position of the 111 bp band was taken as the transcription start site.

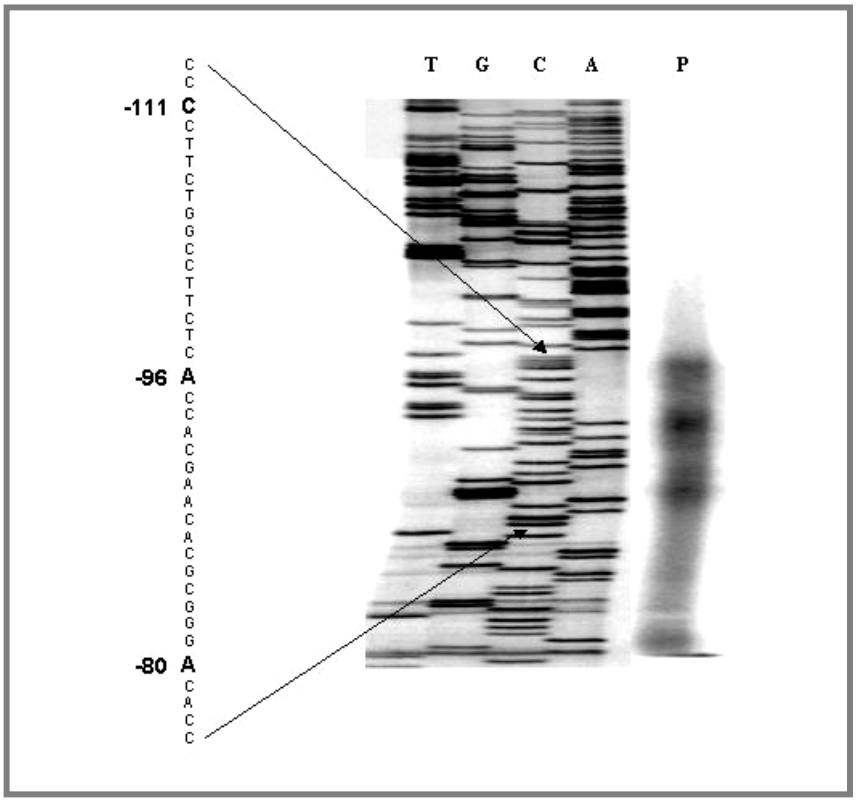

Figure 3.5) Primer extension products generated by a ZmGCN5 specific primer. Reverse transcription products generated from *Z. mays* leaf total RNA using a primer designed to the 5′ UTR of λGCN5.1 (lane P). The sizes of the products were estimated from α [^{33}P] dCTP labelled sequencing reaction on the genomic sequence using the same primer. The sequence between the arrows amplified on the left side.

Analysis of the sequence upstream of the translation start site was done by using time delay neural networks software (TDNN – http://www-hgc.lbl.gov/projects/promoter.html). The program analyses the structure of individual promoter elements such as TATA box, GC box, CAAT box and the transcription start site within a sequence using a novel technique that combines neural networks with pruning. A neural network is pruned to recognise promoter elements until it reaches a local minimum. The procedure eliminates all those weights in the network that add the lowest predictive value to the overall prediction. After pruning the neural network is retrained until it again reaches a local minimum. This procedure is repeated until a defined error level is reached. These single predictions for each element are combined using time-delay neural networks for a complete promoter site prediction. TDNNs are appropriate for recognising promoter elements because they are able to combine multiple features, even those that appear at different relative positions in different sequences. The software identified two

regions between -104 to -153 and -298 to -347 (taking the A residue from ATG as position 0 and counting backwards) as a putative minimal promoter (see figure legend 3.6). The identified regions had an error level of 0.75 and 0.70, which indicates that this region has a very good probability of representing a functional promoter. These regions contain a canonical TATA box, a CAT box as well as the GC box. This is shown in figure 3.6.

Figure 3.6) Predicted promoter region of *ZmGCN5* gene. Sequences predicted to represent potential minimal promoters are shown in yellow. The residues to which the primer extension products were mapped are enlarged and shown in red. The primer sequence used to generate the extension products is shown in red along with an underlined N-terminal ATG.

3.4 The *ZmGCN5* promoter drives the expression of Green fluorescent protein (GFP) in transiently and stably transformed BY2 and SR1 tobacco protoplasts.

In order to confirm the functionality of the *isolated ZmGCN5* promoter, the 2.8Kb promoter fragment was used to drive the transient and stable expression of GFP in protoplasts prepared from either BY2 and/or SR1 tobacco line (see section 2.2.10). For this purpose the promoter fragment was amplified by PCR and transcriptionally fused to the GFP coding sequence as shown in figure 3.7. The primers used for amplifying the *ZmGCN5* promoter (Gcn5PromoterFwd, Gcn5PromoterRev) are listed in section 2.1.3.4.

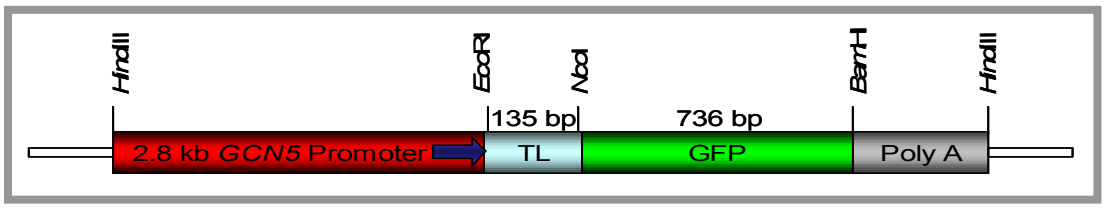

Figure 3.7) *ZmGCN5* promoter transcriptionally fused to GFP (Sheen *et al.* 1995; TL–Translational Enhancer)

The analysis of GFP protein showed that the promoter was active and could drive the GFP expression. GFP itself does not contain any intracellular localisation signal so protein expression was observed throughout the cell (figure 3.8 panels GCN5Prom::GFP). The control protoplasts were transformed with GFP under the 35S promoter from cauliflower mosaic virus (35S::GFP). The protoplasts prepared from stably transformed SR1 plants confirmed the results obtained with the transient analysis (data not shown).

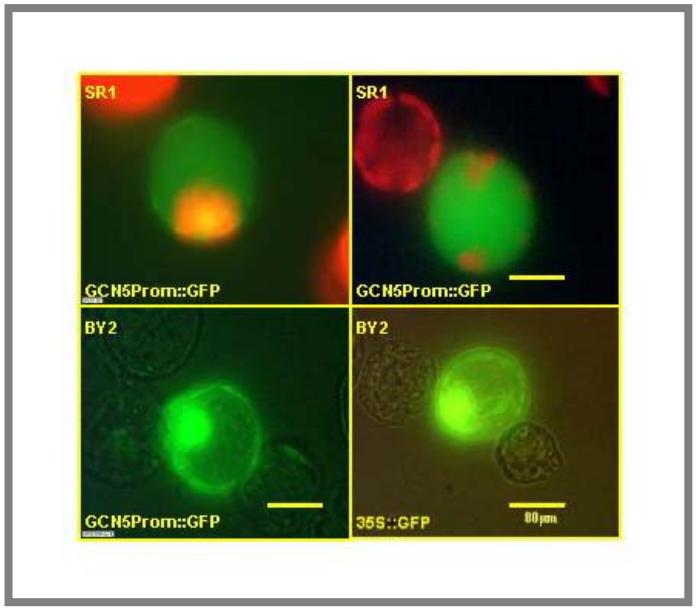

Figure 3.8) GFP expression under the 2.8Kb ZmGCN5 promoter in tobacco BY2 and SR1 protoplasts. Also shown is a control protoplast transfected with 35S::GFP construct.

Localisation and targeting of ZmGcn5

4.1 ZmGcn5 is a nuclear type A histone acetyltransferase

In order to function as a transcriptional co-activator and modify the chromatin, ZmGcn5 should be targeted to the nucleus. This was tested by creating a translational fusion of *ZmGCN5* with the GFP and analysing the fusion protein in tobacco BY2 and SR1 protoplasts. An *Nco*I restricted PCR fragment of full length *ZmGCN5* cDNA was cloned into the *Nco*I site of the vector pGFP-JS (Sheen *et al.,* 1995) to make a C-terminal fusion of *ZmGCN5* with GFP (figure 4.1). The primers used for amplification (*Nco*IGcn5Fwd and *Nco*IGcn5Rev) are listed in section 2.1.3.4. The resultant vector was used to transfect protoplasts isolated from BY2 and/or SR1 tobacco lines (section 2.2.10) and the transient fusion protein expression was observed under a light fluorescence microscope. The results are shown in figure 4.2.

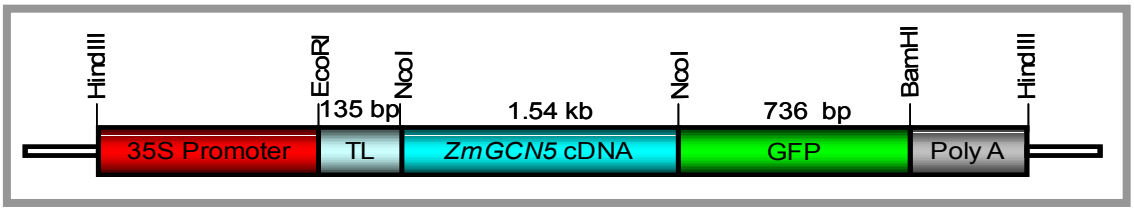

Figure 4.1) Schematic representation of the 35S::GCN5GFP construct used for studying the sub-cellular localisation of ZmGCN5. (TL- Translational Enhancer)

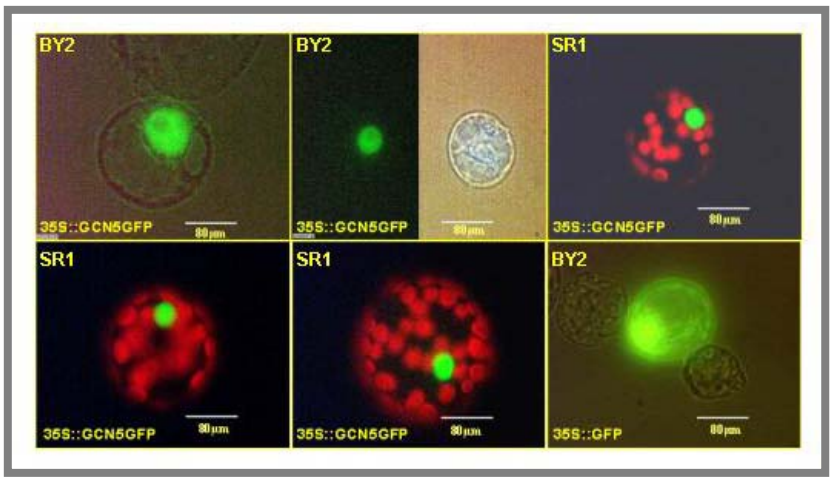

Figure 4.2) Micrographs of protoplasts prepared from BY2 and SR1 tobacco lines transformed with 35S::GCN5-GFP. Also shown are control protoplasts transformed with 35S::GFP only. Upper middle panel shows a transfected protoplast observed under bright field as well as GFP specific excitation.

The fusion protein was exclusively targeted to the nucleus (figure 4.2, panels 35S::GCN5GFP) in comparison to the protoplasts transfected with GFP alone under the control 35S promoter from cauliflower mosaic virus (panel 35S::GFP), where GFP fluorescence was seen throughout the cell.

4.2 The extended N-terminal region of ZmGcn5 contains a functional nuclear localisation sequence (NLS)

Although it seems possible that a protein (up to 40 - 60 kDa in size) without its own nuclear targeting signal may enter the nucleus simply by diffusion (Peters, 1986; Silver, 1991) or via cotransport with a protein that has one (Dingwall *et al.,* 1982; Zhao and Padmanabhan, 1988), many nuclear proteins have their own NLS. A search for potential nuclear targeting residues in ZmGcn5 using the computer program PSORT (http://psort.nibb.ac.jp/) pinpointed a stretch of basic amino acid residues in the extended N-terminal segment of the protein between positions 23-26 (see figure 3.4). Since this extended N-terminal segment shares no homology with other known Gcn5 proteins and is also unique when compared to AtGcn5, we investigated the following possibilities:

1. Is the predicted NLS in the extended N-terminal segment of the protein functional?
2. Is there any cryptic (non-canonical) but functional NLS within the well-characterised domains of ZmGcn5? This could be a possibility because the ScGcn5 (Accession number X68628) does not seem to have a canonical NLS, but is a nuclear HAT, raising the possibility that it is transported to nucleus via a non-canonical NLS.

In order to ascertain the above possibilities, a series of fragments of the coding sequence of *ZmGCN5* were translationally fused to the GFP reporter. The regions used for making translational fusions with GFP are shown in figure 4.3.

Specific primers were designed to amplify the desired regions (between amino acids 1–175, 175–420, 314–515 and 175–515) introducing *Nco*I sites at both N- and C-terminal ends. The primers (*Nco*IGcn5fwd, Gcn5NtermRev, Gcn5HATFwd, Gcn5Ada2IntFwd, Gcn5Ada2IntRev, *Nco*IGcn5Rev) are listed

in section 2.1.3.4. These PCR fragments were then digested with the endonuclease *Nco*I and cloned in the *Nco*I site of vector pGFP-JS (Sheen *et al.,* 1995).

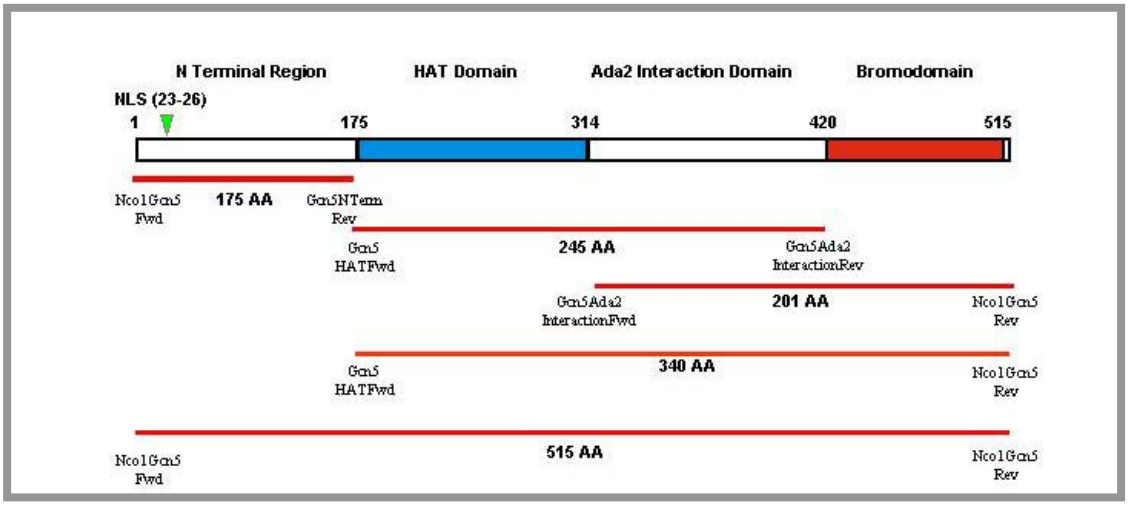

Figure 4.3) Schematic of ZmGCN5 fragments used for translational fusion with GFP. Different domains of ZmGCN5 (shown by red lines) were PCR amplified using specific primers and translationally fused with GFP coding sequence.

Translational Fusion Construct	Protein localisation
35S:: N-terminal domain (1-175) of *ZmGCN5* fused to GFP	Nuclear
35S:: HAT- and ADA2-domain (175-420) of *ZmGCN5* fused to GFP	Cytosolic + Nuclear
35S:: ADA2- and Bromo-domain (314-515) of *ZmGCN5* fused to GFP	Cytosolic + Nuclear
35S:: HAT-, ADA2- and Bromo-domain (175-515) of *ZmGCN5* fused to GFP.	Cytosolic + Nuclear
35S:: Full length (1- 515) *ZmGCN5* fused to GFP	Nuclear
35S:: GFP	Cytosolic + Nuclear

Figure 4.4) Summary of *ZmGCN5* deletions tested by transient gene expression and the location of the encoded fusion proteins.

The resulting plasmids were transfected into BY2 tobacco protoplasts, and the GFP fluorescence was examined under a light fluorescence microscope. Around 75-100 transformed protoplasts were screened for each fusion construct. Nuclear targeting of the GFP was observed only with fusions containing the N-terminal region of the ZmGCN5 or full-length ZmGcn5 protein (see figure 4.4), pinpointing a functional nuclear localization signal in

the N-terminus of the protein, upstream of the region of homology with ScGcn5 or AtGcn5.

The experiment provided support for the hypothesis that, although unrelated to other Gcn5 sequences, the N-terminal extensions in plant Gcn5 proteins might have a specific role to play. In the case of ZmGcn5, the protein encoded cannot function as a transcriptional co-activator unless it is correctly targeted to the nucleus and this is possible only when the protein contains this N-terminal stretch.

In vivo interaction studies between the putative coactivators ZmGcn5, ZmAda2 & a plant transcriptional activator Opaque 2

5.1 Introduction

ZmGcn5 is a putative transcriptional co-activator expressed throughout the plant with highest abundance in tissues containing a high proportion of rapidly dividing cells such as young shoots and endosperm (Marcus Riehl, Diplomarbeit, Universität Giessen, 1999). In yeast the adaptor protein Ada2 has been shown to directly interact with Gcn5 (Marcus *et al.,* 1994). Ada2 is present in several complexes in yeast, not all of which contain Gcn5 (Grant *et al.,* 1997). Ada2 also directly interacts with the bZip type yeast transcriptional activator Gcn4 to evoke specific gene activation (Barlev *et al.,* 1995). Maize transcriptional activator Opaque-2 (O2), expressed during late endosperm development (Gallusci, *et al.,* 1994) shows many similarities to Gcn4 (see introduction section 1.4) and raises the possibility that ZmO2 might also recruit the Gcn5-mediated co-activator complexes via an interaction with ZmAda2.

GST spin-down experiments showed that ZmGcn5 interacts with ZmAda2 *in vitro*. However no interaction could be observed between ZmAda2 and ZmO2 in further GST spin down experiments (Heinz Albert-Becker, Max Planck Institute, personal communication). In view of the fact that Ada2 is part of a multi-protein complex in yeast (Grant *et al.,* 1997) and probably in all higher eukaryotes, it is quite possible that this specific interaction may require the presence of additional components. This is supported by the observation that by co-immunoprecipitation in presence of nuclear extracts, a specific interaction between ZmO2 and ZmAda2 could be detected (Heinz-Albert Becker, personal communication).

In order to define the role of these proteins in the cellular context interactions between ZmGcn5 HAT, adaptor ZmAda2 and plant transcription factor ZmO2 were tested by *in vivo* methods. The split-ubiquitin system was used to check the *in vivo* interaction between Gcn5 and Ada2. The results were further verified by FRET analysis. FRET was also used to determine the interaction between ZmAda2 and the plant transcriptional activator ZmO2.

5.2 The Split-ubiquitin system:

This system was introduced by Johnsson and Varshavsky (1994) and provides an alternative over the yeast two-hybrid system. Ubiquitin is split into N-terminal and C-terminal halves (N_{ub} and C_{ub} respectively) and each half is fused to either protein of interest. C_{ub} is additionally fused at the carboxyl-terminus to a reporter that has been mutated to bear a degradation signal. If the two proteins interact inside living cell, the two halves of ubiquitin are brought into close proximity and a quasi ubiquitin (Ub) moiety is reconstituted and recognised by ubiquitin-specific proteases (UBPs). The fusion containing C_{ub} is cleaved, resulting in the release and degradation of the reporter. This is schematically shown in figure 5.1. Since ubiquitin proteases are present in the cytosol as well as in the nucleus (Varshavsky, 1997; Byrd C., *et al.* 1998), this assay can be used to study interactions reconstituted in the cytosol as well as in the nucleus.

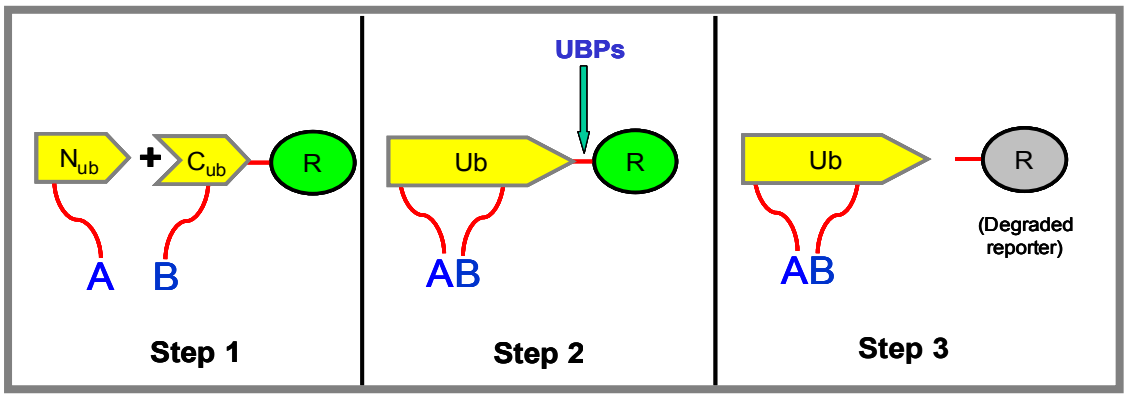

Figure 5.1) Schematic representation of split-ubiquitin system. N_{ub} and C_{ub} are fused to the interacting proteins A and B. The AB interaction brings N_{ub} and C_{ub} into close proximity. A quasi-native Ubiquitin moiety is reconstituted which is recognised and cleaved by UBPs resulting in the release of the reporter R (from Johnsson and Varshavsky, 1994).

5.2.1 Establishment of split-ubiquitin system to study the *in vivo* interaction in plant cells

The N_{ub} fusion vector was created by inserting an *Apa*I/*Sac*I restricted PCR fragment containing N_{ub} into pRT100 (Töpfer *et al.,* 1988), and the C_{ub} fusion vector was created by placing a *Eco*RI/*Apa*I restricted fragment containing a fusion of C_{ub} with green fluorescent protein (GFP), modified to begin with an arginine residue (serving as a degradation signal), into pRT107

(Töpfer *et al.,* 1988). The vectors used for generating the fragments of C_{ub}-Arg-GFP and PCR products of N_{ub}, *viz.* cup-Cub-Rgfp313 and pADNX-NubIB1 respectively, were kindly provided by Dr. Norbert Lehming (Max-Delbrück Lab of the MPG, Köln). PCR fragments containing cDNAs of *ZmADA2* and *ZmGCN5* were cut with *Bgl*II/*Sal*I and *Eco*RI/*Age*I respectively and inserted into two vectors to create the N_{ub}ADA2 and GCN5-C_{ub}-Arg-GFP fusion vectors. The primers used for amplification of N_{ub}, *ZmADA2* and *ZmGCN5* (*viz. Apa*INubFwd, *Sac*INubRev; *Bgl*IIAda2Fwd, *Sal*IAda2Rev; *Eco*RIGcn5Fwd, *Age*IGcn5Rev) are listed in the section 2.1.3.4. The schematic representation of the fusions is shown in figure 5.2 and figure 5.3. The fusion vectors were then used to transfect BY2 protoplasts.

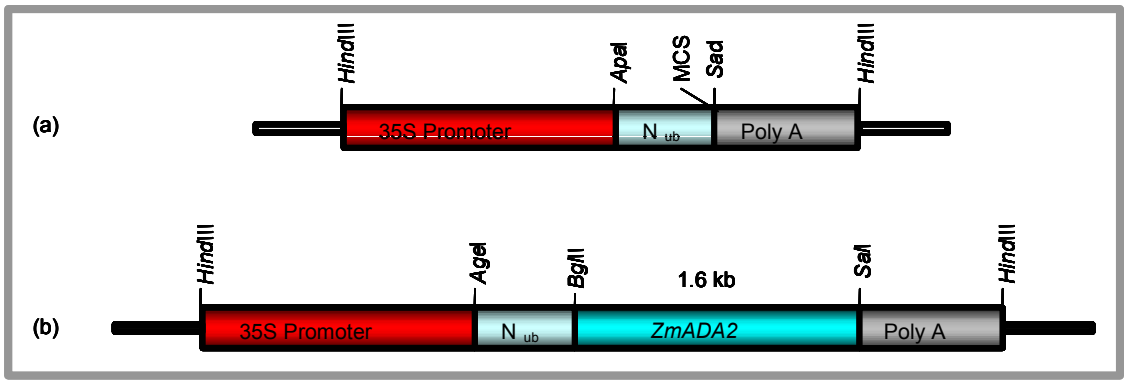

Figure 5.2) Construction of gene specific N_{ub} vectors. (a) Skeleton vector containing 35S::N_{ub} (b) 35S::N_{ub}-ZmADA2. MCS–Multiple cloning site.

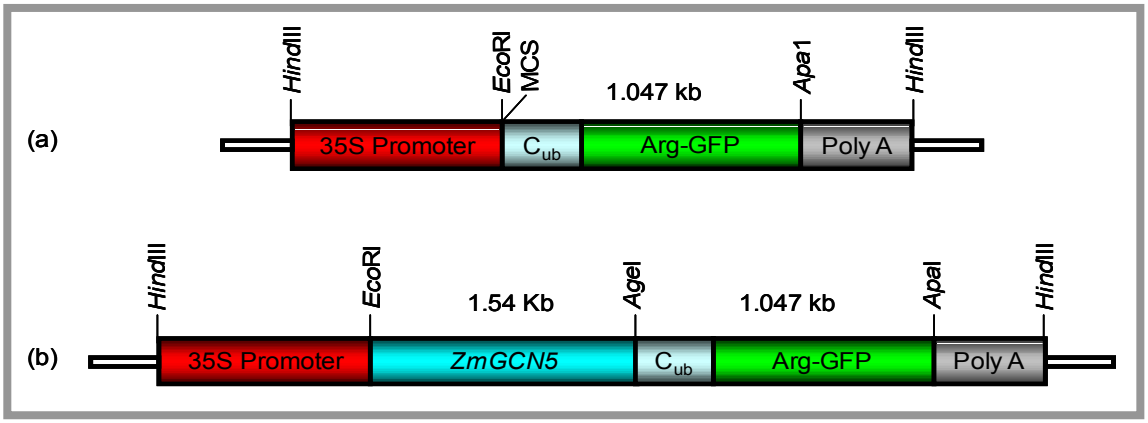

Figure 5.3) Construction of gene specific C_{ub}-Arg-GFP vectors. (a) Skeleton vector containing 35S::C_{ub}-Arg-GFP (b) 35S::ZmGCN5-C_{ub}-Arg-GFP.

In theory, once protoplasts are co-transformed with *ZmGCN5*-C_{ub}-Arg-GFP and Nub-*ZmADA2*, the encoded interacting proteins would come close and a quasi ubiquitin moiety would be reconstituted. This would be recognised by ubiquitin specific proteases (UBP's), which would cleave the Arg-GFP from C_{ub} fusion vectors according to the N-end rule pathway (Varshavsky, 1996) resulting in the loss of fluorescence in the co-transformed cells. [N-end rule refers to the relationship between the metabolic stability of a protein and the identity of its N-terminal residue]. On the other hand, if no interaction takes place the reporter would remain attached to the C_{ub} and can be visualised. When BY2 protoplasts are transfected with a fluorescent protein only about 25-30% of cells show transient protein expression after 18-24 hours. In this situation it would be impossible to identify the cells co-expressing the fusion proteins because if the interaction takes place the reporter would be cleaved and there would be no difference between the transformed and the untransformed cells. In order to circumvent this problem it was decided to use 35S::dsRed as the second fluorescent marker to identify the viable, transformed cells. The assumption being that if cells are co-transfected with equimolar amounts of both N_{ub} and C_{ub} fusion proteins, as well as 35S::dsRed, the interaction between two proteins would lead to the cleavage and degradation of the reporter attached to C_{ub}, while the 35S::dsRed would still be expressed in the cells. This assumption is based on the fact that a cell competent to be transformed does not discriminate between the type of incoming DNA (Potrykus, 1990) and if equimolar ratios of the plasmids are used one can expect the cell to take up equimolar amounts of the different types of incoming DNA provided. In order to test the above assumption BY2 protoplasts were co-transfected with 35S::GCN5-GFP (nuclear targeted) and 35S::dsRed and the protein expression was visualised under fluorescent microscope with filters specific for GFP and dsRed based fluorescence. Out of the total 25-30% transfected protoplasts, almost 95% showed the expression of both fluorescent proteins (see figure 5.4). In the remaining 5% of the cells the expression levels of one or the other fluorescent protein were very low.

Having established that the double transfection was working as predicted, it could be used to detect the specific protein-protein interactions using the modified split-ubiquitin system. BY2 protoplasts were transfected

with different permutations of reporter plasmids (table 5.1) and the possible interactions were checked under the fluorescence microscope.

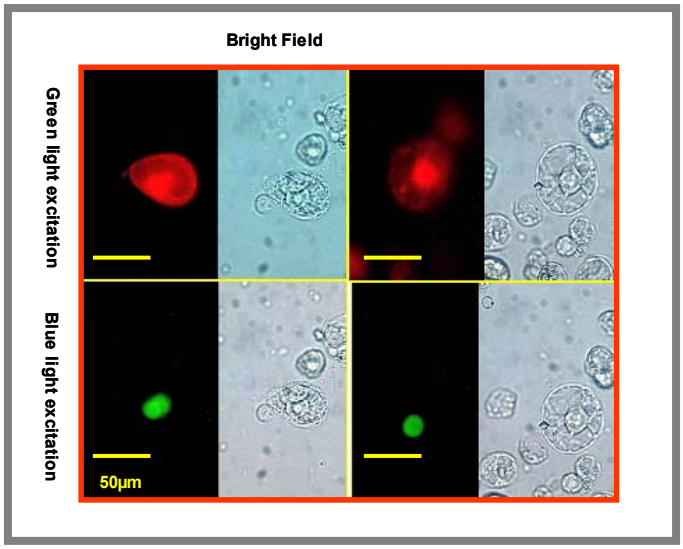

Figure 5.4) Double transfection of BY2 protoplasts with 35S::dsRed and 35S::Gcn5-GFP. Upper panel shows protoplasts seen under dsRed specific excitation and the lower panel shows same protoplasts visualised under GFP specific excitation. For contrast the bright field images are also shown.

Different permutations	1	2	3	4	5	6	7
35S::ZmGCN5-C_{ub}-Arg-GFP	+	-	-	+	+	-	+
35S::N_{ub}-ZmADA2	-	+	-	+	-	+	+
35S::ds Red	-	-	+	-	+	+	+
Expected interaction scenario	GF	NF	RF	NF	GF+RF	RF	RF

GF = Green Fluorescence; NF = No Fluorescence; RF = Red Fluorescence.

Table 5.1) BY2 protoplast transfection scheme for checking interaction between ZmGCN5 HAT and the Adaptor ZmAda2 using modified Split-ubiquitin system.

5.2.2 The split-ubiquitin system detects a strong *in vivo* interaction between ZmGcn5 HAT and the adaptor ZmAda2

The *ZmGCN5* gene encodes a protein of 515 amino acid residues. The central part of the Gcn5 polypeptide is responsible for interaction with adaptor protein Ada2 (Marcus *et al.,* 1994). The modified split-ubiquitin system, as

described above, was used to determine the interaction between ZmGcn5 and ZmAda2 in living plant cells. BY2 protoplasts were transfected with 35S::*ZmGCN5*-C_{ub}-Arg-GFP, 35S::*ZmADA2*-N_{ub} and 35S::dsRed in different combinations and the transient gene expression was observed after 24-36 hours. The results are shown in figure 5.5.

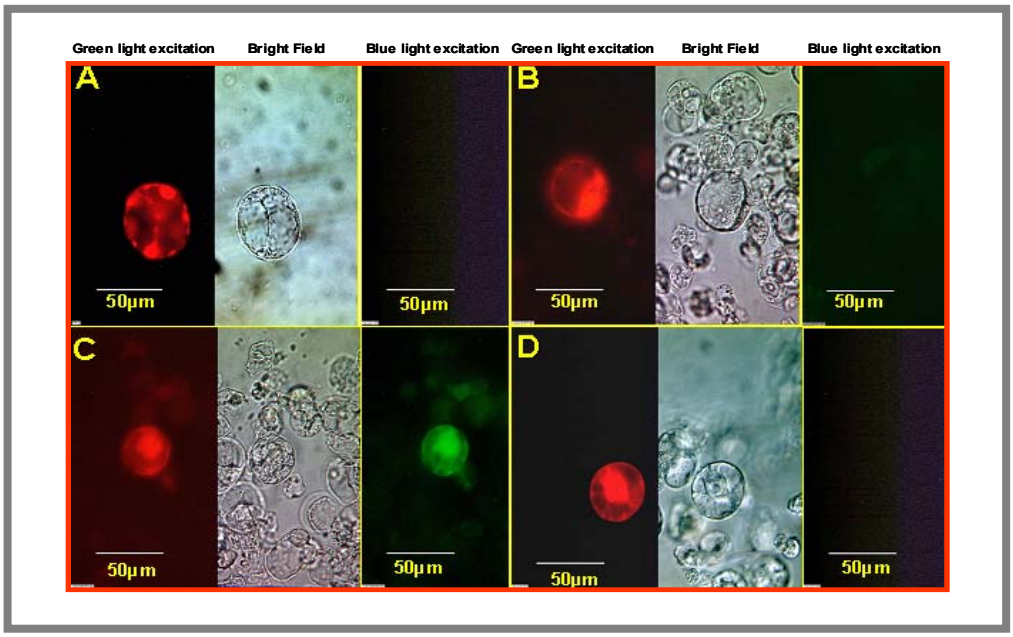

Figure 5.5) Modified Split-ubiquitin system detects specific and strong *in vivo* interaction between ZmGcn5 and ZmAda2 in BY2 protoplasts. (A) Protoplasts transfected with 35S::dsRed alone (B) Protoplasts transfected with 35S::dsRed and ZmADA2-N_{ub} (C) Protoplasts transfected with ZmGCN5-C_{ub}-Arg-GFP and 35S::dsRed (D) Protoplasts transfected with ZmGCN5-C_{ub}-Arg-GFP, ZmADA2-N_{ub} and 35S::dsRed. Protoplasts were transfected with above plasmids and the transient gene expression was observed after 24-36 hours under a fluorescence microscope. Bright field images are shown for comparison.

Co-transfecting protoplasts with 35S::ZmGCN5-C_{ub}-Arg-GFP and 35S::dsRed resulted in the transient expression of both proteins inside the BY2 protoplasts (figure 5.5, C). However it is worth noting that the GFP fluorescence was observed throughout the cell. This was somewhat of a surprise as the ZmGcn5 contains an NLS and the fusion protein (ZmGCN5-C_{ub}-Arg-GFP) should have been targeted to the nucleus. By analysing the C_{ub} portion of the fusion protein using PSORT computer prediction (PSORT-http://psort.nibb.ac.jp/), it became clear that the C_{ub} contains a predictable cytoplasmic localisation signal, thus accounting for the fluorescence in the cytoplasm. On the other hand, co-transfecting BY2 protoplasts with 35S::*ZmGCN5*-C_{ub}-Arg-GFP, 35S::*ZmADA2*-N_{ub} and 35S::dsRed resulted in

the loss of GFP signal in the co-transfected protoplasts while the red fluorescence could still be observed (see figure 5.5, D). This suggested that interaction between ZmGcn5 and ZmAda2 had led to the reconstitution of quasi ubiquitin moiety, which being recognised by UBPs resulted in the cleavage and loss of GFP fluorescence.

Around 100-150 co-transfected protoplasts were analysed for each permutation and the experiment was repeated three times. The same results were obtained each time, suggesting a specific and strong *in vivo* interaction between ZmGcn5 HAT and the adaptor ZmAda2.

5.3 The fluorescence resonance energy transfer (FRET) system

The modified split-ubiquitin system detected a specific and strong interaction between ZmGcn5 HAT and the adaptor ZmAda2. However the system as described above did not differentiate whether the interaction took place in the cytoplasm or in the nucleus. Fluorescence resonance energy transfer (FRET) is an elegant system to address this question. FRET is a dipole-dipole resonance interaction between two close molecules where one molecule, called the “donor” transfers its excitation energy to the other molecule, called the “acceptor” (Mergny *et al.,* 2001, Kenworthy, 2001). FRET occurs when the distance between the donor and the acceptor is less than 1.5 x Förster radius (R_o) for energy transfer (Gadella *et al.,* 1999). Förster radius is the distance between donor and acceptor at which the FRET efficiency is 50% i.e. 50% of the excitation energy absorbed by the donor is transferred to the acceptor. One prerequisite for FRET is that the absorption spectrum of the acceptor fluorophore must overlap with the emission spectrum of the donor. FRET is manifested in different ways:

a) a decrease in the donor fluorescence quantum yield determined by FSPIM (fluorescence spectral imaging microscopy),
b) a decreased donor fluorescence lifetime,
c) an increased stability of the donor if the acceptor fluorophore is photo-bleached (Jovin and Arndt-Jovin, 1989) and
d) an increased (sensitised) acceptor fluorescence emission, if the acceptor is a fluorophore (Wu and Brand 1994; Clegg, 1995).

Chromophore-mutated GFPs show an excellent spectral overlap and hence good FRET pairs can be made using available GFPs (Pollok, *et al.,* 1999). Cyan and yellow fluorescent mutants of GFP *viz.* CFP and YFP have been widely used for FRET studies in living cells (Gadella *et al.,* 1999). Two separate fusion proteins - one containing CFP (cyan emitting GFP) and the other, its putative interacting partner containing YFP (yellow emitting GFP) - are coexpressed in the cell type of choice. If intermolecular FRET is detected (see figure 5.6), it provides direct proof of close proximity of the CFP and YFP chromophores and consequently of the existence of the protein-protein interaction.

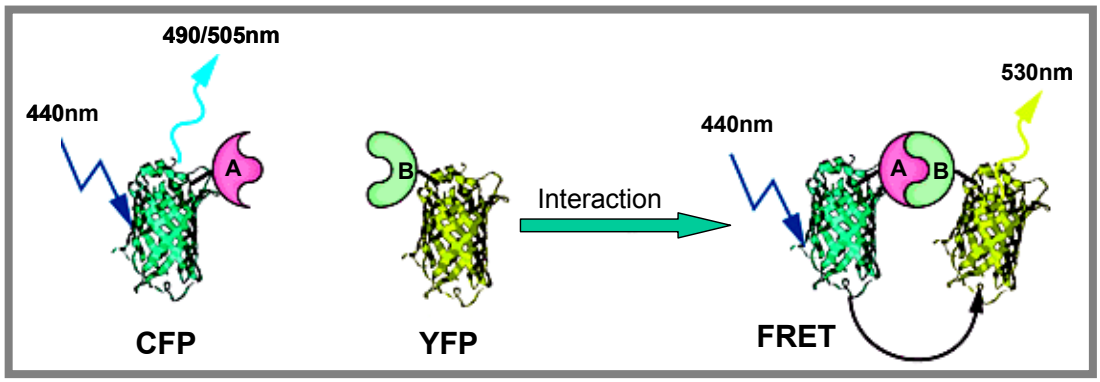

Figure 5.6) Detection of protein interactions with FRET. FRET between cyan fluorescent protein (CFP) fused to protein A and yellow fluorescent protein (YFP) to protein B. Under optimal proximity and angular conditions, interaction between A and B causes a decrease in intensity of CFP fluorescence concomitant with an increase in YFP fluorescence (adopted from Gadella *et al.,* 1999).

FRET has been successfully used to detect protein-protein interactions in plant cells (Gadella *et al.,* 1999). FRET was used to augment the results obtained from modified split-ubiquitin system and also to study the interaction and colocalisation of ZmGcn5 histone acetyltransferase, the adaptor protein ZmAda2 and plant transcriptional activator ZmO2 in living plant cells.

5.3.1 *In vivo* FRET to study interaction between ZmGcn5, ZmAda2 and plant transcriptional activator ZmO2

cDNAs of *ZmGCN5*, *ZmADA2* and *ZmO2* were translationally fused to CFP and YFP in pMon 999 vector (Shah *et al.,* 2001). *Nco*I restricted PCR fragments of *ZmGCN5* and *ZmADA2* were cloned into *Nco*I site of pMON999-

CFP and pMON999-YFP vectors to create *ZmGCN5*-CFP, *ZMGCN5*-YFP, *ZmADA2*-CFP and *ZmADA2*-YFP vectors. Similarly *Cla*I/*Xba*I restricted ZmO2 fragment was cloned into the *Cla*I/*Xba*I digested pMOn999-CFP and pMON999-YFP vectors. The primers used for generating PCR fragments (*viz.* *Nco*IGcn5Fwd, *Nco*IGcn5Rev, *Nco*IAda2Fwd, *Nco*IAda2Rev, *Cla*IO2Fwd, *Xba*IO2Rev) are listed in section 2.1.3.4. Summary maps of the vectors are shown in appendix I.

5.3.2 Colocalisation of ZmGcn5 HAT, adaptor ZmAda2 and plant transcriptional activator ZmO2 in living plant cells

For this purpose transient gene expression in cowpea protoplasts was utilised (see section 2.2.10.2). Protoplasts were co-transfected with either 35S::*ZmGCN5*-CFP/YFP and 35S::*ZmADA2*-YFP/CFP or 35S::*ZmO2*-CFP/YFP and 35S::*ZmADA2*-YFP/CFP. After transfection and incubation for 18-24 hours, the protoplasts were analysed under the confocal laser-scanning microscope (CLSM 510, Zeiss). The results are shown in Figure 5.7.

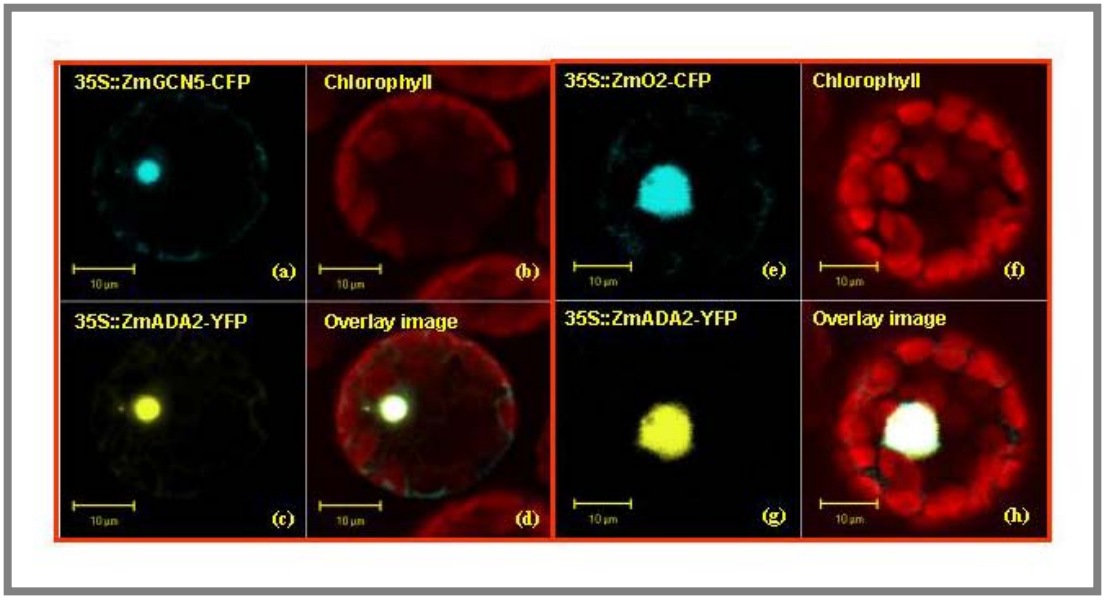

Figure 5.7) Colocalisation of ZmGcn5/ZmAda2 and ZmO2/ZmAda2 in cowpea mesophyll protoplasts. (a-d) Confocal images of the protoplasts co-transfected with 35S::*ZmGCN5*-CFP 35S::*ZmADA2*-YFP. The two fluorophores, CFP and YFP, were simultaneously visualised. Chlorophyll autofluorescence is shown in Red (b). Colocalisation of ZmGcn5 and ZmAda2 is shown in yellowish white fluorescence (d) resulting from the overlay of (a) and (c). **(e-h)** Confocal images of the protoplasts co-transfected with 35S::*ZmO2*-CFP and 35S::*ZmADA2*-YFP. The chlorophyll autofluorescence is shown in red (f). Colocalisation is shown by yellowish white fluorescence (h) resulting from the overlay of (e) and (g).

Figure 5.7 (a-d) shows the colocalisation of ZmGcn5 and ZmAda2 while (e-f) shows the co-localisation of ZmO2 and ZmAda2. For comparison chlorophyll autofluorescence is shown in red. From the combined images (Figure 5.7d) it is clear that the targeting and the localisation pattern of ZmGcn5 and ZmAda2 completely overlap inside the nucleus suggesting that the interaction between these two co-activator proteins occurs inside the nucleus. Hardly any fluorescence is detected outside the nucleus.

The overlay image for ZmO2 and ZmAda2 (figure 5.7 h) also shows considerable overlap inside the nucleus although some ZmO2-CFP fluorescence is scattered outside the nucleus.

5.3.3 FRET studies between ZmGcn5, ZmAda2 and ZmO2

In order to directly study the physical interaction between ZmGcn5 histone acetyltransferase, the adaptor ZmAda2 and plant transcriptional activator ZmO2 in living plant cells, the CFP and YFP fusion proteins were used as a donor-acceptor pair in FRET studies. Fluorescence spectral imaging microscopy (FSPIM) was used as a detection system in all FRET studies (see section 2.2.11.3). Spectral images were taken from small regions within the nucleus co-expressing CFP and YFP fusion proteins, and also outside the nucleus, and the fluorescence emission spectrum corrected for background was generated. In case of FRET, the CFP fluorescence will be quenched and the YFP fluorescence will be increased (sensitised).

FRET was performed between ZmGcn5 HAT and the adaptor ZmAda2 and between transcription factor ZmO2 and the adaptor ZmAda2 proteins fused either to the donor (CFP) or the acceptor (YFP) molecules. This was to ensure that any observed FRET was not due to an unbalanced expression ratio of the target proteins. In all experiments where FRET was observed, the changes in fluorescence intensity were same irrespective of whether donor CFP was fused to one protein or the other.

5.3.2.1 FRET between ZmGcn5 HAT and the adaptor ZmAda2

Protoplasts were co-transfected with either 35S::*ZmGCN5*-CFP and 35S::*ZmADA2*-YFP or 35S::*ZmGCN5*-YFP and 35S::*ZmAda2*-CFP. Both these fusion proteins showed tight nuclear targeting and thus the spectral

images were recorded from the different regions within the nucleus co-expressing ZmGcn5-CFP and ZmAda2-YFP fusion proteins (figure 5.8,a).

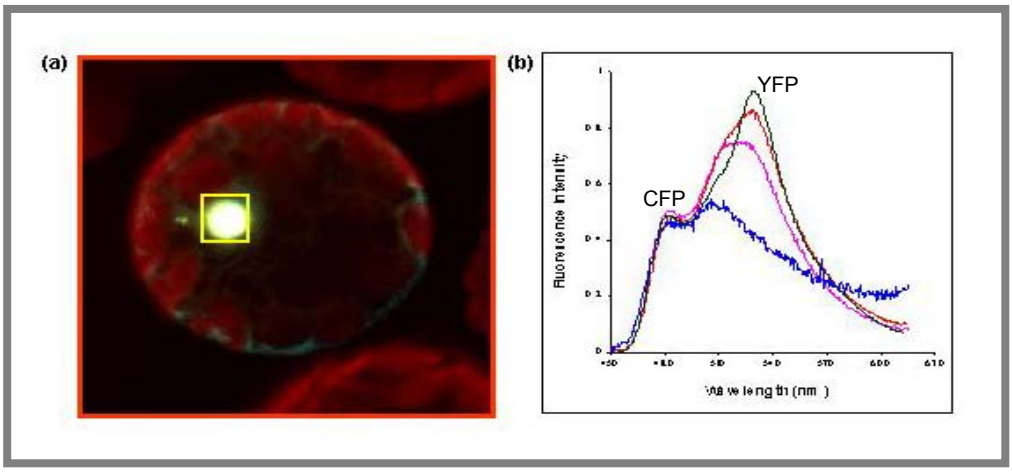

Figure 5.8) FSPIM analysis of fluorescent ZmGcn5-CFP and ZmAda2-YFP fusion proteins. (a) Confocal image of a protoplast co-transfected with 35S::*ZmGCN5*-CFP and 35S::*ZmADA2*-YFP. The two fluorophores, CFP and YFP, were visualised simultaneously and the overlay image is shown. Space within the rectangle shows the region used for spectral measurements. (b) Emission spectra of the ZmGcn5-CFP and ZmAda2-YFP proteins obtained from the nucleus of the co-expressed protoplasts. The X-axis represents the wavelengths of CFP and YFP fluorophores and the Y-axis represents their intensities. CFP emission occurs at 480 and 505 nm while YFP emission occurs at 525-530nm. The blue curve shows the normal spectrum of CFP alone.

In almost all the measurements the YFP/CFP fluorescence intensity ratio was found to be above 1.5. A ratio of fluorescence intensity at 530 nm over 480 nm (designated as the YFP/CFP emission ratio) of 1.3 or above is taken as a sufficient evidence of FRET (Shah *et al.,* 2001). When the spectra were recorded from 15 protoplasts each co-expressing ZmGcn5-CFP and ZmAda2-YFP or ZmGcn5-YFP and ZmAda2-CFP, the YFP/CFP ratio was more than 1.5 in about 95% of the measurements (data not shown).

In order to rule out the possibility that the increased YFP intensity was due to unbalanced ratio of CFP and YFP in the protoplasts, acceptor photobleaching experiments were performed. The rationale behind the experiment is that if the energy transfer from donor fluorophore (CFP) to acceptor fluorophore (YFP) is disrupted by photobleaching of YFP, the donor emission should increase over a short period of time till the acceptor again becomes available and the FRET is re-established. YFP fluorophore was bleached from the ZmGcn5-CFP and ZmAda2-YFP co-expressing cells using the photo bleaching function of Carl-Zeiss laser scanning microscope (3 iterations with 100% laser power at 514nm). The images of both the

fluorophores before and after bleaching were recorded and are shown in figure 5.9.

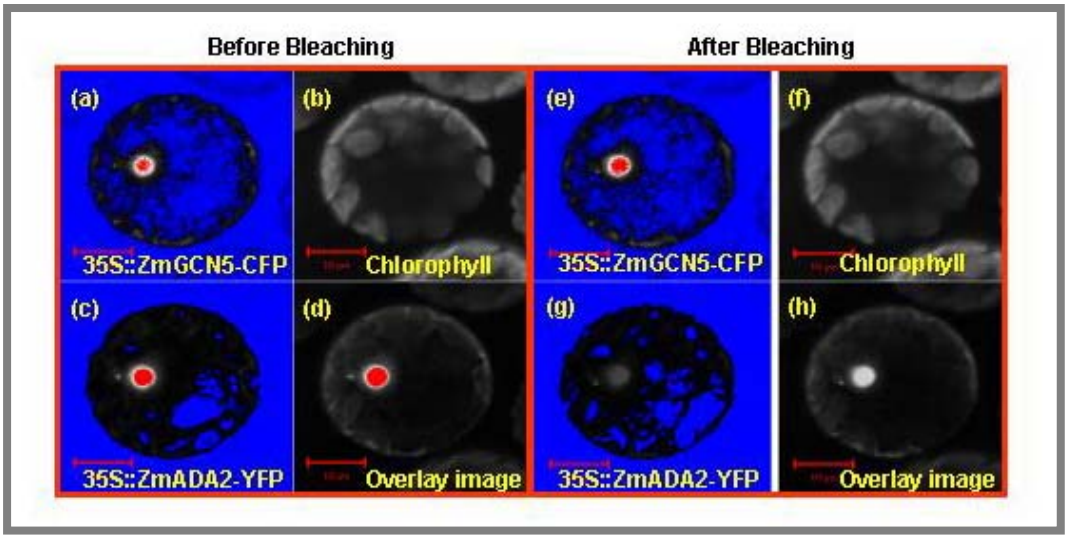

Figure 5.9) Acceptor photobleaching to confirm the FRET between ZmGcn5-CFP and ZmAda2-YFP. (a-d) Confocal images before photobleaching. (a) ZmGcn5-CFP fluorescence before photobleaching of YFP. (c) ZmAad2-YFP fluorescence before photobleaching. (d) The superimposed images of (a) and (c) result in overlay image in (d). **(e-h)** Confocal images of the same protoplasts after photobleaching. (e) Increase in CFP fluorescence after photo bleaching. (g) Photobleached ZmADA2-YFP. (h) Superimposed images of (e) and (g) result in the overlay in (h). (b and f) show chlorophyll autofluorescence. The images are false coloured to show the changes in fluorescence intensities.

When the YFP fluorophore was bleached there was a sharp and sudden increase in the intensity of CFP (figure 5.9, a and e). This proved beyond any doubt that the physical interaction between ZmGCN5 and ZmAda2 brought the fluorophores, CFP and YFP, fused to these proteins, close together to facilitate the energy transfer from the donor to acceptor. These results show that when the ZmGcn5 histone acetyltransferase and the adaptor protein ZmAda2 are targeted to the nucleus they interact physically, supporting the results obtained from modified split-ubiquitin system and the GST spin down experiments.

5.3.2.2 FRET between adaptor ZmAda2 and plant transcriptional activator ZmO2

Protoplasts were co-transfected with either 35S::*ZmO2*-CFP and 35S::*ZmAda2*-YFP or 35S::*ZmO2*-YFP and 35S::*ZmAda2*-CFP. Spectral images of the fusion proteins were recorded from the different regions within

the nucleus co-expressing ZmGcn5-CFP and ZmAda2-YFP fusion proteins. The results are shown in figure 5.10.

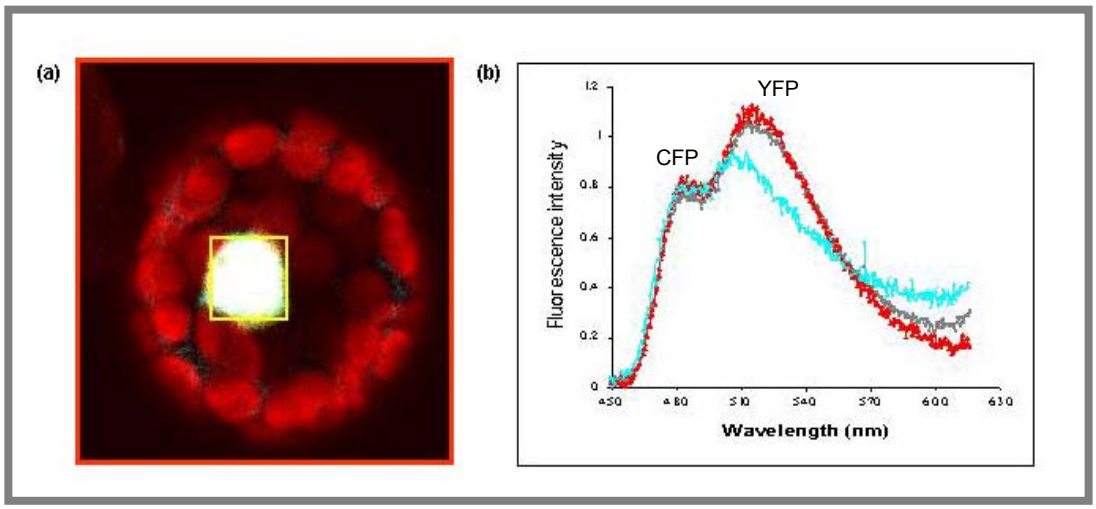

Figure 5.10) FSPIM analysis of fluorescent ZmO2-CFP and ZmAda2-YFP fusion proteins. (a) Confocal images of a protoplast co-transfected 35S::*ZmO2*-CFP and 35S::*ZmADA2*-YFP. The two fluorophores CFP and YFP were visualised simultaneously and the overlay image is shown. Space within the rectangle shows the region used for spectral measurements. (b) Emission spectra of ZmO2 and ZmAda2 proteins obtained from within the nucleus of the co-transfected protoplasts. The blue curve shows the normal spectrum of CFP alone.

When the spectral images were obtained from protoplasts co-expressing ZmO2-CFP and ZmAda2-YFP at the nuclear periphery the YFP/CFP fluorescence intensity ratio were close to 1.0 in all of the measurements suggesting that no interaction occurs between ZmO2 and ZmAda2 at the nuclear periphery (data not shown). However when the spectra were recorded inside the nucleus a noticeable shift in spectra could be observed (figure 5.10 b). The YFP/CFP ratios were close to 1.3 in roughly 3 out of 5 measurements. About 55-60% of the protoplasts showed an increased YFP/CFP ratio of 1.3 when the spectra were recorded from 15 protoplasts co-expressing ZmO2-CFP and ZmAda2-YFP proteins inside the nucleus.

Acceptor photobleaching experiments were performed for this pair of fusion proteins as well. The images of the representative protoplasts before and after photobleaching are shown in figure 5.11. When the YFP fluorophore fused to ZmAda2 was bleached from the cells co-transfected with ZmAda2-YFP and ZmO2-CFP, there was a substantial increase in the CFP

fluorescence (figure 5.11 a and e). Though the increase was not as drastic as seen for ZmGcn5-CFP/ZmAda2-YFP FRET, it could still be clearly observed.

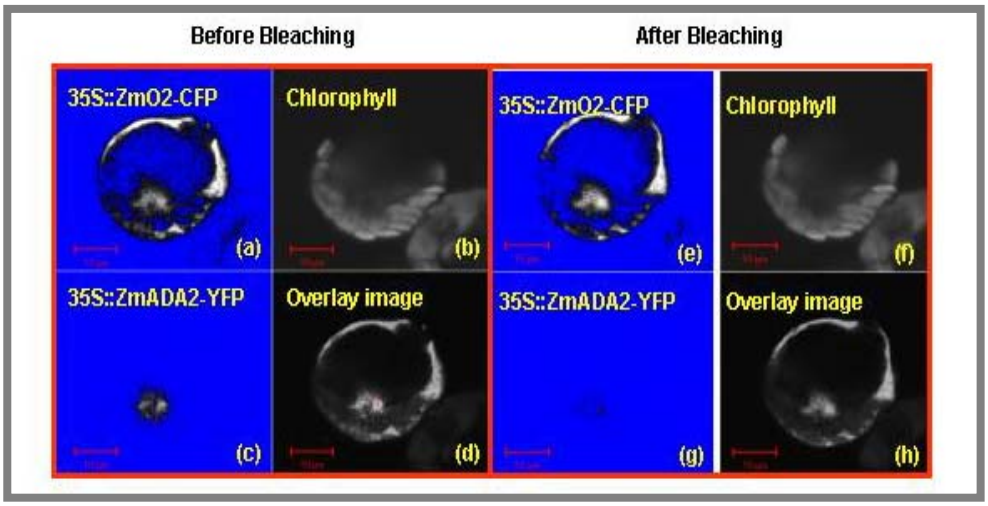

Figure 5.11) Acceptor photobleaching to confirm the FRET between ZmO2-CFP and ZmAda2-YFP. (a-d) Confocal images before photobleaching. (a) ZmO2-CFP fluorescence before photobleaching of YFP. (c) ZmAda2-YFP fluorescence before photobleaching. (d) The superimposed images of (a) and (c) result in overlay image in (d). **(e-h)** Confocal images of the same protoplasts after photobleaching. (e) Increase in CFP fluorescence after photobleaching. (g) Photo-bleached ZmADda2-YFP. (h) Superimposed images of (e) and (g) result in the overlay in (h). (b and f) show chlorophyll autofluorescence. The images are false coloured to show the changes in fluorescence intensities.

Taken together, these results show that the ZmO2 can physically interact with ZmAda2 inside the nucleus. However the interaction seems to be weak and presumably transient in nature.

Biological impact of histone acetylation

6.1 Introduction

Regulation of gene expression mostly occurs at the level of transcription. The transcription initiation machinery includes factors that bind to DNA, cyclin dependent kinases that regulate the polymerase activity and non-DNA binding histone acetylases and other enzymes that modify chromatin (Roth and Allis, 1996). Cells respond to a variety of changes in their environment, growth and development by switching on and off certain gene products. How much each of these factors contributes to the global gene expression is not clearly understood. Moreover the precise interaction of these factors with the transcription machinery is not clear as well. Histone acetylation and deacetylation has long been connected to transcriptional activation and repression (Struhl, 1998). With the isolation of specific histone acetyltransferases and deacetylases from animals, plants and fungi (Lusser *et al.,* 1999), efforts have been directed to dissect the specific role of these enzymes. Genome-wide expression monitoring is increasingly being used as a tool to study the downstream targets of novel genes. Using this approach, ScGcn5 was shown to affect a total of 5% genes in a whole-genome oligonucleotide microarray experiment (Holstege *et al.,* 1998). The microarray technique was employed in the present study to dissect the role of ZmGcn5 acetylation on the overall chromatin status in maize. The study addressed the following questions:

a) How do cells respond to changes in histone acetylation at the transcriptional level? For this purpose histones were hyper-acetylated by using the deacetylase inhibitor Trichostatin A (TSA) on maize HE-89 cell line. The resultant treated and untreated mRNA population was used in a microarray experiment.
b) What are the specific targets of *ZmGCN5* acetylation? For this purpose maize HE-89 cell line was transformed with a construct expressing antisense mRNA strand of *ZmGCN5* coding sequence under the control of 35S promoter from cauliflower mosaic virus. The transgenic material was grown, checked by Northern and Western blots and

maintained as suspension cultures. Microarray experiments were done using the antisense *ZmGCN5* cell line and the control vector transformed cell line.

6.2 Histone Hyper-acetylation studies using Trichostatin A

6.2.1 TSA treatment results in a dosage dependent acetylation response in maize cell lines.

To monitor the relationship between ZmGcn5 expression and changes in the acetylation status of chromatin, maize suspension cell line HE-89 was treated with the deacetylase inhibitor TSA. Cell lines were treated with different concentrations of TSA ranging from 0.5 µM to 5.0 µM for 10 hours and the acetylation status was determined by an immunoblot on crude nuclear extracts, run on a 15% SDS PAGE gel, using an antibody raised against acetylated lysines of histone H4 [(raised against histones acetylated at lysine position 5, 8, 12 and 16; purchased from Serotec) (figure 6.1, 6.2)].

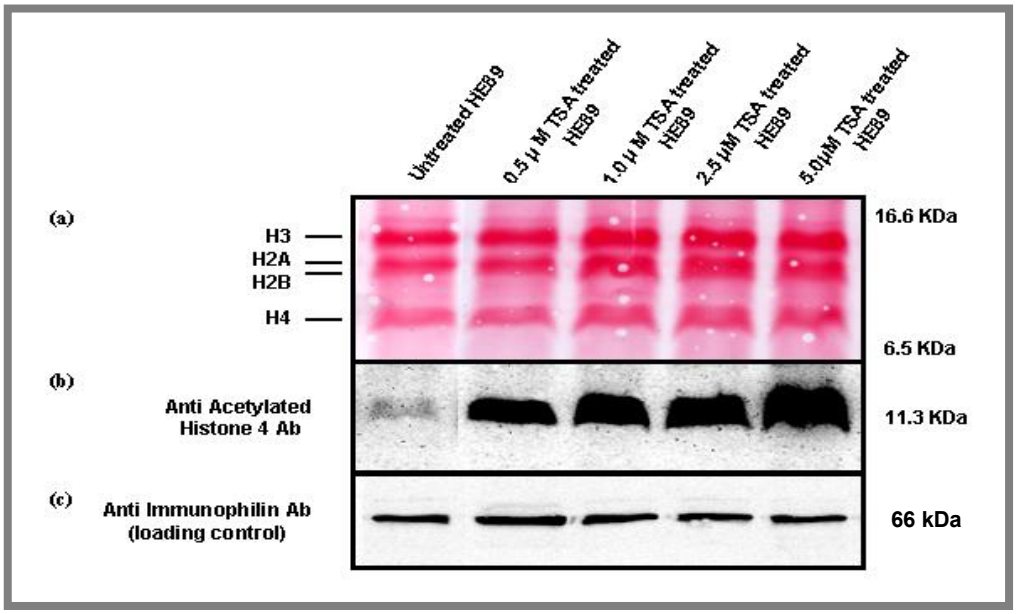

Figure 6.1) Acetylation status of Histone H4 on TSA treatment. Maize HE-89 cell line was treated with different concentrations of TSA for 10 hours and crude nuclear extracts prepared from them were run on a 15% SDS PAGE gel and immunoblotted using anti acetylated histone H4 antibody. (a) Ponceau S staining showing the histone fraction. (b) Dosage dependent acetylation response on histone H4. (c) Immunophilin loading control (Hueros *et al.,* 1998).

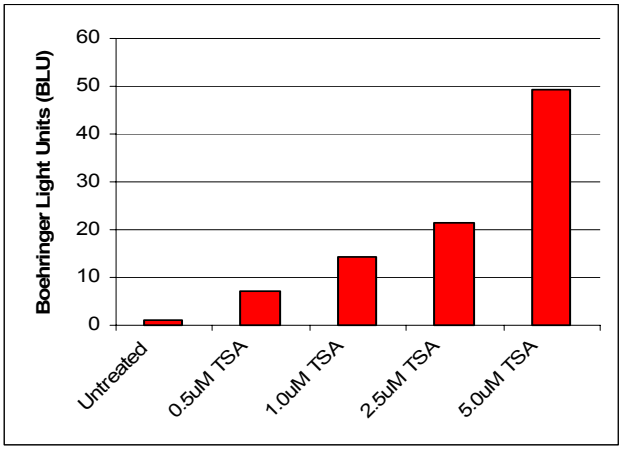

Figure 6.2) Dosage dependent acetylation of Histone H4 on TSA treatment. The Boehringer Light Units (BLU) were calculated using the Lumi-imager software from Boehringer Mannheim and GCN5/Immunophilin ratios were calculated and normalized taking untreated control as 1 BLU.

Acetylation on histone H4 showed an increase with the increasing amounts of TSA (figure 6.1 and 6.2). Even the lowest amount of TSA (0.5 µM) lead to a 7-fold increase in acetylation on histone H4 while the antibody could barely detect the basal/under-acetylated levels in the untreated control.

6.2.2 Increase in acetylation on TSA treatment is accompanied by decrease in ZmGcn5 levels.

In order to look at the levels of ZmGcn5 in TSA treated and untreated maize cell lines, crude nuclei were isolated (section 2.2.7.1) and run on a 10% SDS PAGE gel. The proteins, transferred onto a nitrocellulose membrane were probed with ZmGcn5 specific antibody. The antibody detects a 58 kDa ZmGcn5 histone acetyltransferase. As a loading control an antibody raised against maize immunophilin (Hueros *et al.,* 1998) was used. An Increase in the concentration of TSA resulted in decreasing amounts of the ZmGcn5 protein levels in the cell. The results are shown in figure 6.3.

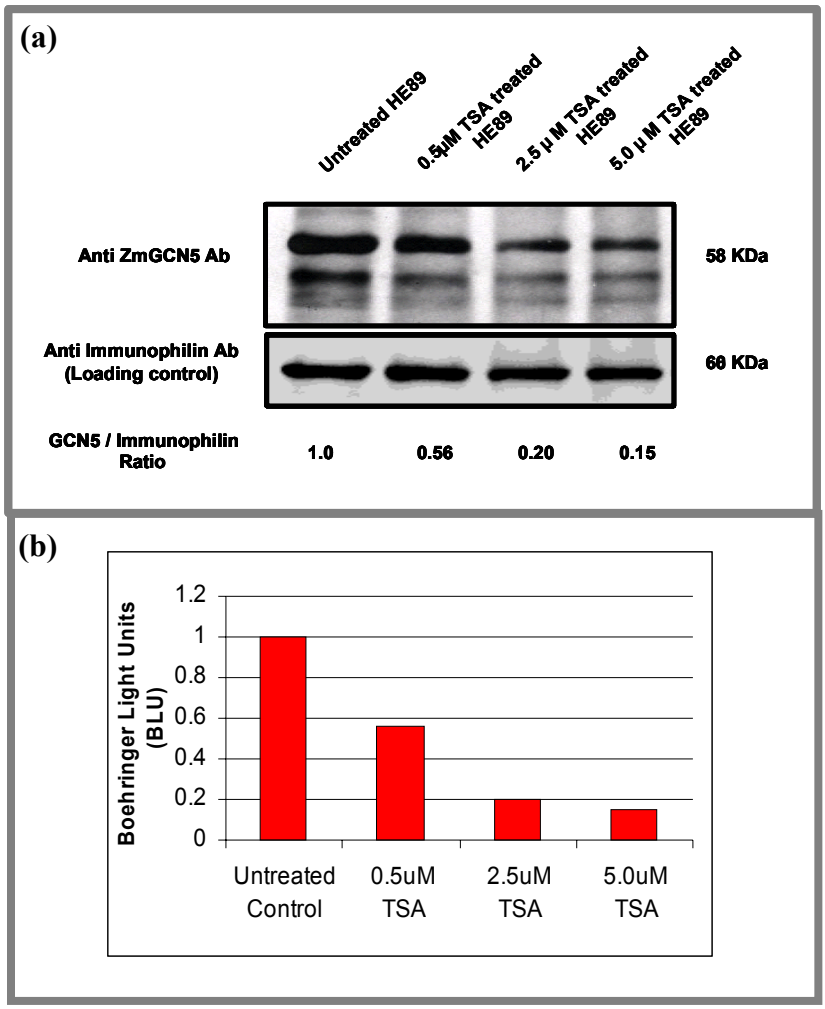

Figure 6.3) ZmGcn5 levels in TSA treated and untreated maize HE-89 cell line. (a) Immunoblot on crude nuclear proteins with anti ZmGcn5 antibody. As a loading control an antibody raised against maize immunophilin was used (Hueros *et al.,* 1998). (b) The BLU values obtained using Lumi-imager software were used to calculate ZmGcn5/Immunophilin ratio and normalised taking untreated control as 1 BLU.

6.2.3 Microarray analysis on TSA treated and untreated cell lines

Microarray technique was used to analyse the changes in gene expression on changing the acetylation status of the cell either by TSA treatment or by genetically manipulating the ZmGcn5 levels (discussed later). Since the changes in the ZmGcn5 protein levels were more pronounced for the 2.5 μM and 5.0 μM TSA concentrations cell lines from these treatments were used in the microarray experiment. Total RNA was isolated from the cell lines after 10 hours of TSA treatment (section 2.2.4.1 and 2.2.13) and used as a template for synthesis of radiolabeled first strand cDNA (see section 2.2.5.2). This was then used to hybridise 2600 maize ESTs spotted onto the

nylon filters. The spotting plan and the complete list of clones along with probable identities can be found at the Thompson Lab web page under http://www.mpiz-koeln.mpg.de/~riehl/ArrayDB/AllPlates.htm and http://www.mpiz-koeln.mpg.de/~riehl/ArrayDB/MzArrayDB.htm.

6.2.3.1 Correction and normalisation of array filters

For the identification of genes that are differentially expressed during different developmental stages or different treatments, two or more filters hybridised with RNA from each stage or treatment need to be compared. However direct comparison of these filters is difficult because of differences due to varying efficiencies of reverse transcription, probe purification, hybridisation and filter quality etc. In order to get reliable and reproducible data, these variations should be compensated for. Different types of controls were used in the present study to compensate for these errors. The controls were spotted at different positions on plate 3. The controls included:

- A cloning vector like pBluescript in order to assess the non-specific hybridisation. pBluescript was spotted in different concentrations (0.1, 1.0, 10 and 100 ng/µl) at positions N4, N6, N8 and N10.
- Reference genes like maize immunophilin (Hueros *et al.,* 1998) and barley ubiquitin (Gausing and Barkardottir, 1986). Different concentrations of Immunophilin (0.1, 1.0, 10 and 100 ng/µl) were spotted at H4, H6, H8 and H10. Similarly ubiquitin was spotted at positions H14, H16, H18 and H20 and also at N14, N16, N18 and N 20.
- An internal control non-coded by plants. These were cDNA's to Nebulin, Desmin and *uid*A gene, cloned into pBluescript SK(-). Nebulin was spotted in different concentrations (0.1, 1.0. 10 and 100 ng/µl) at positions D4, D6, D8 and D10. Similarly Desmin was spotted at position D14, D16, D18 and D20. The *uid*A gene was included at positions F4, F6, F8 and F10. These controls were included in order to provide an internal quantification standard that will not vary between probes and would permit a comparison between independent hybridisations.

6.2.3.2 Development of non-varying Nebulin poly A$^+$ RNA reference

Housekeeping genes are often used as internal references for the normalisation of array filters. However while comparing the unknown states of gene expression, the constancy of housekeeping genes cannot be assumed a priori (Eickhoff *et al.,* 1999). Furthermore there have been studies showing housekeeping genes being regulated (Savonet *et al.,* 1997; Bhatia *et al.,* 1994). A two-pronged strategy was used to circumvent these drawbacks. *Firstly* every hybridisation was repeated three to four times with two filters in each hybridisation. Only those filters that showed a correlation coefficient of 0.90 or higher, when hybridised with same probe, were included for final analysis. This compensated for the differences in filter quality, reverse transcription efficiency and hybridisation. Filters were hybridised with a particular probe only when the incorporation efficiency was more than 30%. Furthermore cross hybridisations were performed to rule out the differences in the amount of DNA spotted onto different filters. Mean or median values were calculated from the filter sets hybridised with same probes. Only after these considerations were the data sets from two different treatments compared. *Secondly* a synthetic Nebulin RNA was synthesised and added to the total RNA prior to cDNA synthesis. Important considerations for the inclusion of a non-varying reference were (i) being an RNA molecule, (ii) presence of an oligo(A) tail for selection with oligo-dT cellulose as primer binding site for reverse transcription (iii) a sequence not related to the plant sequences, (iv) the presence of the hybridisation targets for the standards on the arrays and (v) an easy way of synthesis. Nebulin cDNA cloned into pBluescript SK(-) met all of these criteria.

The corresponding Nebulin gene was included in the gene collection (as described in the section 6.2.3.1). A known concentration of Nebulin RNA was added to each independent reverse transcription reaction, spiked together with plant total RNA used for each probe.

The Nebulin poly(A)$^+$ RNA was generated by an *in-vitro* transcription reaction on the Nebulin cDNA within pBluescript. (The work was done in collaboration with Heinz Albert-Becker, MPIZ). The schematic diagram of Nebulin cloned within the pBluescript SK(-) is shown in figure 6.4.

Figure 6.4) Nebulin cDNA in pBluescript. pBluescript was cut with *Bam*HI and the *in vitro* transcription was done using T7 RNA polymerase.

pBluescript containing the Nebulin cDNA was cut with *Bam*HI so that the *in-vitro* transcription product would terminate after the poly (A) tail and would not run into the vector. *In vitro* transcription was done in the presence of T7 RNA polymerase as described in section 2.2.4.2.

In order to test whether the synthesized Nebulin poly(A) RNA cross hybridises with the plant DNA present in the filters, a test hybridisation was carried out using 5 µg of Nebulin total RNA, which was reverse transcribed and used as a probe. No cross hybridisation was observed to any of the spotted plant DNAs or to the pBluescript background control (figure 6.5)

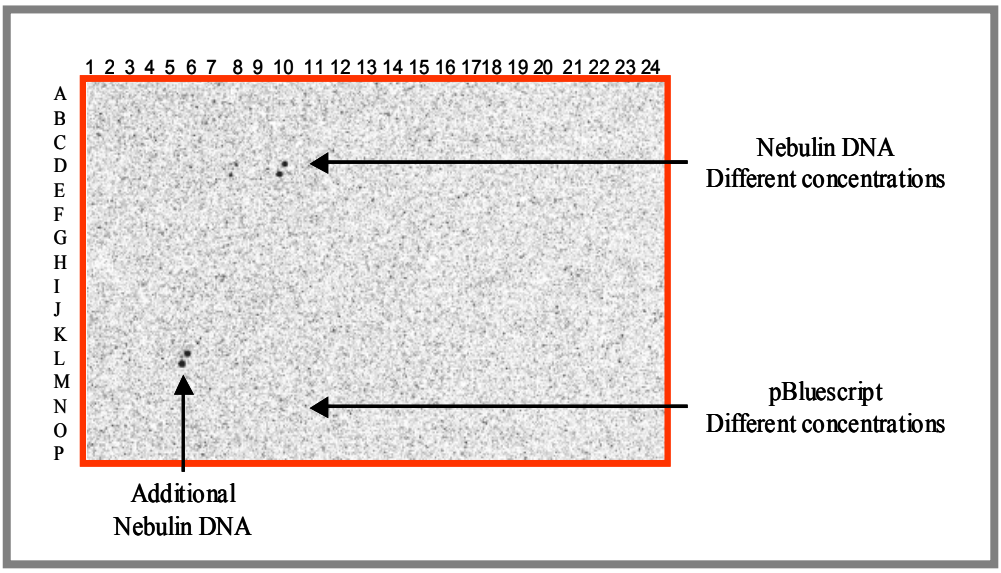

Figure 6.5) Cross-hybridisation test. A nylon filter was hybridised to the synthetic Nebulin cDNA probe. The Nebulin gene with pBluescript was included in the filters at positions D4, D6, D8, D10 and L6 as well as at L6. The pBluscript was included at positions N4, N6, N8 and N10.

6.2.3.3 Sensitivity of the microarray system

In order to determine the sensitivity and the linearity of the microarray system, a series of hybridisations was performed with increasing amounts of synthesised human Nebulin mRNA. Three different filters were hybridised with probes prepared from RNA containing between 0.01, 0.1, and 0.5% of

Nebulin RNA (in relation to the 30 µg of plant total RNA). The corresponding Nebulin cDNA clone was represented on the filters at known concentrations, ranging from 0.1 to 100 ng.

The linearity i.e., the amount of Nebulin probe proportional to the amount of Nebulin DNA on the filter was determined by plotting the amount of spiked Nebulin RNA against the amount of spotted Nebulin DNA. The plotted values are shown in the appendix II. The results are shown in figure 6.6.

When the percentage of Nebulin RNA was 0.01%, the values obtained showed a polynomial behaviour with a correlation coefficient of $R^2 = 0.97$. This implies that when the amount of Nebulin in the probe was 3 ng, inaccurate signal intensities were obtained for Nebulin cDNA spotted at concentrations between 10 -100 ng.

When the percentage of the Nebulin RNA was 0.1%, again the values obtained showed a polynomial behaviour with a correlation coefficient of $R^2 = 0.99$.

When the percentage of Nebulin cDNA in the probe was 0.5%, the resulting signal intensities were proportional to the amount of DNA spotted on the filters and a linear relation was obtained with a correlation coefficient of $R^2 = 0.99$. This implies that the detection system was more accurate and sensitive when the amount of spiked Nebulin was 150 ng and for the DNA spots with a concentration range between 10 to 100 ng.

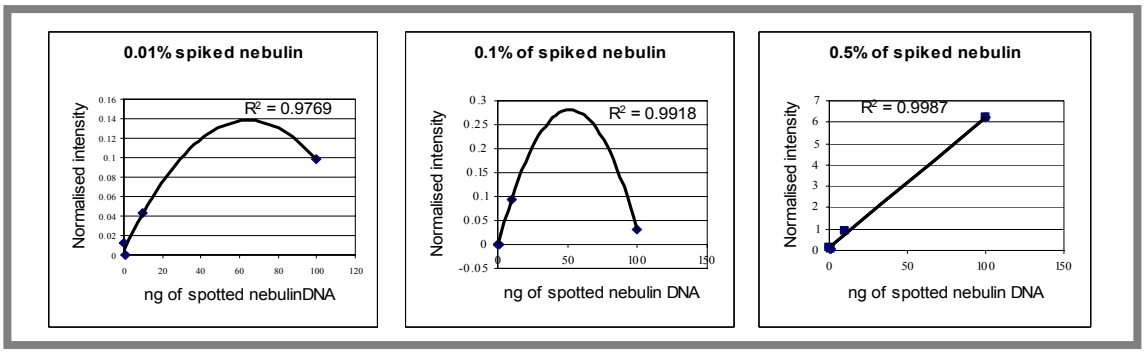

Figure 6.6) Sensitivity of microarray system. Different percentages of synthesised Nebulin were reverse transcribed and used in array filter hybridisations. The graphs show ng amount of Nebulin cDNA plotted against the normalised intensity of each spot after hybridisation with different percentages of synthesised Nebulin. (The plotted values are shown in appendix II).

Based on the above results, 0.5% of the Nebulin RNA was spiked together with the plant total RNA before starting the reverse transcription.

6.2.3.4 Quantification of the TSA treatment transcript profiles

The expression data obtained from the TSA treatments and control was compared and analysed quantitatively using the ArrayVision Software from Imaging Research Inc. Five hybridisations were carried out for each treatment and control with two filters in each hybridisation. In total 10 independent filters each were hybridised to cDNA prepared from 5 µM TSA treated, 2.5 µM TSA treated and untreated HE-89 total RNA respectively. The repetitions were performed in order to compensate for the errors (like varying efficiencies of reverse transcription, probe purification, hybridisation and filter quality etc) that might occur during the whole microarray procedure and thus to ensure the reproducibility of the profiles. Besides, in addition each DNA was spotted on the filters in duplicates, which allowed the assessment of reproducibility within the same experiment. Furthermore 150 ng of the synthetic Nebulin RNA was included in each cDNA probe synthesis reaction from 30 µg of total RNA. The hybridisation, washing and the exposure of the filters were carried out as described in section 2.2.6.3.

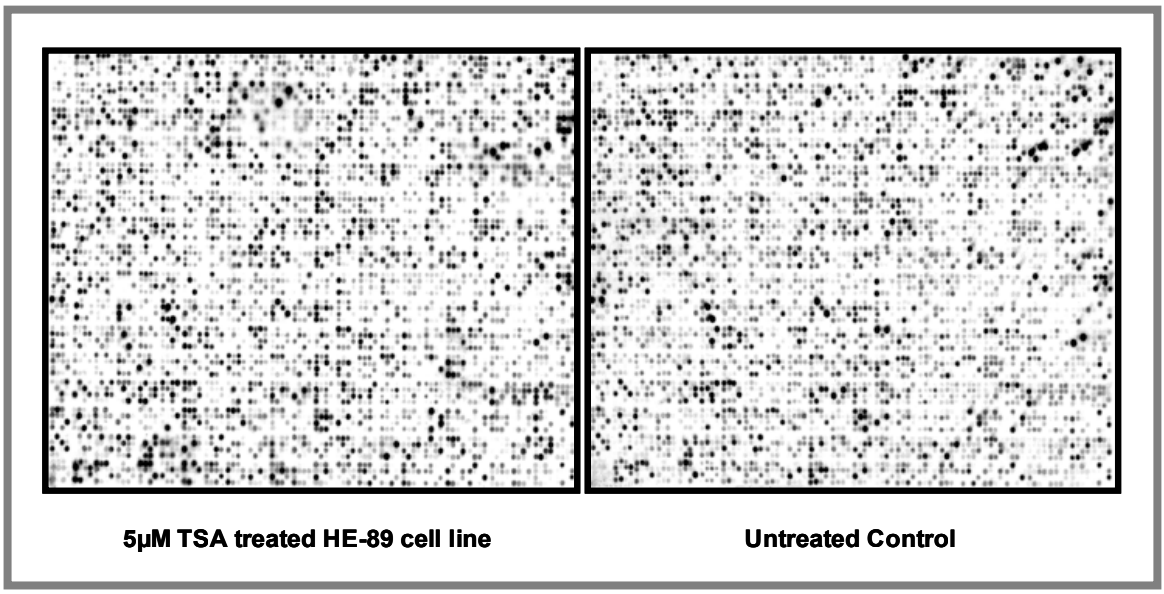

Figure 6.7) Nylon filters probed with radiolabeled cDNA prepared from RNA isolated from TSA treated and untreated *Z. mays* HE-89 cell lines.

After hybridisation and proper exposure, the radioactive signal on the array filters was read with a scanning device (Storm 860, Molecular

Dynamics) and the images were captured. Figure 6.7 shows an example of two filters hybridised with appropriate probes and scanned. The quantification of the signal intensity, normalisation and the subtraction of the local background were carried out using ArrayVision (ARV) software (see section 2.2.6.4).

In order to assess the reproducibility of the system, hybridisation signals obtained from repeats of each double spots on the same filter were compared by plotting the normalised intensity of the spot repetition 1 against the normalised intensity of the spot repetition 2. Comparison between the normalised hybridisation signals for duplicates of control and TSA-treated hybridisation experiments is shown in figure 6.8. The signals were reproducible, except for a small number of clones (between 5 to 10 clones per experiment, representing between 0.25 to 0.5% of the clones present on the filter). These clones were not included in the final analysis for the differential gene expression between the control and the treatment.

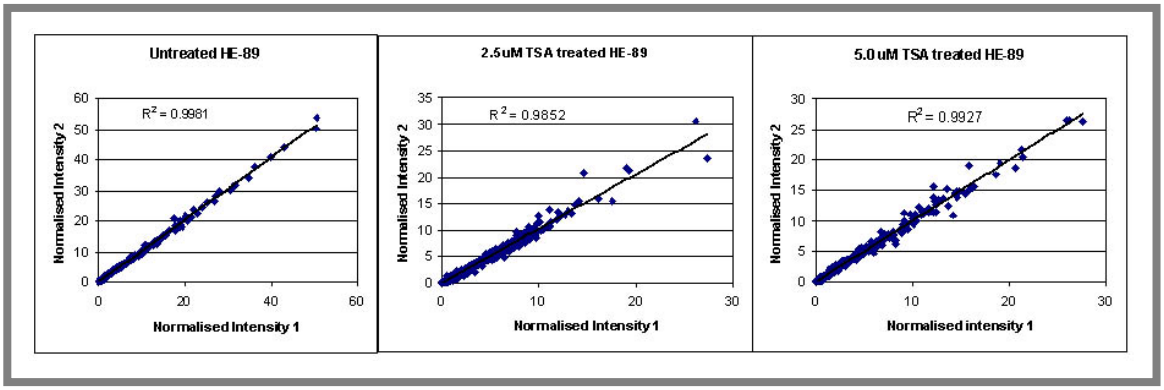

Figure 6.8) Reproducibility of hybridisation signals. Comparison of the normalised hybridisation signals for duplicates of spotted clones in three different hybridisation experiments. cDNA probes were prepared from untreated and TSA treated total RNA. For a small number of cDNA (representing between 0.25-0.5% of all clones) up to 2 fold variation was observed between the repeat values as a result of hybridisation artefacts in the TSA treated lines.

6.2.3.5 Differential gene expression between filters hybridised with cDNA prepared from control and TSA treated cell lines

For the analysis of the differentially expressed transcripts between the treatments and the control, basic mathematical and statistical tools were

applied to the data generated in the microarray analysis. Both concentrations of TSA treatments lead to a general increase in the gene expression levels. This was expected as TSA inhibits deacetylases, leading to hyper-acetylation of core histones associated with increased gene activity. The results are shown in the figure 6.9, where the values obtained from the treatments are plotted against those obtained from the control. The complete quantified and normalised hybridisation results can be viewed at www.mpiz-koeln.mpg.de/~riehl/ArrayDB/MzArrayDB.htm.

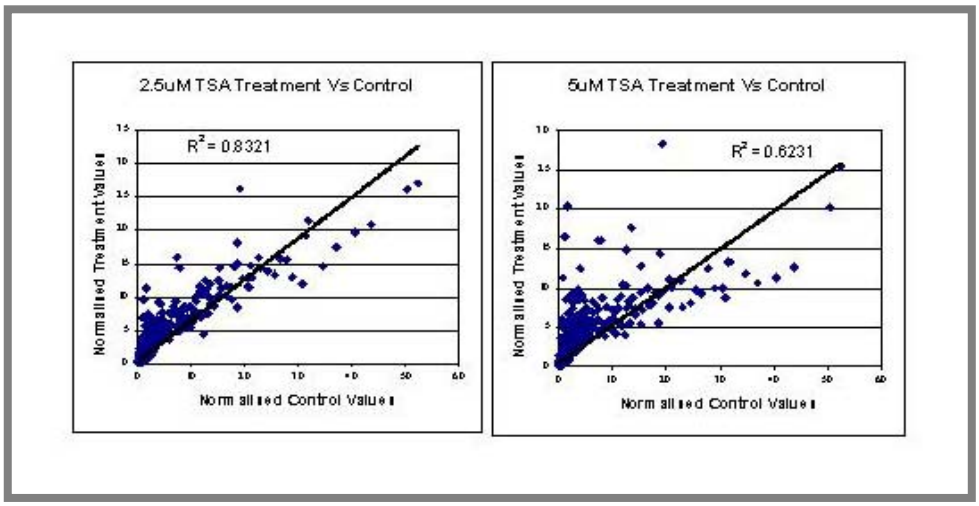

Figure 6.9) Scatter plots of Trichostatin A microarray experiments. Normalised values for TSA treatments were plotted against the normalised values for control.

Difference and ratio scores were used to compare the induction or repression of transcripts. The analysis was done using Microsoft Excel. The following relations were used for the calculation of genes up or down regulated by Trichostatin A treatment.

(a) Up-regulation:

$$\text{Ratio}_K = \frac{\text{Normalised Signal Intensity Sample}_K}{\text{Normalised Signal Intensity Control}}$$

Z score: $$z_k = \frac{(\Delta_K - \Delta mean)}{SD_\Delta}$$

Where : Δ_k = (signal intensity sample *K*) – (signal intensity control)

$$\Delta mean = \frac{\sum_{k=1}^{n} \Delta_k}{n}$$

$$SD_{\Delta} = \sqrt{\frac{\sum_{K=1}^{n} (\Delta_K - \Delta mean)^2}{n}}$$

Where K = 1…..n corresponding to each of the data on the array.

(b) Down-regulation:

$$Ratio_K = \frac{\text{Normalised Signal Intensity Control}}{\text{Normalised Signal Intensity Sample }_K}$$

Z score (as above), substituting the difference value with:

Δ_K = (signal intensity control) – (signal intensity sample *K*)

The normalised averages of the double spots were loaded in an Excel worksheet and the up and down regulated transcripts were identified using the above equations. Some basic criteria were followed in the identification of genes being up or down regulated.

- If the R_K > 2.0 and the Z_K score > 0 in the equation (a) the transcripts were considered to be up regulated.
- If the R_K > 2.0 and Z_K score < -0.15 in the relation b the transcripts were considered down regulated.
- The cut off limit (i.e. ratio between control/sample or sample/control) was taken as 2.0 in order to rule out any possible false positives.

Basic statistical analysis of the treatments permitted the identification of gene expression patterns. The %age of transcripts that were either up or down regulated in both treatments are summarised in table 6.1.

Transcript accumulation	2.5 µM TSA	5.0 µM TSA
Up-regulated	3.4%	3.4%
Down-regulated	0.5%	0.5%

Table 6.1) Percentage of transcripts regulated by Trichostatin A treatment. The percentages were calculated on the basis of a difference of 2 fold in the transcript expression levels of the treatment and control.

Both concentrations of TSA lead to almost same differential expression compared to untreated control. All the transcripts that were seen to be up regulated in 5.0 µM TSA treated material were up regulated in the 2.5 µM

TSA treated material as well, although the signal intensity in both cases showed variation (see figure 6.10). The same was true for the down-regulated clones. The clones that had signal intensity below 0.1 MDC (Molecular dynamics unit) on the filters were weeded out as they might have arisen because of background and therefore might not represent the real differences.

The up-regulated ESTs showing major changes (at least 2.7 fold) in the transcript levels on the TSA treatment (2.5 and 5.0 µM TSA) are shown in table 6.2. The down-regulated clones are shown in table 6.3.

Table 6.2 (Up regulated ESTs showing major changes in transcript levels on TSA treatment)

Array Data			Accession Number	Clone Identity	Random Matching Probability
Control HE-89	TSA treated HE-89	Fold Induction			
1.71	8.76	5.1	T70634	Histone 4/*Stylonychia lemnae*	2e-16
2.10	9.66	4.6	T14716	Histone H2.B/*Triticum aestivum*	2e-12
1.82	8.05	4.4	T14777	Histone H4/*Physarum polycephalum*	1e-20
1.12	4.93	4.4	AA072442	Histone H2.A/*Oryza sativa*	5e-06
1.23	5.32	4.3	T70691	Histone H2.A/*T. aestivum*	2e-08
2.45	9.48	3.8	T15325	Histone 2/*T. aestivum*	3e-21
3.81	12.67	3.3	P40280	Histone 2A/*Z. mays*	9.00E-23
2.71	9.07	3.3	T25236	Histone H2B.2/*O. sativa*	6e-24
2.37	7.73	3.2	W21621	Histone H2.B/*Z. mays*	1.00e-19
1.71	5.55	3.2	H35878	Histone 2B.1/*Z. mays*	1.00e-16
1.24	3.76	3.0	T70646	Histone 3/*Pisum sativum*	8e-39
3.82	10.55	2.8	T23357	Histone 3/*T. aestivum*	2e-50
3.36	9.66	2.7	T14800	Histone 3/*A. thaliana*	1e-55
2.06	5.55	2.7	T23405	Histone 2B/*Z. mays*	3e-15
0.10	0.75	7.0	AAF65195	Leucine rich repeat protein FLR1/*A. thaliana*	1.00E-21
0.47	2.30	4.8	T69041	Cysteine proteinase/*A. thaliana*	8e-50
0.29	1.38	4.7	T18839	Heat Shock Protein 70/*O. sativa*	4e-22
0.65	3.06	4.7	P29023	Endochitinase B Precursor/*Z. mays*	2.00E-106
0.12	0.57	4.6	NP_196305	Polygalacturonase inhibitor protein/*A. thaliana*	2.00E-26
0.92	4.06	4.4	AJ297903	Basal layer antifungal peptide (BAP-2)/*Z. mays*	4.00E-50
0.22	0.97	4.3	P93438	S-adenosyl-L-methionine synthetase/*O. sativa*	1.00E-45
0.16	0.69	4.2	AAB19212.1	Polygalacturonase-inhibiting protein/*Malus domestica*	2.00E-33
0.17	0.72	4.2	BAA92982	Similar to Glycine max GH1 protein/*O. sativa*	6.00E-27
0.29	1.20	4.1	AAK56130	ß-expansin 7/*Z. mays*	4.00E-61
0.49	1.98	4.0	P46611	S-adenosyl methionine synthetase I/*O. sativa*	5.00E-91
1.50	5.87	3.9	X67324	MFS18 protein precursor/*Z. mays*	1e-23
0.36	1.43	3.9	P30571	Metallothionein-like protein/*Z. mays*	9.00E-20
0.23	0.86	3.8	T27554	Aluminium-induced protein/*Brassica napus*	5e-13
0.29	1.08	3.7	P09189	Heat shock protein 70/*Petunia hybrida*	7.00E-98
0.13	0.47	3.7	Z49063	Polygalacturonase inhibitor protein/*Actinidia deliciosa*	7.00E-15

0.54	2.01	3.7	P30571	**Metallothionein-like protein/*Z. mays***	7.00E-20
0.46	1.72	3.7	AAG51670	**Beta-galactosidase/*A. thaliana***	3.00E-74
0.31	1.11	3.5	T02081	**ABA stress ripening protein/*Z. mays***	5e-14
0.39	1.33	3.4	BAB40923.1	**Se-binding protein/*O. sativa***	1.00E-102
0.15	0.52	3.4	AAC09245	**Tonoplast intrinsic protein/*Z. mays***	1.00E-44
0.08	0.29	3.4	P30571	**Metallothionein/*Z. mays***	5e-22
0.40	1.39	3.4	CAA59990	**Elastin like protein/*Drosophila melanogastor***	1.00E-06
1.72	5.72	3.3	S46308	**Initiator-binding protein/*Z. mays***	1.00E-85
0.51	1.56	3.0	P30571	**Metallothionein-like protein/*Z. mays***	5.00E-20
0.12	1.43	11.0	AAG34828	**Glutathione S-transferase GST 20/*Z. mays***	8.00E-76
0.61	6.34	10.0	T02955	**Cytochrome P450 monooxygenase/*Z. mays***	1.00E-35
0.14	0.70	5.1	T18851	**Methionine synthase/*Sorghum bicolor***	2e-27
0.16	0.60	3.7	L77912.1	**Phenylalanine ammonia lyase/*Z. mays***	4e-30
0.12	0.44	3.7	BAA77214.1	**Monodehydroascorbate reductase/*O. sativa***	2e-07
0.27	0.84	3.0	W21658	**S-adenosylmethionine decarboxylase 2/*O. sativa***	2e-29
1.89	8.49	4.5	T23285	**60S Ribosomal protein, L24/*Hordeum vulgare***	6e-39
0.13	0.54	4.2	CAA41024.1	**Acyl carrier protein/*Z. mays***	1e-07
1.24	4.63	3.7	S23780	**Nucleic acid-binding protein/*Z. mays***	6.00E-82
0.85	2.82	3.3	BAB09157	**Small nuclear ribonucleoprotein/*Homo sapiens***	2.00E-06

Table 6.2) Up-regulated ESTs showing major changes in transcript levels on Trichostatin A treatment. The values in the array data correspond to signal intensities on the filters hybridised with cDNA prepared from control or TSA treated lines. Clone identity was established by performing protein Blast analysis (Blast X). Random matching probabilities based on Blast analysis are also given.

Table 6.3(Down regulated ESTs showing major changes in transcript levels on TSA treatment)

Array Data			Accession Number	Clone Identity	Random Matching Probability
Control HE-89	TSA treated HE-89	Fold Attenuation			
37.6	10.5	3.6	NP_199617	**Phosphoribosylanthranilate transferase/*A. thaliana***	1.00E-12
31.0	8.9	3.5	NP_196983.1	**Putative protein/*A. thaliana***	7.00E-34
18.8	5.5	3.4	T03766	**Probable Glutathione reductase/*O. sativa***	4.00E-44
43.8	13.2	3.3	AAC67557.1	**Chlorophyll a/b-binding protein precursor/*O. sativa***	6.00E-22
41.0	12.6	3.3	P49106	**14-3-3-Like protein GF14-6/*Z. mays***	1.00E-102
29.8	9.7	3.1	NP_568368.1	**Putative protein/*A. thaliana***	1.00E-11
15.1	5.3	2.9	Q40784	**Possible apospory related protein/*Pennisetum ciliare***	1.00E-22
20.9	7.5	2.8	U32428.1	**Lipoxygenase/*Triticum aestivum***	6e-05
26.7	9.6	2.8	T00720	**Hypothetical protein/*A. thaliana***	1.00E-15

Table 6.3) Down-regulated ESTs showing major changes in transcript levels on Trichostatin A treatment. Clone identity was established by doing protein blast analysis. Random matching probabilities based on Blast analysis are also given.

6.2.3.6 Inhibiting deacetylases by TSA treatment affects many classes of genes related to stress, development and pathogenesis etc

Analysis of the TSA list for up-regulated clones revealed that about 30% of the clones showing significant changes in transcript levels were histones. Some other classes of sequences related to stress, cell wall turnover, cell senescence, photosynthesis etc were also identified and the significance of these clones is dealt with in the discussion. However it was the up regulation of histone transcripts that posed some interesting questions. Histone protein biosynthesis is tightly regulated inside the cell. In order to verify whether the microarray transcript profiling results could be reproduced on the Northern blot level, total RNA isolated from the control and TSA treated lines was hybridised with two histone (Histone 4 and Histone 2B) and two non-histone clones (Cytochrome P450 monooxygenase and MFS Protein Precursor). The clones for Northern analysis were chosen randomly. As a loading control 18S ribosomal RNA was used. The results of the Northern hybridisations are shown in figure 6.10.

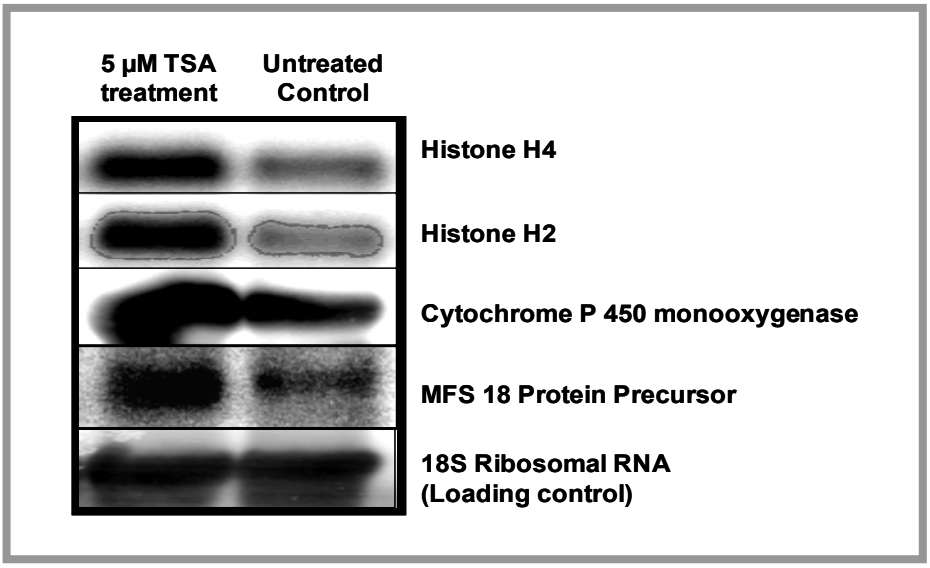

Figure 6.10) Northern confirmation on selected array clones modulated by TSA treatment. HE-89 maize cell line was treated with 5µM TSA For 10 hours. 50 µg of total RNA from the treated and the untreated cell line was blotted onto a nylon membrane and hybridised with selected array clones. Clones for Northern blots were selected randomly.

The Northern blots confirmed the array results. The selected clones were up-regulated in the TSA treated samples as identified through micro-array technique.

6.2.4 Increase in histone transcripts upon TSA treatment does not change the overall histone abundance in the cell

Whether the increase in mRNA levels on TSA treatment is reflected at the protein levels was confirmed by performing an acid extraction to isolate quantitatively the histones from untreated and TSA treated maize HE-89 cell lines (see section 2.2.7.2). The partially purified histones were then run on a 15% SDS PAGE gel and visualised by Ponceau S staining. A Western blot was done on the same membrane with an antibody raised against maize immunophilin to serve as a loading control (figure 6.11)

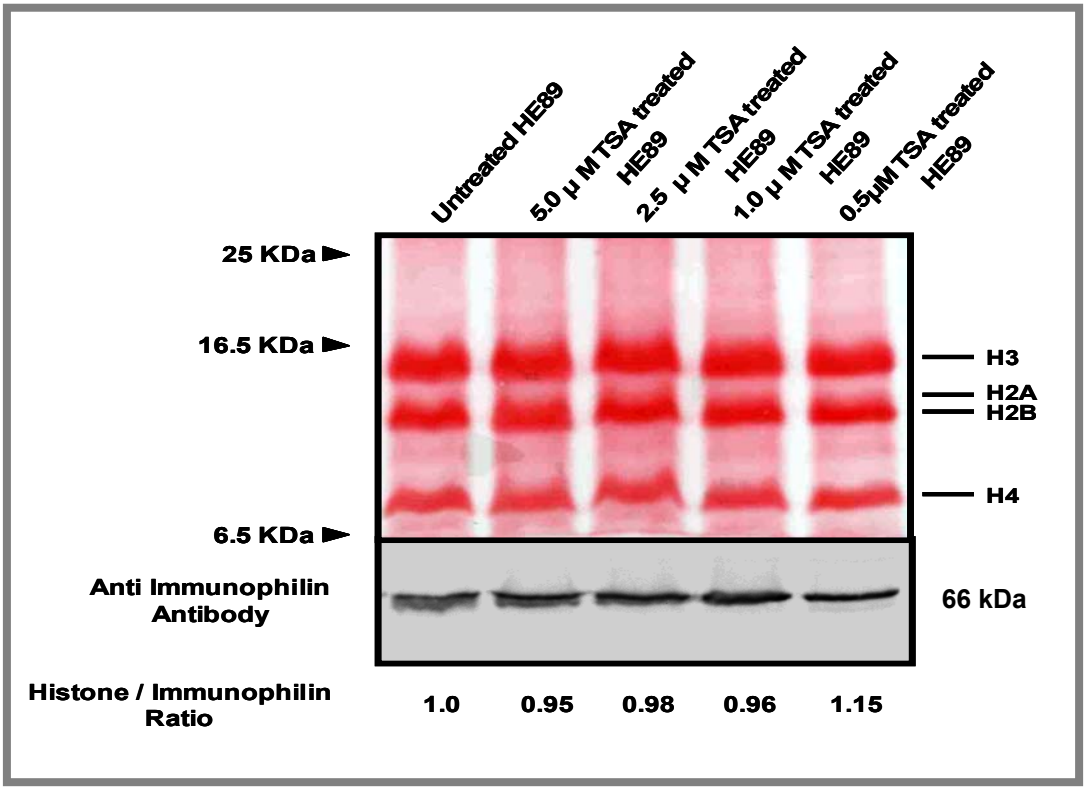

Figure 6.11) Relative amount of histone proteins in TSA treated and untreated HE-89 cell line. Histone fractions were acid extracted, resolved on a 15% SDS PAGE gel and visualised by Ponceau S staining. Anti-immunophilin antibody was used as a loading control.

As can be seen from the figure 6.11, the increase in histone mRNA on TSA treatment (as seen by microarray analysis and Northern blots) is not

reflected at the protein level. The histone protein levels in the cell remain constant relative to a control cytosolic protein immunophilin.

6.3 Transgenic approach to study the impact of histone acetylation

TSA treatment on maze HE-89 suspension cultures provides a general overview of the cellular response to histone hyper-acetylation. TSA, a potent chemical, inhibits the histone deacetylases (Graessle *et al.,* 2001) and leads to hyper-acetylation of histones. Increase in histone acetylation with TSA, also resulted in decreased levels of ZmGcn5 protein in the cell. In order to specifically dissect the role of ZmGcn5 in maintaining acetylation status in maize, a construct expressing antisense mRNA strand of *ZmGCN5* coding sequence was transformed into maize cell line HE-89.

6.3.1 Generation of antisense transgenic cell lines of *ZmGCN5*

An *Nco*I restricted PCR fragment of *ZmGCN5* was cloned into the *Nco*I site of vector pRT104 vector (Töpfer *et al* 1988). A forward primer annealing to the 35S promoter and a reverse primer complementary to the antisense strand of ZmGCN5 were used to identify the bacteria containing the *ZmGCN5* antisense construct (figure 6.12). The primer sequences (*viz.* 35SfwdPrimer and Gcn5AsPrimer) are shown in section 2.1.3.4. The cloned antisense sequence of *ZmGCN5* was verified by sequencing. The resultant vector was

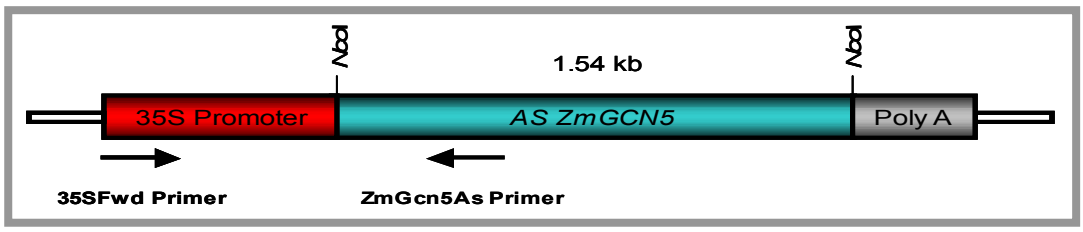

Figure 6.12) Schematic diagram of the *ZmGCN5* antisense construct used for the transformation of maize cell line HE-89. Arrows indicate the primers used to amplify 990 bp insert from transgenic cell lines expressing the antisense construct.

used for the transformation of maize HE-89 cell line. For the selection of the transformants, co-transformation was performed with a vector containing phosphinothricin (BASTA) resistance gene driven by maize polyubiquitin promoter (pAHC25; Christensen and Quail, 1996). The transformation was

kindly performed by A. Seidel/Dr. H. Steinbiss (Monocot transformation group, MPIZ) and Dr. Günter Donn (Aventis Crop Sciences, Frankfurt). The transgenic callus lines were selected on 100 µg/ml BASTA (Phosphinothricin). After several rounds of selection the surviving callus lines were checked for the expression of antisense strand of *ZmGCN5* by PCR, Northern and Western blots.

6.3.2 Characterisation of antisense transgenic lines of *ZmGCN5*

10 callus lines survived the successive selection rounds on Phosphinothricin (BASTA). PCR was performed on these lines with specific primers to amplify a 990 bp insert. The primers used for the PCR were same as described in section 6.3.1. Three lines showed a band of the expected size in varying amounts, possibly due to DNA degradation. Control PCR was performed on the vector-transformed lines. The results are shown in figure 6.13.

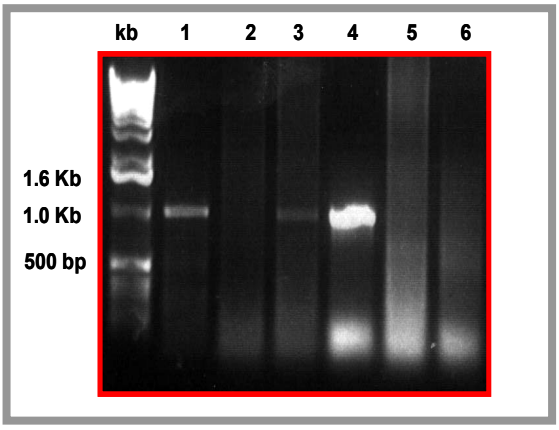

Figure 6.13) PCR analysis on transgenic maize callus containing the *ZmGCN5* antisense construct. PCR was performed with specific primers amplifying 35S promoter and a part of the antisense strand of ZmGCN5. Panel 1-5 shows PCR done on putative ZmGCN5 antisense lines. Panel 6 shows PCR on a control line transformed with vector only.

In order to generate enough material for biochemical studies the PCR positive callus lines were introduced into liquid suspension cultures and maintained under BASTA selection. Further characterisation was performed on the lines 1 and 4. Total RNA isolated from the PCR positive lines as well as a vector transformed control line was transferred onto a nylon membrane

and hybridised with a *ZmGCN5*-specific probe. The same membrane was probed with ubiquitin DNA to serve as a loading control (figure 6.14).

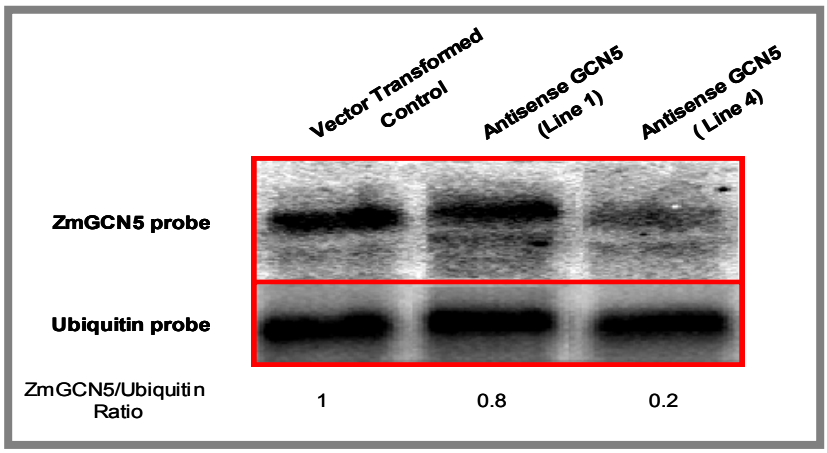

Figure 6.14) Northern analysis of PCR positive *ZmGCN5* antisense cell lines. 100 µg of total RNA was isolated from the frozen tissue and blotted onto a nylon membrane and probed with *ZmGCN5* cDNA. As a loading control the same membrane was probed with Ubiquitin DNA. The bands were quantified using the Image Quant software (Molecular Dynamics), and the *GCN5*/Ubiquitin ratios were determined and normalised to vector transformed line as 1 MDC (molecular dynamics count).

Out of the two putative antisense lines, line 4 showed significantly decreased *ZmGCN5* RNA levels indicating that the antisense of *ZmGCN5* mRNA was being produced in this line. Line 1 also showed some decrease in the transcript levels but it was not as drastic as in the line 4. Crude nuclear proteins, prepared from both antisense and vector transformed control lines were transferred onto a nitrocellulose membrane. Immunoblot was performed on the filters using anti ZmGcn5 and the control anti maize immunophilin specific antibodies. The results are shown in figure 6.15.

Both lines showed decreased ZmGcn5 levels as compared to vector transformed control line. Line 4 showed an almost 5-fold decrease while line 1 showed about a 2-fold decrease in ZmGcn5 protein levels.

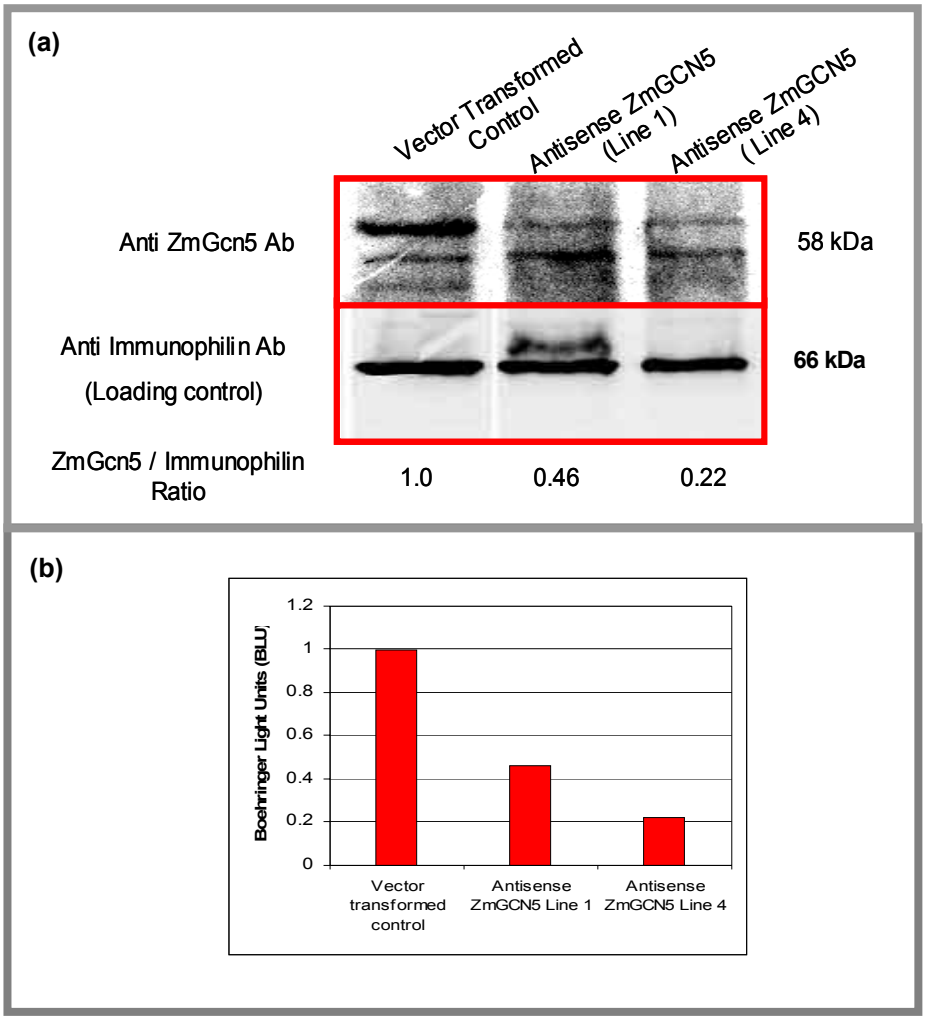

Figure 6.15) ZmGcn5 protein levels in the transgenic maize cell lines. (a) Crude nuclei isolated from the antisense and vector transformed maize lines were transferred onto nitrocellulose membrane and immunoblotted with anti ZmGcn5 antibody and control anti maize immunophilin antibody. (b) ZmGcn5/Immunophilin ratio value plot. The Boehringer Light Units (BLU) were calculated using the Lumi-imager software from Boehringer Mannheim and GCN5/Immunophilin ratios were calculated and normalized taking untreated control as 1 BLU.

6.3.3 Reducing *ZmGCN5* results in decreased protein levels of histone deacetylase HD1B-I (ZmRpd3)

In order to ascertain whether the reduction in ZmGcn5 protein caused changes in deacetylase levels, the crude nuclear extracts transferred on the nitrocellulose membrane (section 6.3.2) were immunoblotted with antibodies raised against two histone deacetylases – HD1B and HD2. The results are shown in figure 6.16.

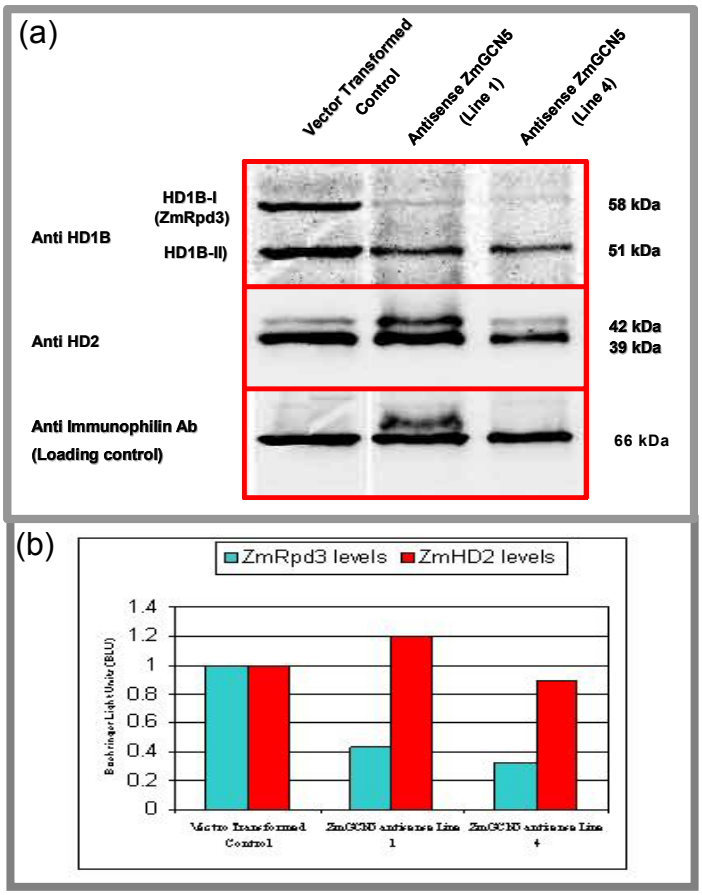

Figure 6.16) ZmRpd3 and ZmHD2 deacetylase protein levels in transgenic maize cell lines containing antisense construct of *ZmGCN5*. As a control a cell line transformed with vector only was used. (a) Immunoblot with deacetylase antibodies. (b) Deacetylase/Immunophilin ratio plot. The Boehringer light units (BLU) were calculated using the Lumi-imager software and the ratio values were normalised to control as 1 BLU.

Anti HD1B antibody was raised against histone deacetylase HD1B-I (also called ZmRpd3, Rossi *et al.,* 1998). The antibody detects a 58 kDa protein (HD1B-I) and a 51 kDa protein HD1B-II, (Lechner *et al.,* 2000). Antibody HD2 detects the histone deacetylase protein HD2 (Lusser *et al.,* 1997). There are several isoforms of this protein and the protein is modified by phosphorylation. The antibody detects the 39 kDa and the 42 kDa forms. A 45 kDa form can also be detected but this form is not abundant (Personal communication Alexandra Pipal, University of Innsbruck, Austria). The antibodies were kindly provided by Prof. Peter Loidl, University of Innsbruck. As a loading control, an antibody raised against maize immunophilin was used.

The Immunoblot showed that the levels of HD1B-I (ZmRpd3) protein were down regulated in the antisense *ZmGCN5* lines. However the levels of

HD1B-II and HD2 protein were not affected as compared to control lines transformed with vector only. The bands were quantified using the Lumi-imager software from Boehringer Mannheim and the ZmRpd3/immunophilin and ZmHD2/Immunophilin ratios were calculated. The values are plotted in the figure 6.16 (b).

6.3.4 Microarray analysis on transgenic maize lines containing the *ZmGCN5* antisense construct

Total RNA, isolated from the antisense *ZmGCN5* line 4 and the vector transformed control line, was used for radioactive cDNA synthesis as described before (see section 2.2.5.2). 2600 maize EST's spotted onto the nylon filters were hybridised with the radiolabeled cDNA. Three hybridisations each were carried out for the antisense *ZmGCN5* and the vector transformed control. In total 9 independent filters each were hybridised to radiolabeled cDNA prepared from antisense *ZmGCN5* line 4 and vector transformed control respectively. The signal intensities were read using the PhosphorImager technology as described in section 2.2.14.1. The filters were normalised as described earlier for TSA microarrays (section 6.2.3.1–6.2.3.3). The expression data from the antisense *ZmGCN5* line 4 and vector transformed control line was compared and analysed quantitatively using ArrayVision software from Imaging Research Inc as described for TSA arrays (section 6.2.3).

6.3.4.1 Differential expression between array filters hybridised with cDNA prepared from antisense *ZmGCN5* and vector transformed control maize cell lines

The hybridisation signals obtained from repeats of each double spot on the same filter were compared as described for TSA arrays (section 6.2.3.4). The signals were reproducible with correlation coefficients above 0.98. The comparison of the normalised values of antisense *ZmGCN5* against the vector-transformed control is shown in figure 6.17.

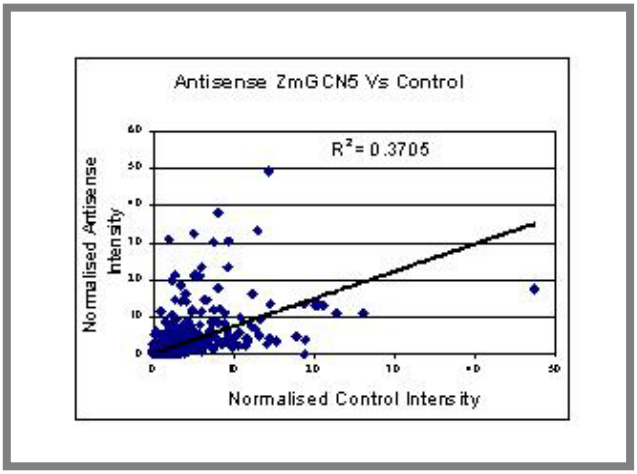

Figure 6.17) Scatter plot of antisense *ZmGCN5* microarray experiment. Normalised values for ZmGCN5 antisense line were plotted against the normalised values for control.

The transcripts up or down regulated by reducing *ZmGCN5* expression were calculated in the same way as described for TSA arrays (see section 6.2.3.5). The percentage of transcripts that were significantly up or down regulated are summarised in table 6.4. The ESTs showing major changes in the transcript levels are shown in appendices III and IV.

Transcript accumulation	Knock out *ZmGCN5*
Up-regulated	2.5%
Down regulated	3.8%

Table 6.4) Percentage of known transcripts regulated by knocking out *ZmGCN5*. The percentages were calculated on the basis of a difference of 2 fold in the transcript expression levels of the treatment and control.

6.3.4.2 Reducing *ZmGCN5* levels affects similar classes of genes to those affected by Trichostatin A treatment

Analysis of the *ZmGCN5* antisense treatment for up-regulated clones (table 6.5) revealed that among the clones showing more than 2 fold increase in transcript levels were again core histones. These were the major transcripts up regulated in TSA microarrays as well. As seen for TSA microarrays, the increase in core histone mRNA was not reflected at the protein levels which remained constant in all cases. This led to the conclusion that the cell was responding to an increase in the degree of histone acetylation or deacetylation by *de novo* histone mRNA synthesis.

Table 6.5) Up-regulated histones between TSA treatment and *ZmGCN5* knockout

Array Data			GenBank	Clone Identity	Random
Control HE-89	As ZmGCN5 HE-89	Fold Induction	Accession Number		Matching Probability
1.55	8.71	5.6	T14716	Histone 2B/*T. aestivum*	2e-12
0.31	1.23	4.0	AA072442	Histone 2A/*O. sativa*	5e-06
2.54	8.57	3.4	T15325	Histone 2/*T. aestivum*	2e-08
4.75	11.81	2.5	T25236	Histone H2B.2/*Z. mays*	6e-24
3.08	7.11	2.3	T23405	Histone 2B/*Z. mays*	3e-15
1.06	2.34	2.2	H35878	Histone 2B.1/*Z. mays*	1.00e-16
6.65	14.52	2.2	T21621	Histone 2B/*Z. mays*	1.00e-19
2.01	4.25	2.1	T70634	Histone 4/*Stylonychia lemnae*	2e-16

Table 6.5) ESTs showing up-regulation in transcript levels on TSA treatment and/or on knocking out *ZmGCN5*. The values in the array data correspond to signal intensities on the filters hybridised with cDNA from control or TSA treated/antisense line. Only those clones are shown where the difference between the control and the antisense lines is 2 fold or more.

Classes of sequences related to stress, cell wall turnover and cell senescence etc that were identified as being up-regulated in TSA microarrays were seen down-regulated on knocking out *ZmGCN5*. Conversely the genes that were seen down-regulated in TSA microarrays were up-regulated on knocking out *ZmGCN5* (tables 6.6, 6.7), confirming that gene regulatory effects observed on TSA treatment are directly related to the acetylation and deacetylation status of the cell.

Table 6.6) Clones up-regulated in knock out *ZmGCN5* microarrays but down-regulated in TSA treatment microarrays

Array Data			GenBank	Clone Identity	Random
Control HE-89	As ZmGCN5 HE-89	Fold Induction	Accession Number		Matching Probability
0.12	0.47	4.0	AA054812	**Chlorophyll a/b binding protein/*Z. mays***	5.00-20
12.95	33.48	2.6	AAC67557.1	**Chlorophyll a/b-binding protein/*O. sativa***	6.00E-22
9.34	30.78	3.3	P49106	**14-3-3-Like Protein GF14-6/*Z. mays***	e-102
0.33	0.77	2.3	Q9SP07	**14-3-3-like protein/*Lilium longiflorum***	e-118
4.08	8.31	2.0	Q40784	**Possible Apospory-associated protein/*Pennisetum ciliare***	1.00E-22
1.85	3.91	2.1	AA030722	**Lipoxygenase -Disease related/*Capsicum annuum***	1.00E-5
0.34	0.69	2.1	AAC28490.1	**Chlorophyll a/b binding protein/*Sorghum bicolor***	1.00E-58
6.01	23.64	3.9	NP_199617.1	**Phosphoribosylanthranilate transferase/*A. thaliana***	1.00E-12

Table 6.6) ESTs showing up-regulation in transcript levels on knocking out *ZmGCN5* but being down regulated on TSA treatment. The values in the array data correspond to signal intensities on the filters hybridised with cDNA from control or antisense line. Only those clones are shown where the difference between the control and the antisense lines is 2 fold or more.

Table 6.7) Clones down-regulated in knock out *ZmGCN5* microarrays but up-regulated in TSA treatment microarrays

Array Data			GenBank	Clone Identity	Random
Control HE-89	As ZmGCN5 HE-89	Fold Attenuation	Accession Number		Matching Probability
1.16	0.22	5.3	T27554	**Aluminum-induced protein/*Brassica napus***	5e-13
18.86	3.91	4.8	T14760	**Salt stress protein/*O. sativa***	9e-07
2.60	0.59	4.4	CAC06433.1	**Expansin/*Festuca pratensis***	4.00E-05
10.61	2.58	4.1	T02955	**Cytochrome P450 monooxygenase/*Z. mays***	1.00E-35
3.18	0.90	3.5	AAL79732.1	**Heat shock protein 90/*O. sativa***	8.00E-86
14.42	4.30	3.4	T23394	**Salt stress protein/*O. sativa***	4e-07
1.77	0.54	3.3	P30571	**Metallothionein-like protein/*Z. mays***	1.00E-19
1.95	0.63	3.1	Q9SW70	**Stress-related protein/*A. thaliana***	8.00E-47
2.62	0.91	2.9	Q10716	**Cysteine proteinase/*Z. mays***	5e-37
1.96	0.82	2.4	P30571	**Metallothionein-like protein/*Z. mays***	6.00E-20
0.77	0.32	2.4	W21658	**S-adenosylmethionine decarboxylase 2/*Z. mays***	2e-29
1.82	0.88	2.1	BAB40923.1	**Putative selenium binding protein/*O. sativa***	e-102

Table 6.7) Down-regulated ESTs showing major changes in transcript levels on knocking out *ZmGCN5* but being up-regulated in TSA treatment microarrays. The values in the array data correspond to signal intensities on the filters hybridised with cDNA from control or antisense line. Only those clones are shown where the difference between the control and the antisense lines is 2 fold or more.

On the other hand there were several classes of genes, which were seen significantly down-regulated by antisense *ZmGCN5* only. A major group among them was clones showing identity to actin and tubulin (table 6.8) that may reflect a role of ZmGcn5 in maintaining the cellular architecture. Linker histones were also reduced in transcript abundance.

Table 6.8) Clones exclusively down-regulated in knock out *ZmGCN5* microarrays

Array Data			GenBank	Clone Identity	Random
Control HE-89	As ZmGCN5 HE-89	Fold Attenuation	Accession Number		Matching Probability
7.48	1.41	5.3	P23444	**Histone H1/*Z. mays***	6.00E-05
11.31	2.51	4.5	AAL73043.1	**Histone H1-like protein/*Z. mays***	7.00E-29
0.97	0.23	4.3	AAK84456.1	**Actin/*O. sativa***	3e-65
2.13	0.60	3.5	P24142	**Prohibitin -inhibitor of cell proliferation/*M. musculus***	3e-10
2.29	0.70	3.3	P14641	**Alpha tubulin/*Z. mays***	2e-36
0.75	0.24	3.1	NP_190236.1	**Actin 12/*A. thaliana***	1.00E-15
9.72	3.65	2.7	P14641	**Tubulin alpha-2 chain/*Z. mays***	2.00E-90
1.60	0.72	2.2	P41210	**Caltractin (mitotic spindle associated protein)/ *Atriplex nummularia***	9e-51

Table 6.8) Down-regulated ESTs showing major changes in transcript levels on knocking out ZmGCN5. The values in the array data correspond to signal intensities on the filters hybridised with cDNA from control or antisense line. Only those clones are shown where the difference between the control and the antisense lines is 2 fold or more.

6.3.4.3 Overall trend of genes differentially expressed on TSA treatment and in the *ZmGCN5* knockout line

Around 200 transcripts were seen to be differentially expressed (significantly) on changing the acetylation status of the cell. This constituted roughly 7.5% of the total clones analysed in microarray experiments (both TSA and *ZmGCN5* microarray experiments). The percentage includes all the transcripts that were up- or down-regulated in both microarray experiments (2-fold induction or above). The overall relationship between the transcripts going up or down is shown in the Venn diagram in figure 6.18.

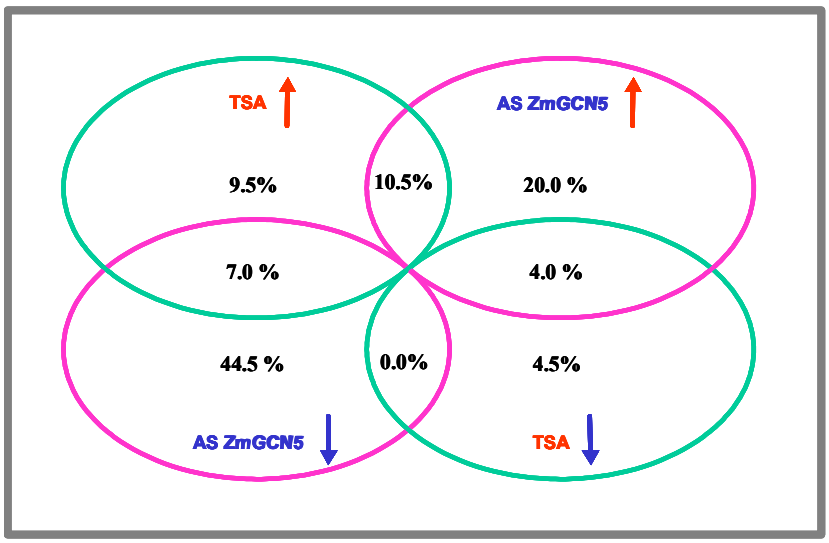

Figure 6.18) Venn diagram of shared and specifically differentially expressed 200 transcripts for TSA and AS *ZmGCN5* microarrays. The percentages of transcripts that were up (↑) and/or down-regulated (↓) are shown.

Discussion and conclusions

7.1 Role of histone acetylation in transcriptional activation

Chromatin structure, or packaging of the DNA in a eukaryotic cell is a highly regulated process and is known to have major impact on the levels of transcription (Lusser *et al.,* 2001). In the last 10 years factors putatively mediating eukaryotic transcriptional activation have been isolated and are being characterised in many laboratories throughout the world. An increasing number of enzymes and protein complexes are now known that facilitate changes in the chromatin structure with resultant effects on gene expression (Greassle, *et al.,* 2001). There is strong evidence to support a role for Gcn5 histone acetyltransferase mediated transcriptional activation in higher eukaryotes (Sterner and Berger, 2000).

Functional analysis of ZmGcn5 - a plant histone acetyltransferase (Becker *et al.,* 1999) - was performed in the present study. The isolated histone acetyltransferase was characterised with respect to its sub-cellular localisation, *in vivo* interaction with adaptor proteins and plant transcription factors. Cellular responses to changes in histone acetylation were performed by modulating the acetylation status of the cell either by chemical induction or by knocking out the *ZmGCN5* HAT in maize cell lines. The resultant RNA populations were reverse transcribed and used to profile 2600 maize ESTs spotted on nylon filters. The results showed that the cell quickly responds to changes in histone acetylation by *de-novo* synthesising core histone and also modulating the levels of acetylases and deacetylases. A general effect on certain classes of genes related to stress, development and pathogenesis was also observed. Taken together, the results presented herein suggest a direct role of histone acetylation in maintaining an overall chromatin status inside the cell.

7.1.1 Plant Gcn5 HAT's do not contain a PCAF domain

ZmGcn5 shows the typical features of being a member of the GNAT (GCN5 related N-acetyltransferase) superfamily (Neuwald and Landsman, 1997), possessing the catalytic histone acetyltransferase-, the adaptor Ada2

interaction-, and bromo-domains, and also being nuclear-localized. Compared to ScGcn5 (yeast), ZmGcn5 has an extended N-terminus (figure 3.1). This N-terminal extension shows no homology with the PCAF (p300/CREB binding protein associated factor) region of mammalian Gcn5. The PCAF domain in mammalian Gcn5 has been implicated in the acetylation of histones in nucleosomes (Xu *et al.,* 1998). It has also been shown to bind to CBP (CREB binding protein; CREB, cAMP responsive element-binding protein) and p300 (Yang, *et al.,* 1996), both of which are transcriptional co-activators and interact with a large number of developmentally important transcription factors (Kamei, *et al.* 1996). ZmGcn5 was shown to acetylate isolated histones but not nucleosomes *in vitro* (Marcus Riehl, Doktorarbeit, Universität Köln, 2002). This raised the possibility that the isolated ZmGcn5 might be missing a function supplied by an N-terminal PCAF type domain. The possibility was investigated by isolating the genomic clone of *ZmGCN5* and performing primer extension (figure 3.3 and 3.5). The results showed that *ZmGCN5*, like *ScGCN5* does not contain a PCAF type domain. Furthermore, database searches for any plant protein showing homology to the PCAF region of mammalian Gcn5 HAT's produced no results. The recent characterisation of AtGcn5 (Stockinger *et al.,* 2001) confirmed that plant *GCN5* genes do not contain the PCAF domain. *AtGCN5* and *TgGCN5* both have an N-terminal extension but interestingly these share no homology with the *ZmGCN5* N-terminal region. The occurrence of the N-terminal PCAF domain in all of the known metazoan Gcn5 proteins suggests that this domain was present in the ancestral metazoan Gcn5, while the absence of the domain in known fungal, plant and protozoan Gcn5 proteins suggests that the PCAF domain may be unique to animals.

7.1.2 The N-terminal region of ZmGcn5 is essential for the nuclear localisation of the protein

The function of ZmGcn5 as a histone acetyltransferase in the chromatin context means that it should be properly targeted to nucleus. Characterisation of the protein by fusion with a GFP (Green fluorescent protein) reporter confirmed that ZmGcn5 is a nuclear type A histone

acetyltransferase (figure 4.2). A search for potential nuclear targeting sequences using the computer programme PSORT identified a stretch of basic amino acid residues in the N-terminal region of ZmGcn5. In order to ascertain the functionality of this N-terminally located nuclear localisation sequence (NLS), and rule out the possibility of any other cryptic NLS within the polypeptide, fragments of ZmGcn5 were translationally fused to GFP and analysed for their targeting properties. Only the full-length protein and the N-terminal region fused to GFP could confer nuclear localisation on the fusion protein (figures 4.3 and 4.4). This raises the possibility that the role of the N-terminal extension might be precise and correct targeting of the protein to the nucleosomal substrates. If the protein does not contain this extension, it will not be properly targeted to the nucleus and thus may not be able to act as a nuclear histone acetyltransferase. This can also possibly explain the non-homologous nature of this N-terminal extension when compared to other HAT's. Nuclear localisation sequences are often redundant and it is quite likely that during evolution a site additional to the original NLS emerged in this N-terminal stretch. Most likely the original NLS was afterwards lost via genetic drift and that is why this N-terminal stretch has been retained in ZmGcn5. However nuclear targeting may not be the only function of this N-terminal region. It would be interesting to replace this region with some other sequence (containing an NLS) and over-express it in maize cell lines to determine whether the encoded nuclear localised protein maintains its function as the transcriptional co-activator.

7.2 ZmGcn5 HAT interacts with the adaptor ZmAda2 *In vivo*

The enzymatic activity of ZmGcn5 histone acetyltransferase was demonstrated by its ability to acetylate free histones, using the *E. coli* expressed GST-fusion protein (Marcus Riehl, Doktorarbeit, Universität Köln, 2002). However, under these conditions, ZmGcn5 was not able to acetylate nucleosomes. Being part of multi-protein complexes inside the cell, like SAGA and ADA, Gcn5 proteins are able to acetylate the nucleosomes only when in complexes, indicating that other proteins are needed to confer this activity (Sterner and Berger, 2000). Gcn5 is linked to the SAGA and ADA complexes by its interaction with the adaptor protein Ada2. In order to study the *in vivo*

interaction between the ZmGcn5 and the adaptor ZmAda2, a modified split-ubiquitin system was used as a sensor for protein-protein interactions *in planta*. Fusion of ZmGcn5 to N_{ub} (N-terminal portion of ubiquitin) and the adaptor ZmAda2 to C_{ub} (C-terminal portion of Ubiquitin) coupled to the GFP reporter, detected a very strong interaction between the two fusions *in vivo*. This was manifested by the formation of a quasi ubiquitin moiety, which being recognised by ubiquitin specific proteases (UBP's) led to the release and degradation of the reporter GFP coupled to C_{ub} (figure 5.5). Since the result relied upon the release and degradation of the reporter gene and was thus negative in nature, it was decided to validate this interaction by using fluorescence resonance energy transfer (FRET) system. It was also of interest to determine the co-localisation of the two proteins and also the sub-cellular compartment where the interaction took place. Co-transfection of protoplasts with ZmGcn5 fused to CFP (Cyan emitting GFP) and the adaptor ZmAda2 fused to YFP (Yellow emitting GFP) resulted in the tight co-localisation of both proteins inside the nucleus (figure 5.7) implying that any interaction between these two proteins presumably occurs exclusively inside the nucleus.

FSPIM (Fluorescence spectral imaging microscopy) inside the nucleus detected a clear shift of CFP fluorescence towards YFP fluorescence indicating a very strong interaction between ZmGcn5 and the adaptor protein ZmAda2 (figure 5.8). When the YFP fluorophore coupled to ZmAda2 was photo-bleached so as to make it unavailable to accept energy from CFP, there was a sudden and sharp increase in fluorescence emitted by CFP fluorophore coupled to ZmGcn5 HAT (figure 5.9). This proved beyond any doubt that the physical interaction between ZmGcn5 and the adaptor ZmAda2 brought the fluorophores, CFP and YFP, fused to these proteins, close together to facilitate the energy transfer from the donor (CFP) to acceptor (YFP). These results show that when the ZmGcn5 and the adaptor protein ZmAda2 are targeted to the nucleus they interact physically, supporting the results obtained from modified Split-ubiquitin system.

7.2.1 FRET analysis identifies a transient interaction between the adaptor ZmAda2 and plant transcriptional activator ZmO2

The biological role of Gcn5-containing complexes may be difficult to establish from gene knockout phenotypes, for example, if these are lethal, or if there is redundancy in functional copies of the coding sequence. In order to establish a role for Gcn5 in maize, its interaction with an endosperm-specific plant transcriptional activator, Opaque-2 (O2) was investigated. Most previous reports indicated Ada2 rather than Gcn5 to be the co-activator component that interacts directly with the activation domain of transcriptional activators (Barlev *et al.,* 1995). Two *A. thaliana* Ada2 proteins were recently shown to interact *in vitro* with CBF1, an acidic transcriptional activator involved in cold regulated gene expression (CBF1: C-repeat/DRE Binding Factor 1; DRE: C-repeat/dehydration responsive element, Stockinger *et al.,* 2001; Stockinger *et al.,* 1997).

GST spin-down experiments failed to show a specific interaction between ZmO2 and either ZmGcn5 or the adaptor ZmAda2 (Heinz-Albert Backer, Max Planck Institute, personal communication). On the assumption that the interaction might require the association of more components of the co-activator complex, the interaction between ZmAda2 and ZmO2 was tested by *in vivo* FRET analysis. Co-transfection of protoplasts with transcriptional activator ZmO2 fused to CFP and the adaptor ZmAda2 to YFP resulted in the predominant localisation of both proteins inside the nucleus although some ZmO2-CFP fluorescence could be detected outside the nucleus (figure 5.7). Spectral images of the co-transfected protoplasts inside the nucleus showed a smaller but noticeable shift of the CFP towards YFP fluorescence indicating a relatively weak and possibly transient interaction between the transcriptional activator ZmO2 and the adaptor protein ZmAda2 (figure 5.10). Although weak, the shift was above the threshold considered meaningful for a successful FRET (Shah *et al.,* 2001). Furthermore acceptor photobleaching confirmed the energy transfer between ZmAda2 and ZmO2 (figure 5.11). A possible explanation for the observed weak interaction could be that since Gcn5 based co-activator complexes are needed at several loci during a limited time-frame within the cell cycle, they may bind to transcriptional activators mediating the

specific co-activator role and then disengage as soon as possible and bind to transcriptional activator molecules located on other promoters i.e., the interaction may need to be transient and short-lived.

7.2.2 Split ubiquitin as a sensor for *in vivo* protein-protein interaction studies in living plant cells

Split ubiquitin is an elegant system to study *in vivo* protein-protein interactions. The system was first described for *S. cerevisiae* and the analysis was performed with Western blots (Dünnwald *et al.,* 1999). Subsequently a selection method in *S. cerevisiae* based on the split-ubiquitin system was demonstrated (Wittke *et al.,* 1999). Recently the system was also used to verify protein-protein interactions implicated in the transcriptional regulation of human genes (Rojo-Nierbach *et al.,* 2000). A modified version of this system was used to study the *in vivo* interaction between ZmGcn5 HAT and the adaptor ZmAda2.

Split-ubiquitin system takes advantage of the protein ubiquitination machinery found in eukaryotes. Eukaryotes contain a highly conserved multi-enzyme system that covalently links ubiquitin to a variety of intracellular proteins that bear degradation signals recognized by this system. The resulting ubiquitin-protein conjugates are degraded by the 26S proteasome, a large ATP-dependent protease (Varshavsky, 1996; 1997). If a reporter gene, coupled to ubiquitin, bears a degradation signal it will be recognised by ubiquitin specific proteases (UBP's) leading to its degradation. In the present study the reporter GFP was modified to begin with an arginine. This arginine residue is a degradation signal recognised by UBP's as per N-end rule pathway. The N-end rule is a relation between the metabolic stability of a protein and the identity of its N-terminal residue (Lehming, 2001, Varshavsky, 1996). Co-transfection of plant protoplasts with ZmAda2-N_{ub} and ZmGcn5-C_{ub}-Arg-GFP resulted in the loss of green fluorescence from the transformed cells indicating an interaction between ZmGcn5 and ZmAda2. Since the result relied on the cleavage and degradation of GFP, the cells were co-transfected with a second fluorescent marker protein (dsRed) to report the successful interaction (figure 5.5). The results were afterwards verified by FRET analysis.

This is for first time that the split-ubiquitin system has been used to detect protein-protein interactions *in planta*.

Split-ubiquitin in essence is a negative system since the reporter gene, instead of being turned on, is cleaved and thus not detected. Furthermore the system described in the present work relies on the accurate and precise reporting of the co-transfected second marker protein (dsRed), which can be misleading if both reporters are not used in equimolar ratios. An improvement on the system would be to clone the second marker protein (under its own promoter) into the same vector containing the C_{ub}-Arg-GFP. This would circumvent the need for co-transfection with second marker and the results would be more reliable. In the long run it would also be advantageous to set up a selection system in plant cells based on split ubiquitin so that the method may be used for screening of *in vivo* interactions out of a population of candidate molecules.

7.3 Contribution of histone acetylation to overall chromatin status in maize

Southern blot hybridisation indicated the presence of only one copy of *ZmGCN5* in the maize genome (Marcus Riehl, Diplomarbeit, Universität Giessen, 1999), although the possibility of more distantly related homologues which do not cross-hybridise, cannot be eliminated. Indeed, in *A. thaliana*, two *GCN5*-related sequences have been detected (Marcus Riehl, Doktorarbeit, Universität Köln, 2002), and yeast also has more than one Type-A HAT, although these appear to have discrete functions (Clarke *et al.,* 1999). Taking the advantage of this single copy in maize, knockout lines of *ZmGCN5* were generated by producing antisense of *ZmGCN5* in maize cell lines and looking at the transcript profiles using cDNA microarrays. As an alternative way of altering the histone acetylation status of the cell, histone hyper-acetylation studies were done by using histone deacetylase (HDAC) inhibitor Trichostatin A (Yoshida *et al.,* 1995) on the untransformed HE-89 cell line. The treated and the control untreated cell lines were also used for transcript profiling.

7.3.1 The cell responds to the changes in histone acetylation by regulating the levels of acetylases and deacetylases

Specific antibodies raised against the acetylated histones or the HAT/HDAC enzymes were used to inspect the levels of acetylation and the abundance of acetylases and deacetylases in transgenic or chemically treated maize cell lines. Treatment of cell lines with TSA resulted in the hyper-acetylation of histones, which was detected by using an antibody raised against the acetylated histone H4 (acetylated at Lys 5, 8, 12 and 16) (figure 6.1 and 6.2). Even the lowest amount of TSA (0.5 µM) led to a 7-fold increase in acetylation on histone H4 while the antibody could barely detect the basal/under-acetylated levels in the untreated control. Using the same antibody on the *ZmGCN5* knockout lines gave no detectable signal (data no shown). This was not surprising as the knockout of *ZmGCN5* HAT activity would lead to under-acetylation of histones and the antibody in the first place barely detected the basal or under-acetylated histones in the untreated cell lines.

When the equilibrium of histone acetylation was disrupted by treatment with TSA, ZmGcn5 protein abundance was rapidly down regulated (figure 6.3). On the other hand using histone deacetylase specific antibodies Rpd3 and HD2 on the knockout lines showed decreased amounts of HD1B-I (ZmRpd3) in these cell lines, although the levels of HD1B-II and HD2 did not change much (figure 6.16). This suggests that the cell efficiently recognises the extent of changes in acetylation or deacetylation patterns so that when a single HAT or HDAC is modulated (as in case of knock-out *ZmGCN5*) the cell tries to balance out this situation by modulating the levels of HDAC or HAT respectively. Taken together these results point towards a general yet presumably complex mechanism by which the cell is able to compensate for the changes in acetylation or deacetylation levels. It is tempting to speculate that there might be some receptor molecules, which are able to perceive the changes in the histone acetylation and gear the cell towards the compensatory response. It will be of interest to investigate the possibility of such receptors and unravel their mechanism of action. The overall response

of the cell also suggests that the histone acetylases and deacetylases contribute significantly to the overall chromatin status.

7.3.2 Histone acetylation affects many classes of genes related to stress, development and pathogenesis etc

Microarray analysis on the TSA treated and knock out *ZmGCN5* maize cell lines recognised a co-ordinated pattern of gene expression. While TSA treatments lead to a general increase in gene expression (table 6.1), knocking out *ZmGCN5* was associated with general decrease in gene expression levels (Table 6.4). About 3.4 % of the genes were significantly up-regulated on TSA treatment (fold induction above 2) while about 3.8% of the genes were down-regulated on knocking out *ZmGCN5* (fold repression above 2). Several classes of genes were regulated by both treatments.

Among the TSA up-regulated transcripts metallothioneins, cysteine proteinases, polygalacturonase inhibitor proteins and Se binding proteins etc are stress-related genes (Hsieh and Huang, 1995; Koizumi *et al.,* 1993; Yao *et al.,* 1999). Chitinases and basal antifungal proteins are involved in cellular responses to pathogens etc (Huynh *et al.,* 1992, Serna *et al.,*2001). MFS 18 protein precursor, found in the vascular bundle in the glumes of male flowers, is a cell wall protein (Wright *et al.,* 1993). Expansins are involved in cell expansion and morphogenesis (Lee and Kende, 200, Lee et al., 2001), beta galactosidase is involved in cell wall breakdown (Smith and Gross, 2000) and initiator-binding protein is a marker for cell elongation and differentiation (Lugert and Werr, 1994).

Phosphoribosylanthranilate transfer like protein produced in response to oxidative stress (Conklin and Robert, 1995) showed a more than 3 fold decrease in transcript levels in TSA microarrays. The same was true for glutathione reductase, chlorophyll a/b binding protein and GF14-6 proteins. Glutathione reductase is regulated via ABA-mediated signal transduction pathway (Kaminaka *et al* 1998). GF14-6 proteins participate in protein/DNA complexes and show homology to a widely distributed protein family referred to as 14-3-3 proteins. These proteins modulate kinase C activity and activate ADP-ribosyltransferase (de Vetten and Ferl, 1994).

Classes of sequences related to stress, cell wall turnover, cell senescence and pathogenesis etc that were identified as being up-regulated in TSA microarrays were down-regulated on knocking out *ZmGCN5*. Conversely the genes related to photosynthesis, ABA signal transduction pathway etc that were down-regulated in TSA microarrays were all up-regulated on knocking out *ZmGCN5* (see sections 6.3.4.2, tables 6.5, 6.6, 6.7). This confirmed that the affects observed on TSA treatment or on knocking out *ZmGCN5* are directly related to the acetylation and deacetylation status of the cell. Microarray analysis also identified some classes of genes as being exclusively regulated by ZmGcn5. Prominent among this group were the transcripts encoding cytoskeletal components *viz.* tubulin and actin. Reducing the *ZmGCN5* levels lead to a decrease in the transcript levels of tubulin and actin (table 6.8) pointing towards an effect of ZmGcn5 on the overall cellular architecture. The regulation of stress, pathogenesis, photosynthesis and development related genes suggest that histone acetylation plays a significant role in plant growth and development.

7.3.3 ZmGcn5 contributes significantly to the overall nuclear histone acetylation in maize

Close inspection of the up-regulated genes from both treatments (TSA and Knock out *ZmGCN5*) revealed that among the clones showing significant changes in transcript levels were core histones (tables 6.2 and 6.5). These were identified among the highest up-regulated sequences in both microarray experiments. This led to postulation that the cell was responding to an increase in the degree of acetylation or deacetylation by *de novo* synthesis of non-acetylated core histone molecules. Histone acetylation is a dynamic process (figure 1.2). Gcn5 based co-activator complexes acetylate histones at specific loci, allowing the transcription machinery access to otherwise repressed DNA and leading to the transcription of desired gene products. Histone deacetylases (like Rpd3, HD2 etc), on the other hand, increase affinity between the negatively charged DNA and the positively charged histones resulting in the restricted access of transcription machinery at specific loci.

At the global level genes are constantly being up- or down-regulated in response to the specific needs of the cell. If this balance is disturbed by changing the acetylation or the deacetylation status of the histones, the cell tries to redress this by modulating the levels of corresponding deacetylase or acetylase enzymes respectively. The cell also responds by *de novo* synthesising core histones, which presumably constantly replace the hyper-acetylated or de-acetylated histones. Linker Histones were seen down-regulated in knock out *ZmGCN5* cell lines. Linker histones are thought to repress transcription (Wolffe and Hayes, 1998). Binding of linker histone leads to a partial rearrangement of core histone interactions in the nucleosome (Lee and Hayes, 1998; Gushchin *et al.,* 1988). Removal of histone H1 is therefore likely to represent a relatively simple means of destabilizing both local and higher order chromatin structures and altering core histone-DNA interactions. With the *GCN5* knockout this seems to be another strategy whereby the cell tries to redress the change in its acetylation status.

Based on the results presented above the whole scenario can be represented in two models.

Model A: Cellular response to histone hyperacetylation on TSA treatment

There is a dynamic equilibrium between the acetylation and deacetylation processes, so that depending on the specific cellular needs HAT's like Gcn5 acetylate histones at specific locations leading to increased levels of transcription while deacetylases like Rpd3, HD2 repress transcription. Reversible inhibition of histone deacetylases with TSA shifts the acetylation-deacetylation equilibrium towards acetylation and the core histones get hyperacetylated (figure 6.1). The cell recognises this change by an unknown mechanism and tries to compensate for an increase in the proportion of acetylated histones by:

1. Down-regulating the production of histone acetyltransferases like Gcn5 (figure 6.3) and
2. *De novo* synthesis of non-acetylated core histones (Table 6.2).

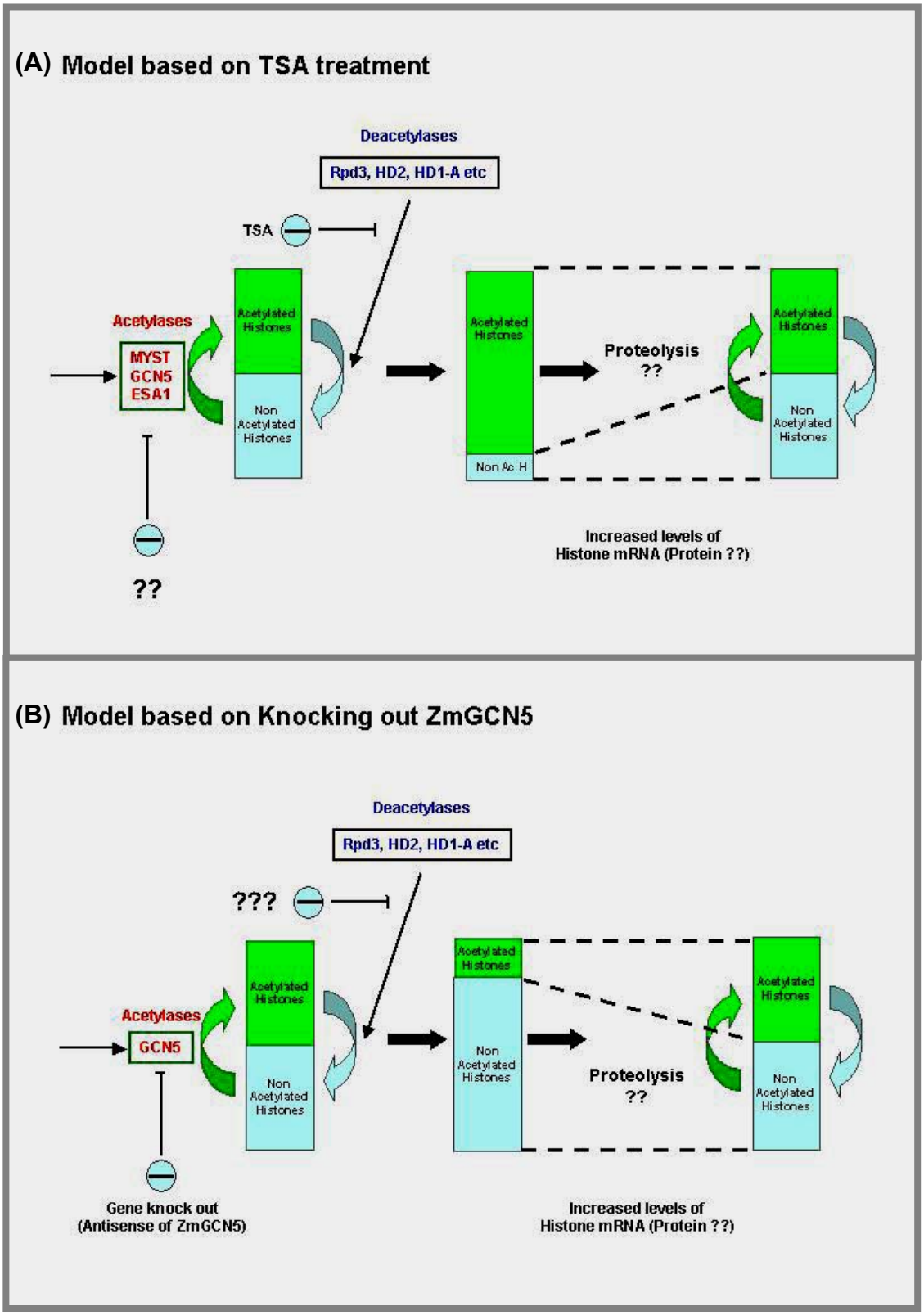

Figure 7.1) Working model for explaining the cellular response to changes in histone acetylation. (A) Cellular response on Trichostatin A treatment. (B) Cellular response on knocking out ZmGCN5 HAT. (Non Ac H – Non acetylated histones)

Model B: Cellular response to knocking out ZmGCN5 histone acetyltransferase

Knocking out ZmGcn5 HAT activity from the cells (figure 6.14 and 6.15) shifts the acetylation-deacetylation equilibrium towards histone deacetylation. The cell again recognises this shift and tries to compensate for it by:

1. Down-regulating the production of histone deacetylases like Rpd3. However it is worth noting that only some and not all deacetylases seem to be down regulated (figure 6.16). This assumes significance, as ZmGcn5 is not the only histone acetyltransferase inside the cell (Lopez-Rodas *et al.,* 1991, Lechner *et al.,* 1996) and presumably there is still competition from other HAT's, so the cell tries to compensate for changes in ZmGcn5 levels only.
2. *De novo* synthesis of non-acetylated core histones (Table 6.5). The newly synthesised histones, destined for deposition on DNA molecules in the nucleus, are acetylated by cytoplasmic B-type HAT's like Hat1 (Parthun *et al.,* 1996),

The increase in histone mRNA on changing the acetylation status of the cell prompted the investigation of possible effect on histone protein abundance in the cells. The results showed that the overall histone abundance in the cell does not alter (Figure 6.11); consistent with other reports indicating that this is tightly regulated (Jackson *et al.,* 1981, Jackson, 1987). To redress the balance between acetylated and non-acetylated histones, therefore, a fraction of the hyper- or under-acetylated histones must be preferentially degraded. The mechanism by which the cell recognises these alterations in the ratio of acetylated/non-acetylated molecules is unknown. Also the mechanism by which the levels of HAT's and HDAC's are regulated is unknown and would warrant further investigation.

7.4 Future directions

There is a pressing need to determine the exact structural and functional consequences of modifying the histones. These modifications are likely to bring about re-arrangements of histone-DNA and histone-protein

interactions, especially those involving the histone tail domains. It is still not known at which point(s) histone acetylation exerts influence on the regulation of transcription. It could be during pre-initiation complex assembly, recruitment of RNA polymerase, escape of RNA polymerase into the transcription unit or transcriptional elongation. Chromatin is conformationally dynamic, with DNA polymerase gaining access to the entire genome once every cell cycle, and RNA polymerase to the active transcription units several times per hour for an active gene (Jackson *et al.,* 1998). Histone modifications and nucleosome disruption follow as a consequence of these events, as chromatin is reassembled after the passage of the polymerase.

The current study was aimed at dissecting the role of histone acetylation in plant gene expression. Efforts to disrupt the balance between acetylation and deacetylation were met with a very quick compensatory response from the cell wherein it tried to restore this balance by up- or down-regulating certain key players in the chromatin. This shows fineness and the complexity of the whole process. How does a cell perceive changes in its acetylation status? Which molecules or receptors are involved in this network? These are some of the questions that one can ask at this point. Furthermore, inducible promoters can be used to drive the expression of HAT or HDAC genes in cell lines, which could then be used for expression profiling using microarrays. This is likely to provide information about the early and specific targets of histone acetylation.

Summary

Transcriptional activation in plants is a relatively poorly studied area. In non-plant eukaryotes, gene activation often involves the action of histone acetyltransferases (HAT's) (Lopez-Rodas *et al.,* 1985), which may associate with transcriptional activators, or are integral parts of them (Barlev *et al.,* 1995). Acetylation of histones in nucleosomes weakens nucleosome-DNA interaction (Loidl, 1988, Oliva *et al.,* 1990), and facilitates transcription (Hendzel *et al.,* 1994). HAT's reside in multi-protein complexes in mammals and yeast, and probably in all higher eukaryotes (Hampsey, 1997). Type A HAT's are nuclear-localized, and involved in promoting transcriptional activation by acetylating histones within nucleosomes, whereas type B HAT's, found in the cytoplasm, acetylate free histones as part of a nucleosome assembly mechanism (Wiegand and Brutlag, 1981; Garcea and Alberts, 1980; Brownell and Allis, 1996).

cDNA clones encoding putative homologues of *GCN5* (General control non-derepressible 5) a type A HAT, and a second coactivator, *ADA2* (Alteration/deficiency in activation) were isolated from maize (Riehl, Doktorarbeit, Universität zu Köln, 2002). With the help of these clones, molecular and biochemical investigations were made to dissect the role of histone acetylation in regulating gene expression in plants, using maize where possible. Gcn5 HAT's contain three typical domains; the catalytic domain at the N-terminus responsible for histone acetyl-transferase activity, a centrally located domain responsible for the interaction with adaptor protein Ada2, and the C-terminal bromo-domain, which interacts with the histone N-termini (Ornaghi *et al.,* 1999). Mammalian Gcn5 HAT's contain an additional N-terminal domain known as PCAF (p300/CREB binding associated factor) homology domain. This domain is thought to be involved in the acetylation of nucleosomes (Xu *et al.,* 1998). Characterisation of *ZmGCN5* revealed a longer N-terminal stretch showing no homology to the PCAF domain in mammalian *GCN5* genes. A genomic clone of *ZmGCN5* was isolated to characterise this N-terminal extension. Studies revealed that plant Gcn5 HAT's do not contain an equivalent PCAF domain.

ZmGCN5 conferred on a 35S::*GCN5*-GFP fusion protein nuclear localization in both BY2 and SR1 tobacco protoplasts, indicating that the isolated gene is a nuclear-located type A histone acetyltransferase. By analysing deletions, the region responsible for the nuclear targeting was mapped to the N-terminus of the protein. Thus an important role for the N-terminus of the ZmGcn5

has been established although it shares no homology with other histone acetyltransferases (plant as well as animal).

In order to monitor protein-protein interactions *in planta*, investigations were made using split-ubiquitin system (Johnsson and Varshavsky, 1994). With this system it could be shown that an interaction between ZmGcn5 and the adaptor ZmAda2 had taken place *in planta*. The results were further validated by using the Fluorescence resonance energy transfer (FRET) system. FRET analysis was also used to detect the *in vivo* interaction between the adaptor protein ZmAda2 and a plant transcriptional activator Opaque 2.

To monitor the relationship between ZmGcn5 expression and changes in the acetylation status of chromatin, transgenic maize cell lines containing an antisense version of *ZmGCN5* were generated. Furthermore, hyperacetylation of core histones was investigated using the deacetylase inhibitor, Trichostatin A. RNA populations from the treated and untreated cell lines were reverse transcribed and used as probes against 2600 maize EST's (Expressed sequence tags) spotted on nylon filters. Several transcripts showing significant changes in expression level on the microarrays were confirmed by Northern blot analysis, and changes in histone acetylation and the corresponding histone acetyltransferase and deacetylase enzymes were monitored using antibodies. Several classes of genes related to stress, pathogenesis, cellular architecture and plant development were seen regulated. However the most prominent response of the cell was to redress the change in acetylation status. The cell responded to inhibition of acetylation or deacetylation by reducing the levels of corresponding deacetylases or acetylases respectively, and by an increase in the abundancy of histone mRNAs. Although acetylated/deacetylated histones did accumulate, as expected, in contrast, there was no overall increase in histone protein concentrations, suggesting selective turnover of histones as part of a compensatory mechanism.

Zusammenfassung

Die Aktivierung der Transkription ist bei Pflanzen ein immer noch lediglich in Anfängen verstandener Prozess. Die Genaktivierung bei Eukaryoten geht meist einher mit einer Aktivierung von Histonacetyltransferasen (HAT's, Lopez-Rodas *et al*., 1985). Diese kommunizieren mit Transkriptionsfaktoren oder sind deren Untereinheiten (Barlev *et al*., 1995). Die Acetylierung der Histone in den Nucleosomen schwächt die Nucleosomen-DNA-Interaktion (Loidl, 1988; Oliva *et al*., 1990) ab und erleichtert so die Transkription (Hendzel *et al*., 1994). Bei Säugern und Hefen befinden sich die HAT's zusammen mit *chromatin remoddeling factors* und TAFs (*transcription activating factors,* Lee *et al*., 1993) in Multiproteinkomplexen (Hempsey, 1997).

Man unterscheidet zwei Gruppen von HAT's: Typ-A-HATs sind im Zellkern lokalisiert und fördern dort die Aktivierung der Transkription der Histone im Nucleosom und Typ B HAT's, lokalisiert im Cytoplasma, acetylieren dort voraussichtlich die freien Histone innerhalb des *nucleosom assembly mechanism* (Wiegand and Brutlag, 1981; Garcea and Alberts, 1980; Brownell and Allis, 1996).

Zur Analyse der Funktion von HATs bei der Genaktivierung in Mais wurden putative Homologe zu einer Typ-A-HAT, *GCN5* (*general control non-derepressible 5*), und einem Koaktivator, *ADA2* (*alteration/deficiency in activation*), isoliert (Riehl, Diplom, 1999; Promotion, 2002).

Für Gcn5-HAT wurden drei Domänen postuliert: die katalytische Domäne am N-Terminus scheint für die Histonacetyltransferaseaktivität verantwortlich zu sein, eine zentrale Domäne übernimmt die Interaktion mit dem adapterprotein Ada2 und C-Terminal befindet sich eine Bromodomäne, welche mit dem Histon-N-Terminus interagiert (Ornaghi et al., 1999). Zusätzlich tragen Gcn5 HATs bei Säugern noch eine N-terminale Domäne, bekannt als PCAF (p300/CREB binding associated factor) *homology domain*, die vermutlich an der Acetylierung der Nucleosomen beteiligt ist (Xu *et al.,* 1998). Der bei der Charakterisierung des *ZmGCN5* gefunde längere N-Terminus weist keine Homologie zu dieser auf. Auch funktionelle Studien ergaben, daß pflanzliche *GCN5*-genes keine PCAF-äquivalente Domäne tragen. Anhand von 35s::*GCN5*-GFP-Fusionsproteinen, mit denen Tabakprotoplasten (BY2/SR1) transformiert wurden, konnte eine Lokalisation dieser Proteine im Zellkern nachgewiesen werden. Dies weist auf

eine Typ A-Histonacetyltransferase hin. Durch Deletionsexperimente wurde die für die Kernlokalisation verantwortliche Sequenz (NLS, *nuclear lokalisation sequence*) N-teminal ausgemacht. Somit wurde, trotz fehlender Homologie mit anderen HATs die wichtige Funktion des N-Teminus des ZmGcn5-HAT deutlich,

Mit dem *split ubiquitin system* konnte eine Protein-Protein-Interaktionen *in planta* zwischen ZmGcn5-HAT und dem Adapter ZmAda2 gezeigt werden (Johnsson and Varshavsky, 1994). Dieses Ergebnis wurde ausserdem durch eine FRET-Analyse (*fluorescence resonance energy transfer*) bestätigt: Eine Kotransfektion von Protoplasten mit *ZmGCN5*-CFP (*cyan fluorescent protein*) und *ZmADA2*-YFP (*yellow fluorescent protein*) resultierte in einem Energietransfer von CFP zu YFP, was eine starke Interaktion zwischen ZmGCN5 und ZmADA2 zeigt. Die Analyse von ZmAda2 und dem Transkriptionsfaktor Opaque2 wies hingegen auf eine schwache Interaktion hin.

Um die Beziehung zwischen ZmGcn5-Expression und Veränderungen im Acetylierungsstatus des Chromatins beobachten zu können, wurden transgene *ZmGCN5-antisense lines* von Mais erstellt. Mit dem Deacetylaseinhibitor Trichostatin A wurde Hyperacetylierung untersucht. Die RNAs dieser Pflanzen wurden revers transkribiert und als Sonden für ein *screening* von 2600 Mais EST (*expressed sequence tag*) auf Nylonfiltern eingesetzt *(microarrays).* Transkripte, welche signifikante Veränderungen ihres Expressionsniveaus aufwiesen, wurden sowohl durch Northern-, als auch durch Western-*blot*-Analyse bestätigt. Die regulierten Gene liessen sich verschiedenen Klassen zuordnen: Stress, Phatogenese, Zytoskelett und Morphogenese. Die Hauptantwort der Zelle bestand jedoch darin, die Veränderung des Acetylierungsstatus durch Inhibition aufzuheben.

Diese kommt durch Konzentrationsabfall der korrespondierenden Deacetylasen oder Acetylasen bzw. eines Anstiegs der Histon-mRNAs zustande.

<u>Appendix I</u>: Schematic of different constructs used for FRET analysis of interactions between putative transcriptional co-activators ZmGcn5, ZmAda2 and transcriptional activator ZmO2.

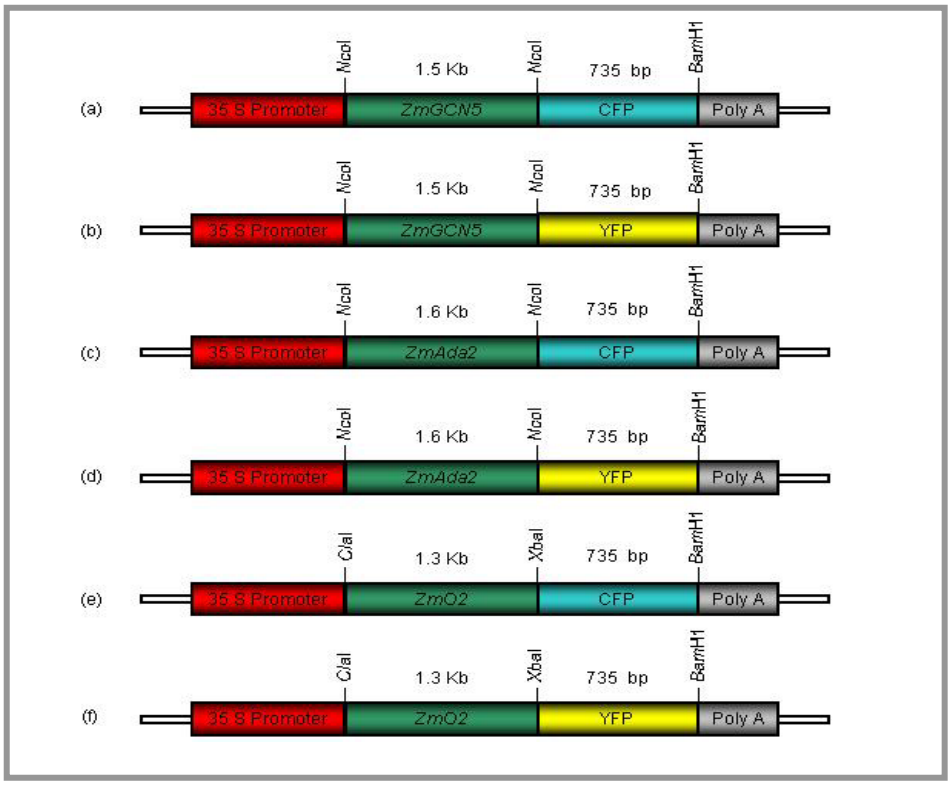

Appendix II: Sensitivity of microarray system

0.01% Spiked Nebulin	
ng of spotted Nebulin DNA	Signal intensity (MDC)
0.1	0.0125
1	0
10	0.0435
100	0.098
0.1% Spiked Nebulin	
ng of spotted Nebulin DNA	Signal intensity (MDC)
0.1	0.019
1	0.068
10	0.0395
100	0.048
0.5% Spiked Nebulin	
ng of spotted Nebulin DNA	Signal intensity (MDC)
0.1	0.1395
1	0.078
10	0.8855
100	6.208

MDC – Molecular dynamics counts.

Appendix III: Clones up-regulated in *ZmGCN5* antisense microarrays

Array Data			GenBank	Clone Identity	Random
Control HE-89	As ZmGCN5 HE-89	Fold Induction	Accession Number		Matching Probability
1.55	8.71	5.6	T14716	Histone 2B	
0.31	1.23	4.0	AA072442	Histone 2A	
2.54	8.57	3.4	T15325	Histone 2	
4.75	11.81	2.5	T25236	Histone H2B.2	
3.08	7.11	2.3	T23405	Histone 2	
1.06	2.34	2.2	H35878	Histone 2B	
6.65	14.52	2.2	T18835	Histone 2B	
2.01	4.25	2.1	T70634	Histone 4	
5.19	20.91	4.0	P36886	Photosystem I reaction centre subunit X	6.00E-14
0.12	0.47	4.0	AA054812	Chlorophyll a/b binding protein, *O. sativa*	5.00E-50
12.95	33.48	2.6	AAC67557.1	Chlorophyll a/b-binding protein, *O sativa*	6.00E-22
0.34	0.69	2.1	AAC28490.1	Photosystem II Chlorophyll a/b binding protein	1.00E-58
3.44	18.67	5.4	O76743	ATP-dependent RNA helicase glh-4	0-19
9.34	30.78	3.3	P49106	14-3-3-Like Protein GF14-6, *Z. mays*	e-102
4.83	11.51	2.4	CAB85491.1	Putative kinetochore protein [H vulgare].	1.00E-23
0.33	0.77	2.3	Q9SP07	14-3-3-like protein, *Lilium longiflorum*	e-118
2.32	5.26	2.3	T69040.1	MFS18 protein precursor, *Z. mays*	
0.29	0.62	2.2	T25298	DNA Repair Protein RADI Homolog	
1.16	2.40	2.1	BAB64785.1	Putative RNA helicase, DRH1 [O sativa].	e-100
1.85	30.96	16.8	AAK63882.1	Thaumatin-like pathogenesis related	5.00E-07
0.10	0.53	5.3	AAK18619.1	Ankyrin-Repeat Protein (Cytokinine signalling)	4.00E-43
0.66	3.20	4.8	T14745	Elongation Factor 1-Alpha (Cytoskeleton protein)	
0.71	3.35	4.8	P29023	Endochitinase Precursor B	e-106
4.02	16.12	4.0	NP_568791.1	Avr9 elicitor response protein-like, A. thaliana	3.00E-43
6.01	23.64	3.9	NP_199617.1	Phosphoribosylanthranilate Transferase	1.00E-12
0.31	1.18	3.8	AAL13304.1	Leucine Zipper Containing Protein	6.00E-30
0.20	0.69	3.4	T18839	HSP70	
1.65	5.27	3.2	U76259	Elongation Factor 1-Alpha	
0.56	1.69	3.0	BAA03751.1	Endochitinase [O. sativa].	8.00E-45
1.99	5.78	2.9	AAF42979.1	Elongation factor 1 alpha [Zea mays].	e-109
0.20	0.58	2.8	BAB01964.1	Leucine-rich repeat protein FLR1 [A. thaliana].	1.00E-21
0.19	0.48	2.5	Q02028	Stromal 70 kDa heat shock-related protein	1.00E-56
2.75	6.04	2.2	O24473	Eukaryotic translation initiation factor	3.00E-79
0.88	1.85	2.1	P33126	Heat Shock Protein 82	e-100
1.85	3.91	2.1	AA030722	Lipoxygenase (Disease related)	
0.29	0.61	2.1	T04146	Glossy1 homolog - *O. sativa* (Cell wall related)	e-108
1.85	3.82	2.1	T03395	Probable Lipase - *Z. mays*. (Cold resistance)	4.00E-25
4.08	8.31	2.0	Q40784	Possible Apospory-associated protein C	1.00E-22
0.12	0.57	5.0	T14661	Sucrose synthase (glucosyltransferase)	
0.12	0.60	4.9	BAA76902.1	Cycloartenol synthase	1.00E-22
3.47	14.33	4.1	NP_174350.1	UDP-galactose 4-epimerase-like protein	9.00E-50
0.21	0.86	4.0	NP_176563.1	Putative aminopeptidase [A thaliana].	2.00E-94
0.11	0.40	3.6	T15306	Protein Disulphide Isomerase	
0.12	0.36	3.1	W21619	ADP-glucose pyrophosphorylase	
0.88	2.31	2.6	S34636	Acetyl CoA carboxylase *Z. mays.*	e-136
0.14	0.37	2.6	T01414	ADP glucose--starch glucosyltransferase	2.00E-46
0.11	0.27	2.6	BAA90672.1	GSH-dependent dehydroascorbate reductase 1	3.00E-20
0.15	0.37	2.5	P93438	S-adenosyl-L-methionine synthetase	5.00E-46
0.34	0.82	2.4	T25208	ATP-dependent Clp protease sub unit	2.00E-51
0.14	0.33	2.4	AAG12489.2	O-deacetylbaccatin III-10-0-acetyltransferase	3.00E-73
0.40	0.95	2.4	T08854	Ferric leghemoglobin reductase - soybean.	7.00E-14
0.21	0.48	2.3	AAL33589.1	Methionine synthase [Zea mays].	e-106
0.25	0.57	2.2	T18321	Ribonuclease PH	
0.19	0.42	2.2	T14676	Protein Phosphatase	
1.69	3.40	2.0	AF308474_1	Asparaginase (transport & metabolism of N)	4.00E-05
2.25	10.69	4.8	Q04832	DNA Binding Protein	3.00E-20
0.21	0.56	2.7	AAG60186.1	Putative Nucleic Acid Binding Protein	2.00E-13
0.40	1.04	2.6	AAG59664.1	Putative RNA binding protein [O sativa].	1.00E-64
0.80	1.99	2.5	AF034945	RNA binding Protein	7.00E-28
0.16	0.39	2.4	T18285	Guanine Nucleotide-binding Protein beta subunit	
1.67	8.44	5.1	W21778	L11 ribosomal protein	
2.92	9.43	3.2	P35685	60S Ribosomal Protein L7A	4.00E-20
0.27	0.81	3.0	T18282	40 S Ribosomal Protein S5, Cytoplasmic	
0.39	0.98	2.5	T18261	40S ribosomal protein S24, cytoplasmic	
0.30	0.63	2.1	AA030697	Ribosomal protein L7	

Appendix IV: Clones down-regulated in *ZmGCN5* antisense microarrays

Array Data			GenBank	Clone Identity	Random
Control HE-89	As ZmGCN5 HE-89	Fold Attenuation	Accession Number		Matching Probability
7.48	1.41	5.3	P23444	**Histone H1.**	6.00E-05
11.31	2.51	4.5	AAL73043.1	**Histone H1-like protein [*Z. mays*]**	7.00E-29
5.92	1.07	5.5	T25279	**Alpha tubulin**	
0.97	0.23	4.3	T23361	**Actin**	
17.86	4.86	3.7	Q41764	**Actin-depolymerising factor 3 - *Z. mays***	4.00E-68
2.13	0.60	3.5	W21711	**Prohibitin (inhibitor of cell proliferation)**	
7.70	2.36	3.3	T70700	**Actin depolymerising factor**	
2.29	0.70	3.3	T15332	**Alpha tubulin**	
0.75	0.24	3.1	NP_190236.1	**Actin 12 [*A. thaliana*].**	1.00E-15
1.63	0.55	2.9	T15329	**Alpha tubulin**	
1.56	0.53	2.9	T25274	**Alpha tubulin**	
1.61	0.59	2.7	W49910	**Tubulin**	
9.72	3.65	2.7	P14641	**Tubulin alpha-2 chain (Alpha-2 tubulin).**	2.00E-90
1.60	0.72	2.2	T18286	**Caltractin (mitotic spindle associated protein)**	
2.61	0.27	9.8	T01354	**Herbicide safener binding protein 1 - *Z. mays*.**	1.00E-81
1.92	0.30	6.3	P29036	**Ferritin 1, (Iron induced protein)**	1.00E-12
2.31	0.41	5.7	AAF33112.1	**RPT2 light receptor A. thaliana.**	1.00E-39
5.96	1.10	5.4	T15276	**Wound inducible protein--basic**	
1.16	0.22	5.3	T27554	**Aluminum-induced protein**	
1.10	0.22	4.9	T50662	**UVB-resistance protein UVR8 - (*A. thaliana*)**	3.00E-86
18.86	3.91	4.8	T14760	***Salt* stress protein**	
2.60	0.59	4.4	CAC06433.1	**Expansin [Festuca pratensis].**	4.00E-05
2.99	0.71	4.2	AAB88876.1	**Putative auxin-repressed protein [*P armeniaca*].**	3.00E-06
3.77	0.98	3.8	T14788	**18 kDa heat shock protein, plastid**	
4.75	1.28	3.7	AA054806	**Ferritin (Iron induced protein)**	
3.18	0.90	3.5	AAL79732.1	**Heat shock protein 90 [*O .sativa*].**	8.00E-86
14.42	4.30	3.4	T23394	***Salt* stress protein**	
1.77	0.54	3.3	P30571	**Metallothionein-like protein**	1.00E-19
1.95	0.63	3.1	Q9SW70	**Stress-related protein.**	2.00E-14
0.97	0.32	3.0	NP_172566.1	**ZIP4, a putative zinc transporter [*A. thaliana*].**	3.00E-56
2.03	0.67	3.0	NP_196092.1	**Disease resistance - like protein [*A. thaliana*].**	3.00E-73
2.62	0.91	2.9	W21641	**Cysteine proteinase**	
1.96	0.82	2.4	P30571	**Metallothionein-like protein**	6.00E-20
0.94	0.40	2.4	AAD26530.1	**101 kDa heat shock protein [*Z. mays*]**	e-107
1.97	0.84	2.3	AAD29676.1	**Plasma membrane MIP protein [*Z. mays*].**	6.00E-68
1.38	0.66	2.1	AAK91502.1	**NADP-dependent malic enzyme [*Z. mays*]**	e-120
1.82	0.88	2.1	BAB40923.1	**Putative selenium binding protein**	e-102
2.46	0.63	3.9	AA051902	**Nucleotide binding protein**	
0.89	0.26	3.5	JE0116	**Zinc-finger protein R2931 [imported] - *O. sativa*.**	1.00E-71
0.86	0.26	3.3	AA054794	**Acyl-CoA binding protein**	
3.42	1.38	2.5	T25214	***Z. mays* GTP- binding protein YPTM2**	
1.28	0.35	3.6	T01210	**Glucose-6-phosphate/phosphate antiporter**	7.00E-37
5.21	1.45	3.6	T23323	**10 kDa zein (delta zein)**	
0.78	0.33	2.4	Q08047	**Starch branching enzyme II**	
0.79	0.37	2.1	AAF36688.1	**Secretory carrier membrane protein [O. sativa].**	9.00E-07
4.19	0.62	6.8	AAF23901.2	**Calcium-dependent protein kinase [O. sativa].**	1.00E-29
1.23	0.20	6.1	W49908	**Carbonic anhydrase**	
1.39	0.27	5.1	W21760	**6-phosphogluconate dehydrogenase**	
14.08	2.97	4.7	T23368	**Peptidyl-prolyl *cis*-trans isomerase**	
1.07	0.24	4.5	AAF66982.1	**Transposase [*Z. mays*].**	e-105
2.44	0.55	4.4	T25264	**Alcohol dehydrogenase**	
10.61	2.58	4.1	T02955	**Cytochrome P450 monooxygenase - *Z. mays***	1.00E-35
2.41	0.60	4.0	P22200	**Pyruvate Kinase, Cytosolic isozyme.**	1.00E-21
0.88	0.24	3.7	P80608	**Cysteine synthase (O-acetylserine sulfhydrylase)**	e-100
1.29	0.35	3.6	W21710	**Proteolipid, vacuolar ATPase**	
1.32	0.37	3.6	T18678	**Pyruvate, orthophosphate dikinase**	
1.99	0.56	3.6	AAL57038.1	**UDP-glucosyltransferase BX9 [Zea mays].**	1.00E-69
5.20	1.52	3.4	T20381	**Phosphoenolpyruvate carboxylase**	
1.86	0.55	3.4	AAF23902.1	**MAP kinase homolog [O. sativa].**	9.00E-56
9.44	2.84	3.3	BAB67990.1	**Putative protein disulfide isomerase [O. sativa].**	1.00E-16
1.10	0.35	3.2	BAA88185.1	**Similar to pyruvate kinase**	7.00E-65
2.88	0.92	3.1	T23349	**Alcohol dehydrogenase**	
3.01	0.99	3.0	T18803	**Cysteine proteinase inhibitor I**	
0.95	0.33	2.9	NP_198236.1	**Epimerase/dehydratase - like protein [A. thaliana].**	5.00E-47
9.77	3.39	2.9	BAB20887.1	**NADP dependent malic enzyme [O. sativa].**	e-120

2.10	0.77	2.7	P26301	**Enolase**	
1.79	0.66	2.7	T15301	**Triosephosphate isomerase**	
2.01	0.74	2.7	T18324	**RNase PH**	
1.97	0.73	2.7	NP_178516.1	**Putative acyl-CoA synthetase [A. thaliana].**	3.00E-92
9.69	3.74	2.6	P12783	**Cytosolic phosphoglycerate kinase 1**	2.00E-83
13.16	5.12	2.6	T14778	**Peptidyl-prolyl *cis*-trans isomerase**	
2.85	1.12	2.5	W21772	**Adenosyl homocysteine hydrolase**	
0.76	0.30	2.5	T02942	**O-succinylhomoserine (thiol)-lyase**	2.00E-81
0.99	0.40	2.5	T70653	**Proteolipid, vacuolar ATPase**	
3.27	1.32	2.5	W49890	**Triose phosphate isomerase**	
0.77	0.32	2.4	W21658	**SAM decarboxylase**	
2.15	0.91	2.4	CAC59823.1	**Xaa-Pro aminopeptidase 1 [*L esculentum*].**	8.00E-23
2.59	1.11	2.3	W21612	**Sucrose synthase**	
2.53	1.09	2.3	T18435	**Triosephosphate isomerase**	
3.80	1.65	2.3	P93629	**Alcohol dehydrogenase**	9.00E-84
1.81	0.82	2.2	CAC09522.1	**S-adenosylmethionine decarboxylase [*O sativa*].**	8.00E-12
1.48	0.68	2.2	Q08062	**Malate dehydrogenase, cytoplasmic. *Z. mays***	e-103
4.28	1.98	2.2	CAA62847.1	**Endoxyloglucan transferase (EXT) [H. vulgare].**	1.00E-04
2.72	1.28	2.1	P46611	**S-adenosylmethionine synthetase [O. sativa].**	e-105
1.38	0.65	2.1	T18824	**6-phosphogluconate dehydrogenase**	
4.36	0.79	5.5	T14781	**Ribosomal protein 27A**	
9.94	1.98	5.0	T18312	**Ribosomal protein 27A**	
7.34	1.69	4.4	AA030700	**Ribosomal protein L18**	
5.54	1.36	4.1	AA072429	**Ribosomal protein L39**	
4.04	1.06	3.8	T14795	**40S ribosomal protein S11, cytoplasmic**	
5.05	1.51	3.3	W49453	**Ribosomal protein S13**	
1.11	0.37	3.0	T18266	**60S ribosomal protein Po, cytoplasmic**	
6.12	2.13	2.9	W49429	**Ribosomal protein L31**	
4.90	1.73	2.8	T14735	**60S ribosomal protein L19**	
4.14	1.83	2.3	T18654	**40S ribosomal protein S28, cytoplasmic**	
4.27	2.00	2.1	T25263	**Ribosomal 5S RNA binding protein - *O. sativa***	
1.17	0.56	2.1	T18653	**Ribosomal protein L24**	

Literature cited

Alland, L., R. Muhle, *et al.* (1997). "Role for N-CoR and histone deacetylase in Sin3-mediated transcriptional repression." Nature **387**(6628): 49-55.

Allfrey, V. G. (1966). "Structural modifications of histones and their possible role in the regulation of ribonucleic acid synthesis." Proc Can Cancer Conf **6**: 313-35.

Allfrey, V. G., R. Faulkner, *et al.* (1964). "Acetylation and methylation of histones and their possible role in the regulation of RNA synthesis." Proc Natl Acad Sci U S A **51**: 786-794.

Allis, C. D., L. G. Chicoine, *et al.* (1985). "Deposition-related histone acetylation in micronuclei of conjugating Tetrahymena." Proc Natl Acad Sci U S A **82**(23): 8048-52.

Alting-Mees, M. A., J. A. Sorge, *et al.* (1992). "pBluescriptII: multifunctional cloning and mapping vectors." Methods Enzymol **216**: 483-95.

Altschul, S. F., W. Gish, *et al.* (1990). "Basic local alignment search tool." J Mol Biol **215**(3): 403-10.

Amedeo, P., Y. Habu, *et al.* (2000). "Disruption of the plant gene MOM releases transcriptional silencing of methylated genes." Nature **405**(6783): 203-6.

An, G. (1995). "Binary Ti plasmid vectors." Methods Mol Biol **44**: 47-58.

Annunziato, A. T., L. L. Frado, *et al.* (1988). "Treatment with sodium butyrate inhibits the complete condensation of interphase chromatin." Chromosoma **96**(2): 132-8.

Aukerman, M. J., R. J. Schmidt, *et al.* (1991). "An arginine to lysine substitution in the bZIP domain of an opaque-2 mutant in maize abolishes specific DNA binding." Genes Dev **5**(2): 310-20.

Baneres, J. L., A. Martin, *et al.* (1997). "The N tails of histones H3 and H4 adopt a highly structured conformation in the nucleosome." J Mol Biol **273**(3): 503-8.

Banerji, J., S. Rusconi, *et al.* (1981). "Expression of a beta-globin gene is enhanced by remote SV40 DNA sequences." Cell **27**(2 Pt 1): 299-308.

Barlev, N. A., R. Candau, *et al.* (1995). "Characterization of physical interactions of the putative transcriptional adaptor, ADA2, with acidic activation domains and TATA-binding protein." J Biol Chem **270**(33): 19337-44.

Bartel, P. L. and S. Fields (1995). "Analyzing protein-protein interactions using two-hybrid system." Methods Enzymol **254**: 241-63.

Bartels, D. and R. D. Thompson (1983). "The characterization of cDNA clones coding for wheat storage proteins." Nucleic Acids Res **11**(10): 2961-77.

Becker, H.-A., M. Riehl, *et al.* (1999). "Components of the maize GCN5/ADA2 coactivator complex." Maize News Letter **73**: 22.

Berger, S. L., B. Pina, *et al.* (1992). "Genetic isolation of ADA2: a potential transcriptional adaptor required for function of certain acidic activation domains." Cell **70**(2): 251-65.

Bevan, M. (1984). "Binary Agrobacterium vectors for plant transformation." Nucleic Acids Res **12**(22): 8711-21.

Bhatia, P., W. R. Taylor, *et al.* (1994). "Comparison of glyceraldehyde-3-phosphate dehydrogenase and 28S-ribosomal RNA gene expression as RNA loading controls for northern blot analysis of cell lines of varying malignant potential." Anal Biochem **216**(1): 223-6.

Birnboim, H. C. and J. Doly (1979). "A rapid alkaline extraction procedure for screening recombinant plasmid DNA." Nucleic Acids Res **7**(6): 1513-23.

Bohm, L. and C. Crane-Robinson (1984). "Proteases as structural probes for chromatin: the domain structure of histones." Biosci Rep **4**(5): 365-86.

Bonne-Andrea, C., M. L. Wong, *et al.* (1990). "In vitro replication through nucleosomes without histone displacement." Nature **343**(6260): 719-26.

Bradbury, E. M. (1992). "Reversible histone modifications and the chromosome cell cycle." Bioessays **14**(1): 9-16.

Brent, R. and M. Ptashne (1985). "A eukaryotic transcriptional activator bearing the DNA specificity of a prokaryotic repressor." Cell **43**(3 Pt 2): 729-36.

Brosch, G., R. Ransom, *et al.* (1995). "Inhibition of maize histone deacetylases by HC toxin, the host-selective toxin of Cochliobolus carbonum." Plant Cell **7**(11): 1941-50.

Brown, S. A., A. N. Imbalzano, *et al.* (1996). "Activator-dependent regulation of transcriptional pausing on nucleosomal templates." Genes Dev **10**(12): 1479-90.

Brownell, J. E. and C. D. Allis (1996). "Special HATs for special occasions: linking histone acetylation to chromatin assembly and gene activation." Curr Opin Genet Dev **6**(2): 176-84.

Brownell, J. E., J. Zhou, *et al.* (1996). "Tetrahymena histone acetyltransferase A: a homolog to yeast Gcn5p linking histone acetylation to gene activation." Cell **84**(6): 843-51.

Byrd, C., G. C. Turner, *et al.* (1998). "The N-end rule pathway controls the import of peptides through degradation of a transcriptional repressor." Embo J **17**(1): 269-77.

Candau, R. and S. L. Berger (1996). "Structural and functional analysis of yeast putative adaptors. Evidence for an adaptor complex in vivo." J Biol Chem **271**(9): 5237-45.

Candau, R., P. A. Moore, *et al.* (1996). "Identification of human proteins functionally conserved with the yeast putative adaptors ADA2 and GCN5." Mol Cell Biol **16**(2): 593-602.

Candau, R., J. X. Zhou, *et al.* (1997). "Histone acetyltransferase activity and interaction with ADA2 are critical for GCN5 function in vivo." Embo J **16**(3): 555-65.

Chee, M., R. Yang, *et al.* (1996). "Accessing genetic information with high-density DNA arrays." Science **274**(5287): 610-4.

Christensen, A. H. and P. H. Quail (1996). "Ubiquitin promoter-based vectors for high-level expression of selectable and/or screenable marker genes in monocotyledonous plants." Transgenic Res **5**(3): 213-8.

Chu CC, Wang CC, *et al.* (1975). "Establishment of an efficient medium for anther culture of rice through comparative experiments on the nitrogen sources." Sci Sin **18**: 659-668.

Clarke, A. S., J. E. Lowell, *et al.* (1999). "Esa1p is an essential histone acetyltransferase required for cell cycle progression." Mol Cell Biol **19**(4): 2515-26.

Clegg, R. M. (1995). "Fluorescence resonance energy transfer." Curr Opin Biotechnol **6**(1): 103-10.

Conklin, P. L. and R. L. Last (1995). "Differential accumulation of antioxidant mRNAs in Arabidopsis thaliana exposed to ozone." Plant Physiol **109**(1): 203-12.

Courey, A. J. and R. Tjian (1988). "Analysis of Sp1 in vivo reveals multiple transcriptional domains, including a novel glutamine-rich activation motif." Cell **55**(5): 887-98.

Covault, J. and R. Chalkley (1980). "The identification of distinct populations of acetylated histone." J Biol Chem **255**(19): 9110-6.

Dasso, M., S. Dimitrov, *et al.* (1994). "Nuclear assembly is independent of linker histones." Proc Natl Acad Sci U S A **91**(26): 12477-81.

Davie, J. R. and D. N. Chadee (1998). "Regulation and regulatory parameters of histone modifications." J Cell Biochem Suppl **30-31**: 203-13.

de Vetten, N. C. and R. J. Ferl (1994). "Two genes encoding GF14 (14-3-3) proteins in Zea mays. Structure, expression, and potential regulation by the G-box binding complex." Plant Physiol **106**(4): 1593-604.

DeRisi, J., L. Penland, *et al.* (1996). "Use of a cDNA microarray to analyse gene expression patterns in human cancer." Nat Genet **14**(4): 457-60.

Desprez, T., J. Amselem, *et al.* (1998). "Differential gene expression in Arabidopsis monitored using cDNA arrays." Plant J **14**(5): 643-52.

Dingwall, C., S. V. Sharnick, *et al.* (1982). "A polypeptide domain that specifies migration of nucleoplasmin into the nucleus." Cell **30**(2): 449-58.

Drysdale, C. M., E. Duenas, *et al.* (1995). "The transcriptional activator GCN4 contains multiple activation domains that are critically dependent on hydrophobic amino acids." Mol Cell Biol **15**(3): 1220-33.

Drysdale, C. M., B. M. Jackson, *et al.* (1998). "The Gcn4p activation domain interacts specifically in vitro with RNA polymerase II holoenzyme, TFIID, and the Adap-Gcn5p coactivator complex." Mol Cell Biol **18**(3): 1711-24.

Dunnwald, M., A. Varshavsky, *et al.* (1999). "Detection of transient in vivo interactions between substrate and transporter during protein translocation into the endoplasmic reticulum." Mol Biol Cell **10**(2): 329-44.

Durrin, L. K., R. K. Mann, *et al.* (1991). "Yeast histone H4 N-terminal sequence is required for promoter activation in vivo." Cell **65**(6): 1023-31.

Edwards, K., C. Johnstone, *et al.* (1991). "A simple and rapid method for the preparation of plant genomic DNA for PCR analysis." Nucleic Acids Res **19**(6): 1349.

Eickbush, T. H. and E. N. Moudrianakis (1978). "The histone core complex: an octamer assembled by two sets of protein-protein interactions." Biochemistry **17**(23): 4955-64.

Eickhoff, B., B. Korn, *et al.* (1999). "Normalization of array hybridization experiments in differential gene expression analysis." Nucleic Acids Res **27**(22): e33.

Fletcher, T. M. and J. C. Hansen (1996). "The nucleosomal array: structure/function relationships." Crit Rev Eukaryot Gene Expr **6**(2-3): 149-88.

Forsberg, E. C., L. T. Lam, *et al.* (1997). "Human histone acetyltransferase GCN5 exists in a stable macromolecular complex lacking the adapter ADA2." Biochemistry **36**(50): 15918-24.

Gadella, T. W., Jr., G. N. van der Krogt, *et al.* (1999). "GFP-based FRET microscopy in living plant cells." Trends Plant Sci **4**(7): 287-291.

Gadella, T. W., Jr., G. Vereb, Jr., *et al.* (1997). "Microspectroscopic imaging of nodulation factor-binding sites on living Vicia sativa roots using a novel bioactive fluorescent nodulation factor." Biophys J **72**(5): 1986-96.

Gallusci, P., F. Salamini, *et al.* (1994). "Differences in cell type-specific expression of the gene Opaque 2 in maize and transgenic tobacco." Mol Gen Genet **244**(4): 391-400.

Garcea, R. L. and B. M. Alberts (1980). "Comparative studies of histone acetylation in nucleosomes, nuclei, and intact cells. Evidence for special factors which modify acetylase action." J Biol Chem **255**(23): 11454-63.

Garcia-Ramirez, M., F. Dong, *et al.* (1992). "Role of the histone "tails" in the folding of oligonucleosomes depleted of histone H1." J Biol Chem **267**(27): 19587-95.

Geisberg, J. V., W. S. Lee, *et al.* (1994). "The zinc finger region of the adenovirus E1A transactivating domain complexes with the TATA box binding protein." Proc Natl Acad Sci U S A **91**(7): 2488-92.

Georgakopoulos, T. and G. Thireos (1992). "Two distinct yeast transcriptional activators require the function of the GCN5 protein to promote normal levels of transcription." Embo J **11**(11): 4145-52.

Giancotti, V., E. Russo, *et al.* (1984). "Histone modification in early and late Drosophila embryos." Biochem J **218**(2): 321-9.

Graessle, S., P. Loidl, *et al.* (2001). "Histone acetylation: plants and fungi as model systems for the investigation of histone deacetylases." Cell Mol Life Sci **58**(5-6): 704-20.

Grant, P. A., D. Schieltz, *et al.* (1998). "A subset of TAF(II)s are integral components of the SAGA complex required for nucleosome acetylation and transcriptional stimulation." Cell **94**(1): 45-53.

Grant, P. A., D. E. Sterner, *et al.* (1998). "The SAGA unfolds: convergence of transcription regulators in chromatin-modifying complexes." Trends Cell Biol **8**(5): 193-7.

Gregory, P. D., A. Schmid, *et al.* (1998). "Absence of Gcn5 HAT activity defines a novel state in the opening of chromatin at the PHO5 promoter in yeast." Mol Cell **1**(4): 495-505.

Grunstein, M. (1997). "Histone acetylation in chromatin structure and transcription." Nature **389**(6649): 349-52.

Guarente, L. (2000). "Sir2 links chromatin silencing, metabolism, and aging." Genes Dev **14**(9): 1021-6.

Guarente, L., R. R. Yocum, *et al.* (1982). "A GAL10-CYC1 hybrid yeast promoter identifies the GAL4 regulatory region as an upstream site." Proc Natl Acad Sci U S A **79**(23): 7410-4.

Gushchin, D., G. A. Nacheva, *et al.* (1988). "[Changes in the interaction of histones with DNA during transcription]." Dokl Akad Nauk SSSR **303**(6): 1504-7.

Hampsey, M. (1997). "A SAGA of histone acetylation and gene expression." Trends Genet **13**(11): 427-9.

Han, M. and M. Grunstein (1988). "Nucleosome loss activates yeast downstream promoters in vivo." Cell **55**(6): 1137-45.

Hansen, J. C. and A. P. Wolffe (1994). "A role for histones H2A/H2B in chromatin folding and transcriptional repression." Proc Natl Acad Sci U S A **91**(6): 2339-43.

Hartings, H., M. Maddaloni, *et al.* (1989). "The O2 gene which regulates zein deposition in maize endosperm encodes a protein with structural homologies to transcriptional activators." Embo J **8**(10): 2795-801.

Hassig, C. A. and S. L. Schreiber (1997). "Nuclear histone acetylases and deacetylases and transcriptional regulation: HATs off to HDACs." Curr Opin Chem Biol **1**(3): 300-8.

Hassig, C. A., J. K. Tong, *et al.* (1998). "A role for histone deacetylase activity in HDAC1-mediated transcriptional repression." Proc Natl Acad Sci U S A **95**(7): 3519-24.

Hayes, J. J. and A. P. Wolffe (1992). "Histones H2A/H2B inhibit the interaction of transcription factor IIIA with the Xenopus borealis somatic 5S RNA gene in a nucleosome." Proc Natl Acad Sci U S A **89**(4): 1229-33.

Heller, R. A., M. Schena, *et al.* (1997). "Discovery and analysis of inflammatory disease-related genes using cDNA microarrays." Proc Natl Acad Sci U S A **94**(6): 2150-5.

Hendzel, M. J., J. M. Sun, *et al.* (1994). "Histone acetyltransferase is associated with the nuclear matrix." J Biol Chem **269**(36): 22894-901.

Hettmann, C. and D. Soldati (1999). "Cloning and analysis of a Toxoplasma gondii histone acetyltransferase: a novel chromatin remodelling factor in Apicomplexan parasites." Nucleic Acids Res **27**(22): 4344-52.

Hinnebusch, A. G. (1990). "Transcriptional and translational regulation of gene expression in the general control of amino-acid biosynthesis in Saccharomyces cerevisiae." Prog Nucleic Acid Res Mol Biol **38**: 195-240.

Hoheisel, J. D., E. Maier, *et al.* (1993). "High resolution cosmid and P1 maps spanning the 14 Mb genome of the fission yeast S. pombe." Cell **73**(1): 109-20.

Holstege, F. C., E. G. Jennings, *et al.* (1998). "Dissecting the regulatory circuitry of a eukaryotic genome." Cell **95**(5): 717-28.

Hope, I. A., S. Mahadevan, *et al.* (1988). "Structural and functional characterization of the short acidic transcriptional activation region of yeast GCN4 protein." Nature **333**(6174): 635-40.

Hope, I. A. and K. Struhl (1986). "Functional dissection of a eukaryotic transcriptional activator protein, GCN4 of yeast." Cell **46**(6): 885-94.

Hope, I. A. and K. Struhl (1987). "GCN4, a eukaryotic transcriptional activator protein, binds as a dimer to target DNA." Embo J **6**(9): 2781-4.

Horiuchi, J., N. Silverman, *et al.* (1995). "ADA3, a putative transcriptional adaptor, consists of two separable domains and interacts with ADA2 and GCN5 in a trimeric complex." Mol Cell Biol **15**(3): 1203-9.

Hsieh, H. M., W. K. Liu, *et al.* (1995). "A novel stress-inducible metallothionein-like gene from rice." Plant Mol Biol **28**(3): 381-9.

Hueros, G., J. Rahfeld, *et al.* (1998). "A maize FK506-sensitive immunophilin, mzFKBP-66, is a peptidylproline cis-trans-isomerase that interacts with calmodulin and a 36-kDa cytoplasmic protein." Planta **205**(1): 121-31.

Hughes, T. R., C. J. Roberts, *et al.* (2000). "Widespread aneuploidy revealed by DNA microarray expression profiling." Nat Genet **25**(3): 333-7.

Huynh, Q. K., C. M. Hironaka, *et al.* (1992). "Antifungal proteins from plants. Purification, molecular cloning, and antifungal properties of chitinases from maize seed." J Biol Chem **267**(10): 6635-40.

Imbalzano, A. N., H. Kwon, *et al.* (1994). "Facilitated binding of TATA-binding protein to nucleosomal DNA." Nature **370**(6489): 481-5.

Ingles, C. J., M. Shales, *et al.* (1991). "Reduced binding of TFIID to transcriptionally compromised mutants of VP16." Nature **351**(6327): 588-90.

Jackson, D. A., F. J. Iborra, *et al.* (1998). "Numbers and organization of RNA polymerases, nascent transcripts, and transcription units in HeLa nuclei." Mol Biol Cell **9**(6): 1523-36.

Jackson, V. (1987). "Deposition of newly synthesized histones: misinterpretations due to cross-linking density-labeled proteins with Lomant's reagent." Biochemistry **26**(8): 2325-34.

Jackson, V., S. Marshall, *et al.* (1981). "The sites of deposition of newly synthesized histone." Nucleic Acids Res **9**(18): 4563-81.

Johnsson, N. and A. Varshavsky (1994). "Split ubiquitin as a sensor of protein interactions in vivo." Proc Natl Acad Sci U S A **91**(22): 10340-4.

Johnston, R. J., S. C. Pickett, *et al.* (1990). "Autoradiography using storage phosphor technology." Electrophoresis **11**: 355-360.

Jovin, T. M. and D. J. Arndt-Jovin (1989). "Luminescence digital imaging microscopy." Annu Rev Biophys Biophys Chem **18**: 271-308.

Junghans, H. and M. Metzlaff (1990). "A simple and rapid method for the preparation of total plant DNA." Biotechniques **8**(2): 176.

Kakutani, T., J. A. Jeddeloh, *et al.* (1995). "Characterization of an Arabidopsis thaliana DNA hypomethylation mutant." Nucleic Acids Res **23**(1): 130-7.

Kamei, Y., L. Xu, *et al.* (1996). "A CBP integrator complex mediates transcriptional activation and AP-1 inhibition by nuclear receptors." Cell **85**(3): 403-14.
Kaminaka, H., S. Morita, *et al.* (1998). "Gene cloning and expression of cytosolic glutathione reductase in rice (Oryza sativa L.)." Plant Cell Physiol **39**(12): 1269-80.
Katagiri, F. and N. H. Chua (1992). "Plant transcription factors: present knowledge and future challenges." Trends Genet **8**(1): 22-7.
Kato, K., T. Matsumoto, *et al.* (1972). "Liquid suspension culture of tobacco cells." Fermentation Technology Today: 689-695.
Kawasaki, H., L. Schiltz, *et al.* (2000). "ATF-2 has intrinsic histone acetyltransferase activity which is modulated by phosphorylation." Nature **405**(6783): 195-200.
Kenworthy, A. K. (2001). "Imaging protein-protein interactions using fluorescence resonance energy transfer microscopy." Methods **24**(3): 289-96.
Kim, Y. J., S. Bjorklund, *et al.* (1994). "A multiprotein mediator of transcriptional activation and its interaction with the C-terminal repeat domain of RNA polymerase II." Cell **77**(4): 599-608.
Kingston, R. E. and G. J. Narlikar (1999). "ATP-dependent remodeling and acetylation as regulators of chromatin fluidity." Genes Dev **13**(18): 2339-52.
Klebanow, E. R., D. Poon, *et al.* (1996). "Isolation and characterization of TAF25, an essential yeast gene that encodes an RNA polymerase II-specific TATA-binding protein-associated factor." J Biol Chem **271**(23): 13706-15.
Kodrzycki, R., R. S. Boston, *et al.* (1989). "The opaque-2 mutation of maize differentially reduces zein gene transcription." Plant Cell **1**(1): 105-14.
Koizumi, M., K. Yamaguchi-Shinozaki, *et al.* (1993). "Structure and expression of two genes that encode distinct drought-inducible cysteine proteinases in Arabidopsis thaliana." Gene **129**(2): 175-82.
Kolle, D., B. Sarg, *et al.* (1998). "Substrate and sequential site specificity of cytoplasmic histone acetyltransferases of maize and rat liver." FEBS Lett **421**(2): 109-14.
Kornberg, R. D. and Y. Lorch (1999). "Twenty-five years of the nucleosome, fundamental particle of the eukaryote chromosome." Cell **98**(3): 285-94.
Kruger, W., C. L. Peterson, *et al.* (1995). "Amino acid substitutions in the structured domains of histones H3 and H4 partially relieve the requirement of the yeast SWI/SNF complex for transcription." Genes Dev **9**(22): 2770-9.
Kuo, M. H. and C. D. Allis (1998). "Roles of histone acetyltransferases and deacetylases in gene regulation." Bioessays **20**(8): 615-26.
Kuo, M. H., J. E. Brownell, *et al.* (1996). "Transcription-linked acetylation by Gcn5p of histones H3 and H4 at specific lysines." Nature **383**(6597): 269-72.
Kuo, M. H., J. Zhou, *et al.* (1998). "Histone acetyltransferase activity of yeast Gcn5p is required for the activation of target genes in vivo." Genes Dev **12**(5): 627-39.
Kwon, H., A. N. Imbalzano, *et al.* (1994). "Nucleosome disruption and enhancement of activator binding by a human SW1/SNF complex." Nature **370**(6489): 477-81.
Landschulz, W. H., P. F. Johnson, *et al.* (1988). "The leucine zipper: a hypothetical structure common to a new class of DNA binding proteins." Science **240**(4860): 1759-64.
Lane, T., C. Ibanez, *et al.* (1990). "Transformation by v-myb correlates with trans-activation of gene expression." Mol Cell Biol **10**(6): 2591-8.
Lechner, T., A. Lusser, *et al.* (1996). "A comparative study of histone deacetylases of plant, fungal and vertebrate cells." Biochim Biophys Acta **1296**(2): 181-8.
Lechner, T., A. Lusser, *et al.* (2000). "RPD3-type histone deacetylases in maize embryos." Biochemistry **39**(7): 1683-92.
Lee, K. M. and J. J. Hayes (1998). "Linker DNA and H1-dependent reorganization of histone-DNA interactions within the nucleosome." Biochemistry **37**(24): 8622-8.
Lee, Y., D. Choi, *et al.* (2001). "Expansins: ever-expanding numbers and functions." Curr Opin Plant Biol **4**(6): 527-32.
Lee, Y. and H. Kende (2001). "Expression of beta-expansins is correlated with internodal elongation in deepwater rice." Plant Physiol **127**(2): 645-54.
Levinger, L. and A. Varshavsky (1982). "Selective arrangement of ubiquitinated and D1 protein-containing nucleosomes within the Drosophila genome." Cell **28**(2): 375-85.
Lin, H., K. E. Yutzey, *et al.* (1991). "Muscle-specific expression of the troponin I gene requires interactions between helix-loop-helix muscle regulatory factors and ubiquitous transcription factors." Mol Cell Biol **11**(1): 267-80.

Lockhart, D. J., H. Dong, *et al.* (1996). "Expression monitoring by hybridization to high-density oligonucleotide arrays." Nat Biotechnol **14**(13): 1675-80.

Lohmer, S., M. Maddaloni, *et al.* (1991). "The maize regulatory locus Opaque-2 encodes a DNA-binding protein which activates the transcription of the b-32 gene." Embo J **10**(3): 617-24.

Loidl, P. (1988). "Towards an understanding of the biological function of histone acetylation." FEBS Lett **227**(2): 91-5.

Loidl, P. (1994). "Histone acetylation: facts and questions." Chromosoma **103**(7): 441-9.

Lopez-Rodas, G., E. I. Georgieva, *et al.* (1991). "Histone acetylation in Zea mays.I. Activities of histone acetyltransferases and histone deacetylases." J Biol Chem **266**(28): 18745-50.

Lopez-Rodas, G., J. E. Perez-Ortin, *et al.* (1985). "Partial purification and properties of two histone acetyltransferases from the yeast, Saccharomyces cerevisiae." Arch Biochem Biophys **239**(1): 184-90.

Luger, K., A. W. Mader, *et al.* (1997). "Crystal structure of the nucleosome core particle at 2.8 A resolution." Nature **389**(6648): 251-60.

Lugert, T. and W. Werr (1994). "A novel DNA-binding domain in the Shrunken initiator-binding protein (IBP1)." Plant Mol Biol **25**(3): 493-506.

Lusser, A., A. Eberharter, *et al.* (1999). "Analysis of the histone acetyltransferase B complex of maize embryos." Nucleic Acids Res **27**(22): 4427-35.

Lusser, A., D. Kolle, *et al.* (2001). "Histone acetylation: lessons from the plant kingdom." Trends Plant Sci **6**(2): 59-65.

Ma, J. and M. Ptashne (1987). "Deletion analysis of GAL4 defines two transcriptional activating segments." Cell **48**(5): 847-53.

Ma, J. and M. Ptashne (1987). "A new class of yeast transcriptional activators." Cell **51**(1): 113-9.

Maddaloni, M., L. Barbieri, *et al.* (1991). "Characterisation of an endosperm-specific developmentally regulated protein synthesis inhibitor from maize seeds." J. Genet. & Breed. **45**: 377-380.

Mahadevan, L. C., A. C. Willis, *et al.* (1991). "Rapid histone H3 phosphorylation in response to growth factors, phorbol esters, okadaic acid, and protein synthesis inhibitors." Cell **65**(5): 775-83.

Maliga, P., A. Sz-Breznovits, *et al.* (1973). "Streptomycin-resistant plants from callus culture of haploid tobacco." Nat New Biol(244): 29-30.

Maniatis, T., E. F. Fritsch, *et al.* (1989). "Molecular cloning; a laboratory manual,." Cold spring harbour laboratory press(2nd edition).

Marcus, G. A., J. Horiuchi, *et al.* (1996). "ADA5/SPT20 links the ADA and SPT genes, which are involved in yeast transcription." Mol Cell Biol **16**(6): 3197-205.

Marcus, G. A., N. Silverman, *et al.* (1994). "Functional similarity and physical association between GCN5 and ADA2: putative transcriptional adaptors." Embo J **13**(20): 4807-15.

Marmorstein, R. (2001). "Structure and function of histone acetyltransferases." Cell Mol Life Sci **58**(5-6): 693-703.

Marmorstein, R. and S. Y. Roth (2001). "Histone acetyltransferases: function, structure, and catalysis." Curr Opin Genet Dev **11**(2): 155-61.

Mauri, I., M. Maddaloni, *et al.* (1993). "Functional expression of the transcriptional activator Opaque-2 of Zea mays in transformed yeast." Mol Gen Genet **241**(3-4): 319-26.

Melcher, K. and S. A. Johnston (1995). "GAL4 interacts with TATA-binding protein and coactivators." Mol Cell Biol **15**(5): 2839-48.

Moehs, C. P., F. E. McElwain, *et al.* (1988). "Chromosomal proteins of Arabidopsis thaliana." Plant Mol Biol **11**: 507-515.

Mergny, J. L. and J. C. Maurizot (2001). "Fluorescence resonance energy transfer as a probe for g-quartet formation by a telomeric repeat." Chembiochem **2**(2): 124-32.

Morcz, S., G. Donn, *et al.* (1990). "An improved system to obtain fertile regenerants via maize protoplasts isolated from a highly embryogenic suspension culture." Theor Appl Genet **80**(721-726).

Nagata, T., K. Okada, *et al.* (1981). "Delivery of Tobacco Mosaic Virus RNA into Plant Protoplasts by Reverse-Phase Evaporation Vesicles (Liposomes)." Mol Gen Genet **184**: 161-165.

Negrutiu, I., R. Shillito, *et al.* (1987). "Hybrid genes in the analysis of transformation conditions." Plant Molecular Biology **8**: 363-373.

Neuwald, A. F. and D. Landsman (1997). "GCN5-related histone N-acetyltransferases belong to a diverse superfamily that includes the yeast SPT10 protein." Trends Biochem Sci **22**(5): 154-5.

Nightingale, K. P., R. E. Wellinger, *et al.* (1998). "Histone acetylation facilitates RNA polymerase II transcription of the Drosophila hsp26 gene in chromatin." Embo J **17**(10): 2865-76.

Ogryzko, V. V., R. L. Schiltz, *et al.* (1996). "The transcriptional coactivators p300 and CBP are histone acetyltransferases." Cell **87**(5): 953-9.

Oliva, R., D. P. Bazett-Jones, *et al.* (1990). "Histone hyperacetylation can induce unfolding of the nucleosome core particle." Nucleic Acids Res **18**(9): 2739-47.

Ornaghi, P., P. Ballario, *et al.* (1999). "The bromodomain of Gcn5p interacts in vitro with specific residues in the N terminus of histone H4." J Mol Biol **287**(1): 1-7.

Owen-Hughes, T., R. T. Utley, *et al.* (1996). "Persistent site-specific remodeling of a nucleosome array by transient action of the SWI/SNF complex." Science **273**(5274): 513-6.

Parthun, M. R., J. Widom, *et al.* (1996). "The major cytoplasmic histone acetyltransferase in yeast: links to chromatin replication and histone metabolism." Cell **87**(1): 85-94.

Perry, M. and R. Chalkley (1982). "Histone acetylation increases the solubility of chromatin and occurs sequentially over most of the chromatin. A novel model for the biological role of histone acetylation." J Biol Chem **257**(13): 7336-47.

Peters, R. (1986). "Fluorescence microphotolysis to measure nucleocytoplasmic transport and intracellular mobility." Biochim Biophys Acta **864**(3-4): 305-59.

Peterson, C. L. and J. W. Tamkun (1995). "The SWI-SNF complex: a chromatin remodeling machine?" Trends Biochem Sci **20**(4): 143-6.

Pina, B., S. Berger, *et al.* (1993). "ADA3: a gene, identified by resistance to GAL4-VP16, with properties similar to and different from those of ADA2." Mol Cell Biol **13**(10): 5981-9.

Pogo, B. G., V. G. Allfrey, *et al.* (1966). "RNA synthesis and histone acetylation during the course of gene activation in lymphocytes." Proc Natl Acad Sci U S A **55**(4): 805-12.

Pollard, K. J. and C. L. Peterson (1997). "Role for ADA/GCN5 products in antagonizing chromatin-mediated transcriptional repression." Mol Cell Biol **17**(11): 6212-22.

Pollard, K. J. and C. L. Peterson (1998). "Chromatin remodeling: a marriage between two families?" Bioessays **20**(9): 771-80.

Pollok, B. A. and R. Heim (1999). "Using GFP in FRET-based applications." Trends Cell Biol **9**(2): 57-60.

Potrykus, I. (1990). "Gene transfer methods for plants and cell cultures." Ciba Found Symp **154**: 198-208; discussion 208-12.

Ptashne, M. and A. Gann (1997). "Transcriptional activation by recruitment." Nature **386**(6625): 569-77.

Qiagen (2000). "Qiagen plasmid purification handbook."

Roberts, S. M. and F. Winston (1996). "SPT20/ADA5 encodes a novel protein functionally related to the TATA-binding protein and important for transcription in Saccharomyces cerevisiae." Mol Cell Biol **16**(6): 3206-13.

Robles, J. (1994). "p-GEM-T vector ysytems trouble shooting guide." Promega notes 45 **19**: 19.

Rojo-Niersbach, E., D. Morley, *et al.* (2000). "A new method for the selection of protein interactions in mammalian cells." Biochem J **348 Pt 3**: 585-90.

Rossi, V., H. Hartings, *et al.* (1998). "Identification and characterisation of an RPD3 homologue from maize (Zea mays L.) that is able to complement an rpd3 null mutant of Saccharomyces cerevisiae." Mol Gen Genet **258**(3): 288-96.

Roth, S. Y. and C. D. Allis (1996). "Histone acetylation and chromatin assembly: a single escort, multiple dances?" Cell **87**(1): 5-8.

Ruiz-Carrillo, A., L. J. Wangh, *et al.* (1975). "Processing of newly synthesized histone molecules." Science **190**(4210): 117-28.

Rundlett, S. E., A. A. Carmen, *et al.* (1996). "HDA1 and RPD3 are members of distinct yeast histone deacetylase complexes that regulate silencing and transcription." Proc Natl Acad Sci U S A **93**(25): 14503-8.

Rundlett, S. E., A. A. Carmen, *et al.* (1998). "Transcriptional repression by UME6 involves deacetylation of lysine 5 of histone H4 by RPD3." Nature **392**(6678): 831-5.

Saleh, A., V. Lang, *et al.* (1997). "Identification of native complexes containing the yeast coactivator/repressor proteins NGG1/ADA3 and ADA2." J Biol Chem **272**(9): 5571-8.

Sauve, D. M., H. J. Anderson, *et al.* (1999). "Phosphorylation-induced rearrangement of the histone H3 NH2-terminal domain during mitotic chromosome condensation." J Cell Biol **145**(2): 225-35.

Savonet, V., C. Maenhaut, *et al.* (1997). "Pitfalls in the use of several "housekeeping" genes as standards for quantitation of mRNA: the example of thyroid cells." Anal Biochem **247**(1): 165-7.

Schena, M., D. Shalon, *et al.* (1995). "Quantitative monitoring of gene expression patterns with a complementary DNA microarray." Science **270**(5235): 467-70.

Schmidt, R. J., F. A. Burr, *et al.* (1990). "Maize regulatory gene opaque-2 encodes a protein with a "leucine-zipper" motif that binds to zein DNA." Proc Natl Acad Sci U S A **87**(1): 46-50.

Schmidt, R. J., F. A. Burr, *et al.* (1987). "Transposon tagging and molecular analysis of the maize regulatory locus opaque-2." Science **238**(4829): 960-3.

Schmitz, D., S. Lohmer, *et al.* (1997). "The activation domain of the maize transcription factor Opaque-2 resides in a single acidic region." Nucleic Acids Res **25**(4): 756-63.

Serna, A., M. Maitz, *et al.* (2001). "Maize endosperm secretes a novel antifungal protein into adjacent maternal tissue." Plant J **25**(6): 687-98.

Shah, K., T. W. Gadella, Jr., *et al.* (2001). "Subcellular localization and oligomerization of the Arabidopsis thaliana somatic embryogenesis receptor kinase 1 protein." J Mol Biol **309**(3): 641-55.

Sheen, J., S. Hwang, *et al.* (1995). "Green-fluorescent protein as a new vital marker in plant cells." Plant J **8**(5): 777-84.

Shen, X., L. Yu, *et al.* (1995). "Linker histones are not essential and affect chromatin condensation in vivo." Cell **82**(1): 47-56.

Silver, P. A. (1991). "How proteins enter the nucleus." Cell **64**(3): 489-97.

Silverman, N., J. Agapite, *et al.* (1994). "Yeast ADA2 protein binds to the VP16 protein activation domain and activates transcription." Proc Natl Acad Sci U S A **91**(24): 11665-8.

Smith, D. L. and K. C. Gross (2000). "A family of at least seven beta-galactosidase genes is expressed during tomato fruit development." Plant Physiol **123**(3): 1173-83.

Smith, E. R., J. M. Belote, *et al.* (1998). "Cloning of Drosophila GCN5: conserved features among metazoan GCN5 family members." Nucleic Acids Res **26**(12): 2948-54.

Sogo, J. M., H. Stahl, *et al.* (1986). "Structure of replicating simian virus 40 minichromosomes. The replication fork, core histone segregation and terminal structures." J Mol Biol **189**(1): 189-204.

Stagljar, I., C. Korostensky, *et al.* (1998). "A genetic system based on split-ubiquitin for the analysis of interactions between membrane proteins in vivo." Proc Natl Acad Sci U S A **95**(9): 5187-92.

Sterner, D. E. and S. L. Berger (2000). "Acetylation of Histones and Transcription-Related Factors." Microbiol. Mol. Biol. Rev. **64**(2): 435-459.

Sterner, D. E., X. Wang, *et al.* (2002). "The SANT Domain of Ada2 Is Required for Normal Acetylation of Histones by the Yeast SAGA Complex." J Biol Chem **277**(10): 8178-86.

Stockinger, E. J., S. J. Gilmour, *et al.* (1997). "Arabidopsis thaliana CBF1 encodes an AP2 domain-containing transcriptional activator that binds to the C-repeat/DRE, a cis-acting DNA regulatory element that stimulates transcription in response to low temperature and water deficit." PNAS **94**(3): 1035-1040.

Stockinger, E. J., Y. Mao, *et al.* (2001). "Transcriptional adaptor and histone acetyltransferase proteins in Arabidopsis and their interactions with CBF1, a transcriptional activator involved in cold-regulated gene expression." Nucleic Acids Res **29**(7): 1524-33.

Struhl, K. (1995). "Yeast transcriptional regulatory mechanisms." Annu Rev Genet **29**: 651-74.

Struhl, K. (1998). "Histone acetylation and transcriptional regulatory mechanisms." Genes Dev **12**(5): 599-606.

Studitsky, V. M., D. J. Clark, *et al.* (1994). "A histone octamer can step around a transcribing polymerase without leaving the template." Cell **76**(2): 371-82.

Tamkun, J. W., R. Deuring, *et al.* (1992). "brahma: a regulator of Drosophila homeotic genes structurally related to the yeast transcriptional activator SNF2/SWI2." Cell **68**(3): 561-72.

Taunton, J., C. A. Hassig, *et al.* (1996). "A mammalian histone deacetylase related to the yeast transcriptional regulator Rpd3p." Science **272**(5260): 408-11.

Tian, L. and Z. J. Chen (2001). "Blocking histone deacetylation in Arabidopsis induces pleiotropic effects on plant gene regulation and development." Proc Natl Acad Sci U S A **98**(1): 200-5.

Topfer, R., J. Schell, *et al.* (1988). "Versatile cloning vectors for transient gene expression and direct gene transfer in plant cells." Nucleic Acids Res **16**(17): 8725.

Tse, C. and J. C. Hansen (1997). "Hybrid trypsinized nucleosomal arrays: identification of multiple functional roles of the H2A/H2B and H3/H4 N-termini in chromatin fiber compaction." Biochemistry **36**(38): 11381-8.

Tse, C., T. Sera, *et al.* (1998). "Disruption of higher-order folding by core histone acetylation dramatically enhances transcription of nucleosomal arrays by RNA polymerase III." Mol Cell Biol **18**(8): 4629-38.

Tsukiyama, T., P. B. Becker, *et al.* (1994). "ATP-dependent nucleosome disruption at a heat-shock promoter mediated by binding of GAGA transcription factor." Nature **367**(6463): 525-32.

Ura, K., H. Kurumizaka, *et al.* (1997). "Histone acetylation: influence on transcription, nucleosome mobility and positioning, and linker histone-dependent transcriptional repression." Embo J **16**(8): 2096-107.

Varshavsky, A. (1996). "The N-end rule: functions, mysteries, uses." Proc Natl Acad Sci U S A **93**(22): 12142-9.

Varshavsky, A. (1997). "The ubiquitin system." Trends Biochem Sci **22**(10): 383-7.

Verreault, A. (2000). "De novo nucleosome assembly: new pieces in an old puzzle." Genes Dev **14**(12): 1430-8.

Verreault, A., P. D. Kaufman, *et al.* (1996). "Nucleosome assembly by a complex of CAF-1 and acetylated histones H3/H4." Cell **87**(1): 95-104.

Vidal, M. and R. F. Gaber (1991). "RPD3 encodes a second factor required to achieve maximum positive and negative transcriptional states in Saccharomyces cerevisiae." Mol Cell Biol **11**(12): 6317-27.

Vignali, M., A. H. Hassan, *et al.* (2000). "ATP-dependent chromatin-remodeling complexes." Mol Cell Biol **20**(6): 1899-910.

Vinson, C. R., P. B. Sigler, *et al.* (1989). "Scissors-grip model for DNA recognition by a family of leucine zipper proteins." Science **246**(4932): 911-6.

Wade, P. A., D. Pruss, *et al.* (1997). "Histone acetylation: chromatin in action." Trends Biochem Sci **22**(4): 128-32.

Wade, P. A. and A. P. Wolffe (1997). "Histone acetyltransferases in control." Curr Biol **7**(2): R82-4.

Wang, L., L. Liu, *et al.* (1998). "Critical residues for histone acetylation by Gcn5, functioning in Ada and SAGA complexes, are also required for transcriptional function in vivo." Genes Dev **12**(5): 640-53.

Waterborg, J. H., R. E. Harrington, *et al.* (1990). "Dynamic histone acetylation in alfalfa cells. Butyrate interference with acetate labeling." Biochim Biophys Acta **1049**(3): 324-30.

Wei, Y., C. A. Mizzen, *et al.* (1998). "Phosphorylation of histone H3 at serine 10 is correlated with chromosome condensation during mitosis and meiosis in Tetrahymena." Proc Natl Acad Sci U S A **95**(13): 7480-4.

Wiegand, R. C. and D. L. Brutlag (1981). "Histone acetylase from Drosophila melanogaster specific for H4." J Biol Chem **256**(9): 4578-83.

Wittke, S., N. Lewke, *et al.* (1999). "Probing the molecular environment of membrane proteins in vivo." Mol Biol Cell **10**(8): 2519-30.

Wolffe, A. P. (1997). "Histones, nucleosomes and the roles of chromatin structure in transcriptional control." Biochem Soc Trans **25**(2): 354-8.

Wolffe, A. P. (1997). "Transcriptional control. Sinful repression." Nature **387**(6628): 16-7.

Wolffe, A. P. and D. Guschin (2000). "Review: chromatin structural features and targets that regulate transcription." J Struct Biol **129**(2-3): 102-22.

Wolffe, A. P. and J. J. Hayes (1999). "Chromatin disruption and modification." Nucleic Acids Res **27**(3): 711-20.

Wright, S. Y., M. M. Suner, *et al.* (1993). "Isolation and characterization of male flower cDNAs from maize." Plant J **3**(1): 41-9.

Wu, K., K. Malik, *et al.* (2000). "Functional analysis of a RPD3 histone deacetylase homologue in Arabidopsis thaliana." Plant Mol Biol **44**(2): 167-76.

Wu, K., L. Tian, *et al.* (2000). "Functional analysis of HD2 histone deacetylase homologues in Arabidopsis thaliana." Plant J **22**(1): 19-27.

Wu, P. and L. Brand (1994). "Resonance energy transfer: methods and applications." Anal Biochem **218**(1): 1-13.

Xu, W., D. G. Edmondson, *et al.* (1998). "Mammalian GCN5 and P/CAF acetyltransferases have homologous amino-terminal domains important for recognition of nucleosomal substrates." Mol Cell Biol **18**(10): 5659-69.

Yang, X. J., V. V. Ogryzko, *et al.* (1996). "A p300/CBP-associated factor that competes with the adenoviral oncoprotein E1A." Nature **382**(6589): 319-24.

Yao, C., W. S. Conway, *et al.* (1999). "Gene encoding polygalacturonase inhibitor in apple fruit is developmentally regulated and activated by wounding and fungal infection." Plant Mol Biol **39**(6): 1231-41.

Yoshida, M., S. Horinouchi, *et al.* (1995). "Trichostatin A and trapoxin: novel chemical probes for the role of histone acetylation in chromatin structure and function." Bioessays **17**(5): 423-30.

Zhang, D. E. and D. A. Nelson (1988). "Histone acetylation in chicken erythrocytes. Rates of deacetylation in immature and mature red blood cells." Biochem J **250**(1): 241-5.

Zhao, L. J. and R. Padmanabhan (1988). "Nuclear transport of adenovirus DNA polymerase is facilitated by interaction with preterminal protein." Cell **55**(6): 1005-15.

Ziff, E. B. (1990). "Transcription factors: a new family gathers at the cAMP response site." Trends Genet **6**(3): 69-72.

Erklärung

"Ich versichere, daß ich die von mir vorgelegte Dissertation selbständig angefertigt, die benutzten Quellen und Hilfsmittel vollständig angegeben und die Stellen der Arbeit - einschließlich Tabellen, Karten und Abbildungen -, die anderen Werken im Wortlaut oder dem Sinn nach entnommen sind, in jedem Einzelfall als Entlehnung kenntlich gemacht habe; daß diese Dissertation noch keiner anderen Fakultät oder Universität zur Prüfung vorgelegen hat; daß sie - abgesehen von unten angegebenen Teilpublikationen - noch nicht veröffentlicht worden ist sowie, daß ich eine solche Veröffentlichung vor Abschluß des Promotionsverfahrens nicht vornehmen werde. Die Bestimmungen dieser Promotionsordnung sind mir bekannt. Die von mir vorgelegte Dissertation ist von Priv.-Doz. Dr. Richard D. Thompson betreut worden."

Köln, im July 2002

Riyaz Ahmad Bhat

Publications:

Riyaz A. Bhat, Marcus Riehl, Geraldina Santandrea, Riccardo Velasco, Stephen Slocombe, Richard D. Thompson, Heinz-Albert Becker

Alteration of *GCN5* levels in maize reveals dynamic responses to manipulating histone acetylation (The Plant Journal, *in press*).

Riyaz A. Bhat, Marcus Riehl, Jan Willum Borst, Heinz Albert Becker, Richard D. Thompson

In vivo protein-protein interactions between putative transcriptional co-activators ZmGcn5 HAT, adaptor ZmAda2 and plant transcriptional activator ZmO2 (in preparation)

Sequences:

Zea mays GCN5 gene for histone acetyltransferase, complete cds.

Accession Number: AJ428542

Acknowledgements

It is a heart warming and rewarding experience to pay tributes to the people whose invaluable contributions helped me throughout my time as a PhD researcher at Max Planck Institute, Köln.

My sincere and profound gratitude goes to Dr. Richard D. Thompson for giving me an opportunity to join his group and for the trust that he put into me. It was a unique experience to work with him. His excellent and matchless scientific guidance helped me immensely and expanded my capabilities. I thank Prof. Dr. Francesco Salamini for the scientific support that I received in his department. I also thank Prof. Dr. Ulf Ingo Fleugge for giving me an opportunity to join the GraduirtenKolleg at the University of Köln.

I wish to extend my gratitude to Dr. Timothy Patrick O'Connell, Dr. Heinz Albert-Becker and Dr. Jonathan Philips for providing all the scientific and moral support at the start of my PhD research. It was a relief to know that there was someone who had solutions to my problems (well those days everything was a problem).

My special thanks go to the present and the past members of the Thompson family. Marcus thanks for being an excellent lab mate. It was a very nice experience to work with you. Thanks for all the help and discussions. Violeta and Sonja, thanks for all the support. Ursula, many thanks for setting up the microarray facility in our group. But for your help it would have been impossible to even think about microarrays. Also thanks for being an excellent company and bringing many a smile on my face when needed. Brigitte, I don't know how to describe my gratitude and appreciation. Your golden tissue culture fingers did the magic. Thanks for being there for me when needed. You are one of the few persons who influenced me a lot during my time at MPI. Thanks for supporting me, for taking care of me. There is no way I can pay back for all your help and support.
I also thank the Monocot transformation group (Dr. Hans Henning Steinbiss, Anja Seidel and Sabine Schulze) for their help with the plant transformation. Anja thank you very much for taking care of my transformation experiments. They all worked fine. Sabine thanks for providing the BY2 cell line. I thank Dr. Günter Donn, Aventis Crop Sciences for help with maize transformation.

I also wish to thank all my friends and colleagues at MPI. Special thanks are also due to Konstanze for all the help.
Finally appreciation and praise is due to my family, especially my parents, without whom I would have given up long time back. Mama and Papa, thank you very much for your prayers and support. You have served as guiding stars throughout my stay outside Kashmir.

Lebenslauf

Persönliche Daten

Daten zur Person

Name:	Riyaz Ahmad Bhat
Anschrift:	Kolibriweg 3, Vogelsang, 50829 Köln
Email:	riyazbhat@yahoo.com
Geburtsdatum:	29.11.1970
Familienstand:	Ledig
Staatsangehörigkeit:	Indisch

Ausbildung:

1975 - 1980	Grundschule
1981 - 1986	Höhere Schule
1987 - 1989	Präuniversität
1991 – 1995	Studium der Landwirtschaft an der *Sheri-Kashmir University of Agricultural Sciences and Technology*, Kashmir, Indien *Bachelor of science*
1997 – 1998	Magisterstudium in *Food Biotechnology* an der *University of Strathclyde*, Glasgow, UK *Master of science in Food Biotechnology* Magisterarbeit am *Scottish Crop Research Institute*, Dundee, UK in der Arbeitsgruppe von Prof. Gordon Machray Thema: *Biolistic transformation studies in Barley (Hordeum vulgare* L.*)*
1999 – 2002	Promotion am Max-Planck-Institut für Züchtungsforschung in Köln in der Arbeitsgruppe von PD Dr. Richard D. Thompson Abteilung Prof. Dr. F. Salamini Thema: *Evidence for the biological functions of histone acetyltransferase Gcn5 and adaptor protein Ada2 in Zea mays* L. Promotion an der Mathematisch-Naturwissenschaftliche Fakultät der Universität zu Köln